

**GENOMIC IMPRINTING: ESTABLISHMENT, MAINTENANCE AND
STABILITY OF DNA METHYLATION IMPRINTS**

Lara K. Abramowitz

A DISSERTATION

in

Cell and Molecular Biology

Presented to the Faculties of the University of Pennsylvania

in

Partial Fulfillment of the Requirements for the

Degree of Doctor of Philosophy

2013

Supervisor of Dissertation

Marisa S. Bartolomei, PhD., Professor of Cell and Developmental Biology

Graduate Group Chairperson

Daniel S. Kessler, PhD., Associate Professor of Cell and Developmental Biology

Dissertation Committee

Eileen M. Shore, PhD., Cali and Weldon Professor, Orthopedic Surgery

Craig H. Bassing, PhD., Associate Professor of Pathology and Laboratory Medicine

Kenneth S. Zaret, PhD., Joseph Leidy Professor

Zhaolin Zhou, PhD., Assistant Professor of Genetics

This dissertation is dedicated to the memory of Annie Le.
Her dedication, work ethic and love of research was an inspiration to all those around her.

ACKNOWLEDGMENTS

This work would not have been possible without the contribution and support from many others. First, I would like to thank my advisor, Dr. Marisa Bartolomei, whose support and guidance throughout the years has been invaluable. I appreciate the confidence she has had in me and the opportunities she has given me to pursue a variety of projects. She has an inspirational enthusiasm for science that nurtures an environment of creativity and is truly a role model for women in science.

I also would like to thank all of the talented postdocs, students and technicians of the Bartolomei lab that I have had the pleasure of working with. I appreciate all of the conversations, help and advice I have gotten from everyone in the lab. It really has been a fun environment to work in. I would like to thank former lab members Dr. Winnie Mak, Dr. Shu Lin, Dr. Jamie Weaver and current lab members Dr. Sebastien Vigneau, Robert Plasschaert, Dr. Martha Susiarjo, Dr. Jennifer Kalish, Dr. Eric de Waal, and Stella Hur. Although each member of the lab has helped to advance my research, I would like to particularly thank Dr Nora Engel, Dr. Joanne Thorvaldsen, Dr. Folami Ideraabdullah, and Christopher Krapp who have all directly contributed to the work described in this dissertation.

Throughout my graduate career, I have had the great opportunity to collaborate with some of the brightest minds in science. I would like to thank Dr. Ralph Brinster, Dr Andrew Schmidt, Dr. Xin Wu and Dr. Sean Goodyear for giving me the opportunity to contribute to their studies on spermatogonial stem cell culture and transplantation. Their

revolutionary work will one day allow germline preservation for thousands of infertile men. I am grateful to Dr. Guo-Liang Xu and Bang-An Wang for the opportunity to participate in studies to understand Tet-mediated DNA demethylation in primordial germ cells. The ability to work with so many fantastic researchers has been invaluable in teaching me a variety of scientific approaches.

I would also like to thank my thesis committee, Dr. Eileen Shore, Dr. Kenneth Zaret, Dr. Zhaolin Zhou and Dr. Craig Bassing. They have always been there to give advice and guidance and I have left all committee meetings reinvigorated and ready to pursue new questions. I would especially like to thank Dr. Zhaolin Zhou who has been an invaluable resource both for insightful discussions and generously supplying reagents for the MBD project.

Finally, I would like to thank my family and friends. None of this would have been possible without the support from my wonderful husband. He continually puts my needs first and has supported me in pursuing my dreams. I am so grateful that I have not only a loving and caring, but also an intelligent and hardworking person to go home to. I feel lucky to have found a partner who is also my role model. I would also like to thank my amazing parents, brother and sister. They have taught me from an early age that if I am going to pursue something, I need to give it my all and really master it. It was with their support and these values that motivated me to pursue a doctorate. I am also grateful to my in-laws for their continual love and support. Lastly, I would like to thank my friends for making these past six years such a fun experience.

ABSTRACT

GENOMIC IMPRINTING: ESTABLISHMENT, MAINTENANCE AND STABILITY OF DNA METHYLATION IMPRINTS

Lara K. Abramowitz

Marisa S. Bartolomei

Genomic imprinting is an epigenetic phenomenon in which genes are monoallelically expressed according to their parent-of-origin. Imprinted expression entails marking parental chromosomes so that a specific parental allele is stably repressed or expressed. Differential DNA methylation is essential for marking and regulating imprinted genes and is often found at imprinting control regions (ICRs). These DNA methylation imprints must be maintained throughout early development despite genome-wide epigenetic reprogramming to allow for stable allelic expression in differentiated tissues. Moreover, marking of the alleles must be erased in the germline so that establishment of sex-specific marks can occur during gametogenesis. These processes are critical for normal imprinting, however, the precise mechanisms and factors involved remain largely unknown. Of particular concern, environmental perturbations occurring during times of epigenetic reprogramming have been reported to disrupt imprinting. In this dissertation I investigate both *cis* and *trans* mechanisms by which DNA methylation confers imprints and how environmental stresses can disrupt imprinted regulation. I show that decreased CpG content at the endogenous paternal *H19* ICR in mouse renders the ICR unable to silence paternal *H19*, indicating a *cis*-regulatory role for CpG density

in imprinted regulation of *H19*. I also investigate the role that methyl-CpG-binding domain (MBD) proteins, involved in DNA methylation dependent repression, have in genomic imprinting. Through analysis of *Mbd1* and *Mbd2* mutant mice, I find that individual MBD proteins are dispensable for normal imprinting. In a collaborative effort to identify factors necessary for resetting of imprints in germ cells, we examine the cooperative function of Ten-eleven-translocation (TET)1 and TET2 in the erasure of imprints, and show that both TET1 and TET2 are required for demethylation at imprinted loci in the germline. Furthermore, as a collaborative effort, we investigate possible deregulation of imprints upon environmental stress through analysis of spermatogonial stem cells (SSCs) undergoing aging and cryopreservation. We find that stressed SSCs stably maintain methylation imprints and can produce sperm to be used in intracytoplasmic sperm injection that result in normal offspring. These results provide novel insights into mechanisms involved in normal imprint establishment and maintenance, as well as the stability of these marks despite environmental perturbations.

TABLE OF CONTENTS

ACKNOWLEDGMENTS	III
ABSTRACT	V
TABLE OF CONTENTS	VII
LIST OF TABLES	XII
LIST OF FIGURES	XIII
CHAPTER ONE: INTRODUCTION	1
1.1 Genomic imprinting	1
1.2 DNA methylation	3
1.3 Mechanisms of genomic imprinting	4
1.3.1 Insulator model of imprinted regulation	5
1.3.2 long non-coding RNA model of imprinted regulation	9
1.4 Genomic imprinting and human disease	12
1.5 Epigenetic reprogramming in mammalian development	15
1.5.1 Erasure of DNA methylation in primordial germ cells	16
1.5.2 Establishment of DNA methylation in the germline	19
1.5.3 Reprogramming in the preimplantation embryo	24
1.6 Models for DNA methylation dependent repression	29
1.6.1 MBD proteins and transcriptional repression	31
CHAPTER TWO: THE ROLE OF CPG CONTENT IN ICR-MEDIATED REPRESSION OF PATERNAL <i>H19</i>	39
2.1 Generation of the <i>H19</i>^{ICR-SnrCG} allele and experimental design	43

2.2 Aberrant <i>H19</i> expression from the paternal <i>H19</i> ^{ICR-8nrCG} allele.....	46
2.3 Aberrant <i>H19</i> expression from the paternal <i>H19</i> ^{ICR-8nrCG} correlates with developmental and tissue-specific expression of total <i>H19</i>	46
2.4 The paternal <i>H19</i> ^{ICR-8nrCG} allele remains hypermethylated despite paternal <i>H19</i> expression.....	51
2.5 Normal imprinting when the <i>H19</i> ^{ICR-8nrCG} allele was maternally inherited.....	54
2.6 An <i>in vitro</i> repressor assay to assess contribution of methylation at the ICR on repression of a reporter gene.....	54
CHAPTER THREE: THE ROLE OF METHYL-CPG-BINDING DOMAIN PROTEINS IN IMPRINTED GENE REPRESSION	61
3.1 Experimental design.....	62
3.2 Normal imprinting in <i>Mbd1</i> mutant mice	64
3.3 Normal imprinting in <i>Mbd2</i> mutant mice	67
3.4 Loss of MBD1 or MBD2 is not compensated by upregulation of transcripts from other MBD proteins.....	69
3.5 Assessing functional redundancy among the MBD proteins	73
3.5.1 Transient siRNA depletion of MBD proteins in MEFs and TS cells.....	73
3.5.2 Stable shRNA depletion of MBD proteins in <i>Mbd2</i> ^{-/-} MEFs and TS cells.....	76
3.5.3 Overexpression of the MBD in MEFs.....	82
3.6 Breeding to generate <i>Mbd1</i> ^{-/-} <i>Mbd2</i> ^{-/-} mice	85
CHAPTER FOUR: TET-MEDIATED ERASURE OF IMPRINTS IN THE MAMMALIAN GERMLINE	87
4.1 TET1 and TET2 deficient PGCs lack 5hmC.....	88
4.2 TET1 and TET2 deficient PGCs retained DNA methylation at imprinted loci.....	90
4.3 Abnormal methylation at imprinted loci in TET1/TET2 deficient sperm	93
4.4 Aberrant methylation in fetuses from TET1/TET2 deficient females	98
CHAPTER FIVE: STABILITY OF DNA METHYLATION IN SPERMATOGONIAL STEM CELLS DESPITE ENVIRONMENTAL PERTURBATIONS	100
5.1 Analysis of aged SSCs	102

5.1.1 Normal methylation detected in <i>in vivo</i> aged SSCs	102
5.1.2 Normal methylation detected in <i>in vitro</i> aged SSCs.....	108
5.1.3 Normal methylation in offspring derived from aged SSCs, transplantation and ICSI	108
5.1.4 Aged SSCs have decreased stem cell function.....	109
5.2 Analysis in mice derived from SSCs cryopreserved for ~14 years.....	109
5.2.1 Normal methylation profiles in mice derived from SSCs cryopreserved for ~14 years	110
CHAPTER SIX: DISCUSSION AND FUTURE DIRECTIONS	116
6. 1 Non-promoter methylation in gene silencing	117
6.2 CpG content mediates paternal <i>H19</i> repression	118
6.3 CpG content does not have a role in methylation maintenance	119
6.4 Further elucidation of the mechanism for paternal repression of <i>H19</i>	120
6.5 <i>H19^{ICR-SnrCG}</i> allele and implications for human disease	121
6.6 Individual MBD proteins are dispensable for normal imprinting in the mouse.....	122
6.7 MBD2 and MBD3 form functionally distinct NuRD complexes <i>in vivo</i>	124
6.8 MBD proteins: gene-specific or global regulators of repression	125
6.9 TET1 and TET2 mediate DNA demethylation at imprinted loci in PGCs.....	126
6.10 Locus-specific susceptibility to TET deficiency.....	128
6.11 Comparison of two independent <i>Tet1^{-/-}Tet2^{-/-}</i> mutant mice.....	129
6.12 Future directions for analysis of TET-mediated erasure of imprints	130
6.13 Stability of methylation imprints in spermatogonial stem cells.....	132
6.14 Decreased stem cell function in aged SSCs.....	133
6.15 ICSI and disruption of imprinting	134
6.16 Conclusion.....	136
CHAPTER SEVEN: MATERIALS AND METHODS	138
7.1 Targeting and mouse generation of the <i>H19^{ICR-SnrCG}</i> allele	138
7.2 Mice	139

7.3 Genotyping	140
7.4 DNA isolation	141
7.5 Methylation sensitive southern at <i>H19</i>	142
7.6 Bisulfite mutagenesis	142
7.7 PCR amplification of bisulfite DNA for sequencing or COBRA	142
7.8 Bisulfite assays	143
7.9 Luminometric Methylation Assay	146
7.10 Pyrosequencing of bisulfite treated DNA	147
7.11 RNA extraction	148
7.12 Reverse transcription	148
7.13 <i>H19</i> allele-specific RNase protection assay	148
7.14 Allele-Specific expression by RT-PCR and restriction digest	149
7.15 Allele-Specific Lightcycler assay	151
7.16 Relative quantification of expression	151
7.17 Cloning CpGfree1 and CpGfree3	152
7.18 <i>In vitro</i> repressor assay in Hep3b cells	153
7.19 <i>In vitro</i> repressor assay in F9 cells	154
7.20 Isolation of F1 hybrid mouse embryonic fibroblasts	155
7.21 siRNA knockdown in MEFs	155
7.22 Culturing trophoblast stem cells	157
7.23 siRNA knockdown in TS cells	158
7.24 Cloning shRNA into a lentiviral vector	158
7.25 shRNA knockdown in MEFs	161
7.26 shRNA knockdown in TS cells	161
7.27 Western blot analysis	162
7.28 Cloning of MBD overexpression vector	163

7.29 MBD overexpression in F1 hybrid MEFS.....	164
7.30 Statistical analysis.....	165
REFERENCES.....	166

LIST OF TABLES

Table 3.1 Allele-specific expression analysis of imprinted genes in F1 hybrid <i>Mbd1</i> mutant samples	68
Table 3.2 Allele-specific expression analysis of imprinted genes in F1 hybrid <i>Mbd2</i> mutant samples	70
Table 3.3 Allele-specific expression analysis of imprinted genes in F1 hybrid MEFS transiently depleted of MBD1, MBD2, MBD3 or MBD1, MBD2 and MBD3....	75
Table 3.4 Allele-specific expression analysis of imprinted genes in F1 hybrid <i>Mbd2</i>^{-/-} MEFS depleted of MBD1, MECP2 or MBD1 and MECP2.....	78
Table 3.5 Allele-specific expression analysis of imprinted genes in F1 hybrid MEFS which overexpress the MBD	84
Table 7.1 Genotyping PCRs.....	141
Table 7.2 Pyrosequencing assays.....	147
Table 7.3 Allele-specific RT-PCR assays for imprinted genes on mouse chromosome 7	150
Table 7.4 Real time PCR assays.....	152
Table 7.5 siRNA sequences.....	156
Table 7.6 RT-PCR assays for pluripotency markers.....	158
Table 7.7 Antibodies used for western blot	162

LIST OF FIGURES

Figure 1.1 Genomic Imprinting	2
Figure 1.2 Insulator model of imprinting at the mouse <i>H19/Igf2</i> locus.....	7
Figure 1.3 lncRNA model of imprinting at the mouse <i>Igf2r</i> locus.....	11
Figure 1.4 lncRNA model of imprinting at the mouse <i>Kcnq1</i> locus	13
Figure 1.5 Epigenetic reprogramming in primordial germ cells.....	18
Figure 1.6 Epigenetic reprogramming in the preimplantation embryo	25
Figure 1.7 TET mediated oxidation of 5mC and models of DNA demethylation	27
Figure 1.8 Models of DNA methylation dependent repression.....	30
Figure 1.9 Methyl-CpG-binding domain proteins	32
Figure 2.1 Mutant paternal ICRs and corresponding phenotypes.....	40
Figure 2.2 8nrCG mutant ICR	42
Figure 2.3 Generation of the <i>H19^{ICR-8nrCG}</i> allele	44
Figure 2.4 Mating schemes to analyze effect of <i>H19^{ICR-8nrCG}</i> on imprinted <i>H19</i> expression	45
Figure 2.5 Aberrant <i>H19</i> expression from the paternal <i>H19^{ICR-8nrCG}</i> allele.....	47
Figure 2.6 Mutants carrying a paternal <i>H19^{ICR-8nrCG}</i> allele have normal weights and <i>Igf2</i> expression	48
Figure 2.7 Aberrant paternal <i>H19</i> expression throughout development in 8nrCG mutants	50
Figure 2.8 Hypermethylation throughout the paternal 8nrCG mutant ICR.....	52
Figure 2.9 Hypermethylation at the promoter region of the paternal <i>H19^{ICR-8nrCG}</i> allele	53

Figure 2.10 Imprinting analyses of the maternally inherited <i>H19</i> ^{ICR-8nrCG} allele	55
Figure 2.11 CpGfree1 repression assay	57
Figure 2.12 CpGfree3 repression assay	60
Figure 3.1 Expression of <i>H19</i> and <i>Igf2</i> in tissues used in the MBD study	63
Figure 3.2 Experimental design and expression of <i>Mbd1</i> in wild type tissues.....	65
Figure 3.3 Experimental design and expression of <i>Mbd2</i> in wild type tissues.....	66
Figure 3.4 Normal Methylation at the <i>Peg3</i> DMR in <i>Mbd2</i> mutants.....	71
Figure 3.5 Expression of other MBD family members in <i>Mbd1</i> and <i>Mbd2</i> mutant embryos.....	72
Figure 3.6 Depletion of MBD1, MBD2 and MBD3 in MEFs or TS cells	74
Figure 3.7 Stable depletion of MBD1 and MECP2 in <i>Mbd2</i> ^{-/-} MEFs.....	77
Figure 3.8 Infection of shRNA constructs in TS cells.....	80
Figure 3.9 Expression of pluripotency and differentiation markers in TS cells	81
Figure 3.10 Overexpression of the MBD in F1 hybrid MEFs.....	83
Figure 4.1 Mating schemes for analysis of TET1/TET2 deficiency in imprint erasure	89
Figure 4.2 Reduction of 5hmC in TET1/TET2 deficient PGCs.....	91
Figure 4.3 Retention of methylation at imprinted loci in TET1/TET2 deficient E13.5 PGCs	92
Figure 4.4 Retention of methylation at imprinted loci in TET1/TET2 deficient mature sperm	94
Figure 4.5 Normal genomic methylation levels of adult TET1/TET2 deficient testes	96

Figure 4.6 Normal methylation levels at imprinted loci in kidneys of TET1/TET2 deficient mice.....	97
Figure 4.7 Retention of methylation at paternally-methylated DMRs in offspring of a TET1/TET2 deficient female	99
Figure 5.2 Experimental design for <i>in vitro</i> aging analysis	104
Figure 5.3 Experimental design for analysis of offspring derived from aged SSCs, transplantation and ICSI	105
Figure 5.4 Maintenance of DNA methylation at paternally-methylated DMRs	107
Figure 5.5 Experimental design to analyze offspring derived from SSCs cryopreserved ~14 years.....	111
Figure 5.6 Normal genome-wide DNA methylation detected in offspring derived from ICSI using sperm from cryopreserved SSCs	112
Figure 5.7 Normal methylation at paternally-methylated DMRs in mice derived from ICSI using sperm from cryopreserved SSCs.....	114
Figure 5.8 Normal methylation at maternally-methylated DMRs in mice derived from ICSI using sperm from cryopreserved SSCs	115

CHAPTER ONE

Introduction

1.1 Genomic imprinting

In the mammalian genome, the vast majority of genes are either biallelically expressed or repressed. However, there is a small subset of genes in which expression is dependent on the parent-of-origin, these are known as imprinted genes (figure 1.1). In the mouse there has been 150 imprinted genes verified. Imprinted genes have high conservation among mammals, and play essential roles in fetal growth and development as well as metabolism and behavior (www.mousebook.org/catalog.php?catalog=imprinting). Whereas many imprinted genes are ubiquitously imprinted, some exhibit tissue specific imprinted patterns, for example, those imprinted in the placenta (figure 1.3- 1.4) (Frost and Moore, 2010).

Imprinted gene expression accounts for the fact that the two parental genomes are not equal, as suggested by experiments conducted by the Surani and Saltor laboratories throughout the 1980's. Pronuclear transfer experiments were used to generate either a diploid bimaternal (gynogenetic) or diploid bipaternal (androgenetic) conceptus. These embryos failed to develop. The gynogenote developed mostly embryonic tissues, but failed to develop extra-embryonic tissues, whereas the androgenote developed extra-embryonic tissues and failed to develop embryonic tissues. These experiments demonstrated the necessity of transcripts from both parental genomes for normal

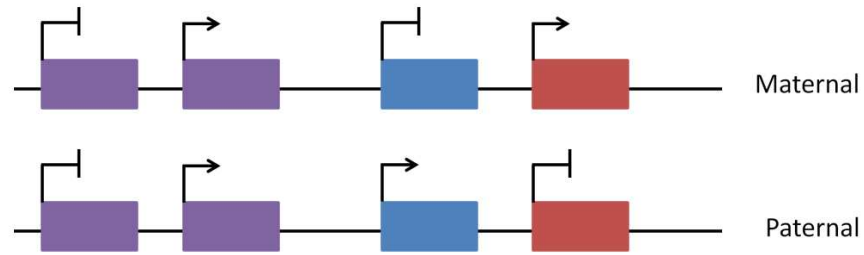


Figure 1.1 Genomic Imprinting. Unlike the majority of genes in the mammalian genome which are biallelically expressed or repressed (purple boxes), imprinted expression is dependent upon the parent-of-origin (blue and red boxes). Expression is indicated by arrows. Parental origin of chromosomes is indicated to the right.

development (McGrath and Solter, 1983; McGrath and Solter, 1984; Surani and Barton, 1983; Surani et al., 1984).

In order for genes to be expressed based on their parent-of-origin, the cell must be able to recognize the parental origin of each chromosome. Therefore, one critical attribute of imprinted genes is that there is a parental-specific mark. There are several key characteristics that this mark must exhibit to allow for stable parental-specific expression. First, the mark must be able to influence transcription. The mark must also be stable and heritable so that imprinting is maintained throughout development. The mark is likely to be established in the germline when the maternal and paternal genomes do not in occupy the same nucleus. Finally, the mark must be erasable to allow for resetting of the appropriate parental-specific marks to be inherited in the next generation (Abramowitz and Bartolomei, 2012). DNA methylation is the only epigenetic modification that fulfills all these criteria. Accordingly, allele-specific DNA methylation has been detected at all imprinted regions identified to date.

1.2 DNA methylation

DNA methylation in mammals occurs predominantly at the 5-position carbon on cytosine residues (5mC) (figure 1.7) followed by guanines (though non-CpG methylation has been described in embryonic stem (ES) cells, induced pluripotent stem (iPS) cells and oocytes (Lister et al., 2011; Tomizawa et al., 2011)). This modification is generally associated with a repressed chromatin state and silencing of gene expression, as will be discussed in section 1.6 (Bird and Wolffe, 1999).

Mammalian DNA methyltransferases fit into two categories, based on their preferred substrate; the *de novo* DNA methyltransferases, DNMT3a and DNMT3b, and the maintenance methyltransferase, DNMT1. DNMT3a and DNMT3b methylate previously unmethylated sequences, while DNMT1 copies existing methylation marks onto the daughter strand during replication. An E3 ubiquitin protein ligase, UHRF1 (also known as NP95 in mouse), is an essential co-factor in maintenance methylation, recruiting DNMT1 to hemimethylated sequences (Sharif et al., 2007). Thus, DNA methylation is a stable and heritable mark. Additionally, there are two non-canonical family members, DNMT3L and DNMT2. Although catalytically inactive, DNMT3L associates with DNMT3a and DNMT3b and stimulates their activity (Suetake et al., 2004). DNMT2 has been shown to methylate tRNA (Goll et al., 2006) and is not likely to be involved in DNA methylation as targeted deletion in ES cells had no effect on global DNA methylation levels (Okano et al., 1998).

DNA methylation is essential for viability, as mice deficient in DNA methyltransferases die in early embryogenesis (Li et al., 1992; Okano et al., 1999). Importantly, when tested prior to death, these embryos exhibit loss of imprinting at many imprinted loci (Kaneda et al., 2004; Li et al., 1993), indicating that DNA methylation is not only found at imprinted loci but is critical for imprinted regulation.

1.3 Mechanisms of genomic imprinting

In the mammalian genome there are approximately 150 imprinted genes which are clustered throughout the genome. Generally, a cluster is ~1MB in size, contains both

maternally and paternally expressed genes, at least one non-coding RNA, and differentially methylated regions (DMRs) (Bartolomei, 2009). Genes within a cluster are co-regulated by a *cis*-acting regulatory element termed an imprinting control region (ICR). These ICRs have been identified genetically, and when deleted in the mouse cause loss of imprinting of the entire cluster (Arney, 2003; Fitzpatrick et al., 2002; Lin et al., 2003; Thorvaldsen et al., 1998; Wutz et al., 1997; Yang et al., 1998). All identified ICRs are also DMRs, in which allele-specific methylation is acquired in the parental germline (also termed primary or germline DMR). Since establishment of DNA methylation at ICRs occurs at a time when the paternal and maternal genomes are in separate compartments (either oocyte or sperm) it allows for parental specific marking of imprinted genes. These DNA methylation marks are then maintained in the offspring by DNMT1 (Li et al., 1993), despite genome-wide DNA demethylation in the preimplantation embryo (Reik et al., 2001). Additionally, differential DNA methylation can also be established after fertilization in the postimplantation embryo, these regions are known as secondary DMRs (Bartolomei, 2009). The vast majority of ICRs are maternally methylated, with methylation at promoters. In contrast, only three paternally-methylated ICRs (*H19*, *Rasgrf1*, IG-DMR) have been identified each with intergenic methylation (Ferguson-Smith, 2011). Various models for imprinted gene regulation have been described, with the best defined being the insulator and long non-coding RNA (lncRNA) models (Bartolomei, 2009).

1.3.1 Insulator model of imprinted regulation

The insulator model of imprinting has been best described in regulation of the *H19/Igf2* locus, which is located on mouse chromosome 7 and human chromosome 11p15.5. This model of imprinted regulation is the most evolutionarily ancient (Smits et al., 2008). Maternally expressed *H19* is a lncRNA that encodes ~2.2kb transcript (Bartolomei et al., 1991). Although the precise function of *H19* remains unclear, it harbors a microRNA (miR-675) at its first exon (Mineno et al., 2006). Recently, miR-675 has been described to play a role in growth suppression (Keniry et al., 2012), which supports the hypothesis that *H19* acts as a tumor suppressor (Hao et al., 1993; Yoshimizu et al., 2008). Paternally expressed *Igf2* encodes a fetal growth factor, *Insulin like growth factor 2* (DeChiara et al., 1990; DeChiara et al., 1991). Imprinted expression at this locus is regulated by two *cis*-acting elements; (1) shared enhancers located downstream of *H19* such as those that drive expression in endodermal (Leighton et al., 1995) and mesodermal (Kaffer et al., 2001) tissues, and (2) an ICR located between the two genes, ~2-4kb upstream of the *H19* transcriptional start site (Thorvaldsen et al., 1998). This element is paternally methylated, with methylation established during spermatogenesis and maintained throughout development (figure 1.2) (Davis et al., 2000; Tremblay et al., 1997; Tremblay et al., 1995).

The insulator model at this locus has been worked out through a series of targeted mutations in the mouse and *in vitro* experiments. Maternal inheritance of a mutant chromosome in which the ICR was deleted, resulted in biallelic *Igf2* expression and a reduction in total *H19* expression. Conversely, when a paternal chromosome was inherited in which the ICR was deleted, *H19* was biallelically expressed and total *Igf2*

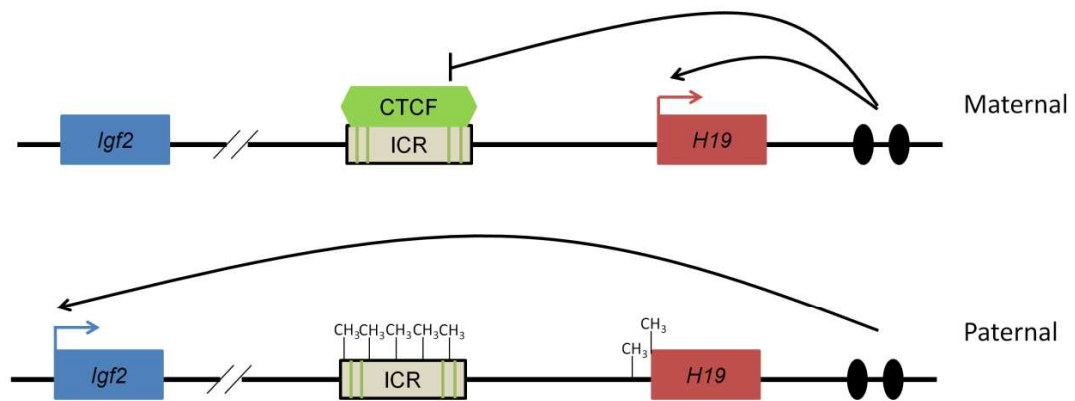


Figure 1.2 Insulator model of imprinting at the mouse *H19/Igf2* locus. Imprinting of maternally expressed *H19* (red box) and paternally expressed *Igf2* (blue box) is regulated by a paternally methylated ICR (grey box) harboring 4 CTCF binding sites (green lines). The unmethylated maternal allele binds CTCF (green hexagon) blocking shared enhancers (black ovals) from accessing *Igf2*. CTCF cannot bind the methylated (CH₃) ICR, allowing interaction of *Igf2* with the enhancers on the paternal chromosome. Expression is indicated by arrows. Parental origin of chromosomes is indicated to the right.

expression was reduced (Thorvaldsen et al., 1998; Thorvaldsen et al., 2002). Interestingly, when enhancers were inserted between the ICR and *Igf2*, *Igf2* became biallelically expressed with no effect on *H19* expression (Webber et al., 1998). Subsequently, it was shown that CTCF, a protein that acts as an enhancer blocker at the chicken β -globin locus (Bell et al., 1999), binds at the ICR in a methylation sensitive manner (Bell and Felsenfeld, 2000; Hark et al., 2000; Kaffer et al., 2000; Kanduri et al., 2000; Szabo et al., 2000). The unmethylated ICR was demonstrated to function as an insulator *in vitro* (Bell and Felsenfeld, 2000; Hark et al., 2000; Kaffer et al., 2000; Kanduri et al., 2000). Thus, the following model for imprinted regulation at the *H19* locus has been proposed (Figure 1.2); CTCF binds the unmethylated maternal ICR, establishing an insulator, and blocking shared enhancers from accessing *Igf2* promoters. CTCF is unable to bind to the methylated ICR, allowing the shared enhancers to interact with *Igf2* on the paternal allele. Furthermore, methylation at the paternal ICR leads to secondary methylation at the *H19* promoter, silencing paternal *H19* (Srivastava, 2002; Thorvaldsen et al., 1998; Tremblay et al., 1997). Therefore, the insulator activity of the ICR regulates maternal *H19* and paternal *Igf2* expression.

Various mouse mutants have subsequently supported the role of the ICR as a methylation sensitive insulator regulating imprinted activity of the locus. When CTCF was unable to bind the maternal ICR (either by deletion or mutations of CTCF binding sites), *Igf2* was biallelically expressed with reduction of *H19* expression (Engel et al., 2006; Pant et al., 2004; Schoenherr et al., 2003; Szabo et al., 2004; Thorvaldsen et al.,

1998). Furthermore, paternal inheritance of a mutant ICR that allowed binding of CTCF, lead to biallelic *H19* expression and a reduction of *Igf2* expression, (Engel et al., 2004).

Although the *H19/Igf2* locus has been the only locus characterized to be regulated by the insulator model, allelic CTCF binding has been described at other imprinted loci (Fitzpatrick et al., 2007; Hikichi et al., 2003; Kernohan et al., 2010; Lin et al., 2011; Yoon et al., 2005). At the *Rasgrf1* locus there is evidence suggesting insulator activity (Yoon et al., 2005), however, further investigation is necessary to determine if imprinting at this locus is regulated in the same manner as *H19/Igf2*, which requires identification of enhancers.

1.3.2 long non-coding RNA model of imprinted regulation

The majority of imprinted loci use the lncRNA model of imprinted regulation (Koerner et al., 2009; Santoro and Barlow, 2011). At these imprinted loci, a promoter for a lncRNA is within the ICR. Transcription of the lncRNA is necessary for the imprinted regulation of the cluster in *cis*. The best characterized loci that use the lncRNA mechanism of imprinted expression are the *Igf2r* and *Kcnq1* imprinted clusters. Imprinting at the *Igf2r* cluster is coordinated by the paternally expressed lncRNA *Airn*, which contains a differentially methylated promoter that acts as the ICR (Wutz et al., 1997). Here, transcription of *Airn* represses *Igf2r* ubiquitously, and *Slc22a2* and *Slc22a3* in the placenta. Thus, *Igf2r* is maternally expressed in all tissues where *Airn* is expressed, and *Slc22a2* and *Slc22a3* are maternally expressed in the placenta. Also at this locus are biallelically expressed genes *Slc22a1* and *Mas1*, which are interspersed between the

imprinted genes. In addition to the ICR, a secondary DMR is found at this cluster at the paternally-methylated *Igf2r* promoter (Stoger et al., 1993). Interestingly, inheritance of a paternal allele carrying a truncated *Airn* transcript resulted in loss of imprinting of the entire cluster in embryonic and placental tissues, whereas maternal truncation had no effect (Sleutels et al., 2002). Thus, transcription of the full length lncRNA *Airn* is required for proper imprinting of the locus (figure 1.3). Recently, different mechanisms for *Airn* mediated repression have been proposed for regulation of *Igf2r* and *Slc22a3*. Analysis of a series of *Airn* truncation mutant ES cells indicated that silencing of *Igf2r* required transcriptional overlap of the *Igf2r* promoter. Thus, transcriptional interference, rather than the *Airn* product is critical for *Igf2r* silencing (Latos et al., 2012). In contrast, it has been proposed that *Airn* interacts with the *Slc22a3* promoter and recruits the histone methyltransferase G9a in placenta (Nagano et al., 2008). Therefore, *Airn* mediated repression could be acting through different mechanisms to confer tissue-specific imprinted expression.

Imprinting at the *Kcnq1* cluster exhibits many features similar to that at the *Igf2r* cluster. Imprinting is dependent upon a paternally expressed lncRNA, *Kcnq1ot1*, whose promoter is an ICR exhibiting maternal-specific methylation (Smilinich et al., 1999). Additionally, a secondary DMR is located at the promoter for *Cdkn1c* (Bhogal et al., 2004). Expression of *Kcnq1ot1* is necessary for maternal specific expression of neighboring genes in *cis* (Fitzpatrick et al., 2002; Mancini-Dinardo et al., 2006). Interestingly, only *Cdkn1c* is ubiquitously imprinted, *Kcnq1* only exhibits imprinted

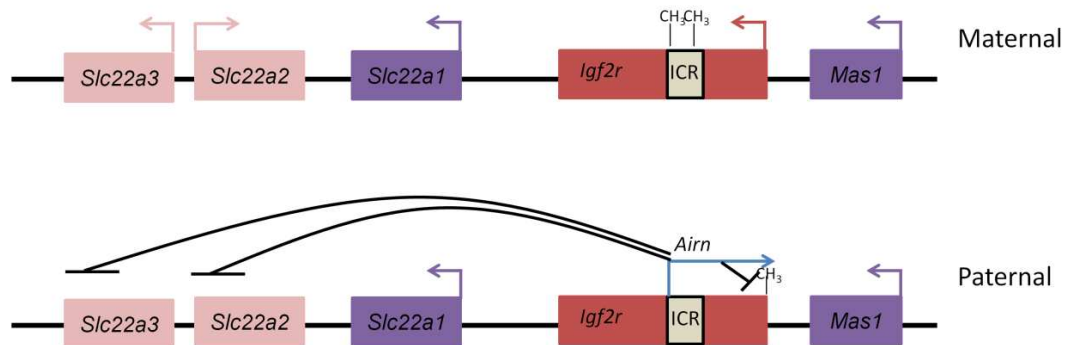


Figure 1.3 lncRNA model of imprinting at the mouse *Igf2r* locus. Imprinting is coordinated by paternal expression of the lncRNA *Airn* (blue arrow). The promoter of *Airn* is located within the intron of *Igf2r*, is maternally methylated (CH₃) and acts as the ICR (grey box). Expression of *Airn* represses paternal *Igf2r* (red box) ubiquitously and paternal *Slc22a3* and *Slc22a2* (pink boxes) in the placenta. Also at this locus are biallelically expressed genes (purple boxes). Expression is indicated by arrows. Parental origin of chromosomes is indicated to the right.

expression until ~E15.5 (Mancini-Dinardo et al., 2006; Umlauf et al., 2004). Additionally, several genes, such as *Osbp15*, *Cd81*, *Tssc4*, are imprinted exclusively in the placenta (figure 1.4) (Green et al., 2007; Umlauf et al., 2004). Similar to *Airn*, paternal inheritance of a truncated *Kcnq1ot1* transcript resulted in a loss of imprinting of the cluster (Mancini-Dinardo et al., 2006; Shin et al., 2008), except for *Cdkn1c* which maintained proper imprinted expression in a subset of embryonic tissues (Shin et al., 2008). Details of the mechanism by which *Kcnq1ot1* acts to repress other genes in the cluster remains to be elucidated.

1.4 Genomic imprinting and human disease

Imprinted genes play essential roles in prenatal and postnatal growth and development, as well as metabolism and behavior. Because dosage of these genes is tightly regulated, disease can result from chromosomal abnormalities, genetic or epigenetic mutations. There are a number of human congenital diseases associated with imprinted clusters (Thorvaldsen and Bartolomei, 2007), including Prader-Willi Syndrome (PWS), Angelman Syndrome (AS), Beckwith-Wiedemann Syndrome (BWS) and Silver-Russell Syndrome (SRS). Additionally, loss of imprinting contributes to a variety of malignancies (Girardot et al., 2012).

Failure to express genes within the *SNRPN* imprinted domain, located in the proximal arm of chromosome 15, results in PWS and AS. Silencing of paternally expressed genes within this domain causes PWS, a condition characterized by infantile hypotonia, early childhood obesity, short stature, small hands and feet, growth hormone

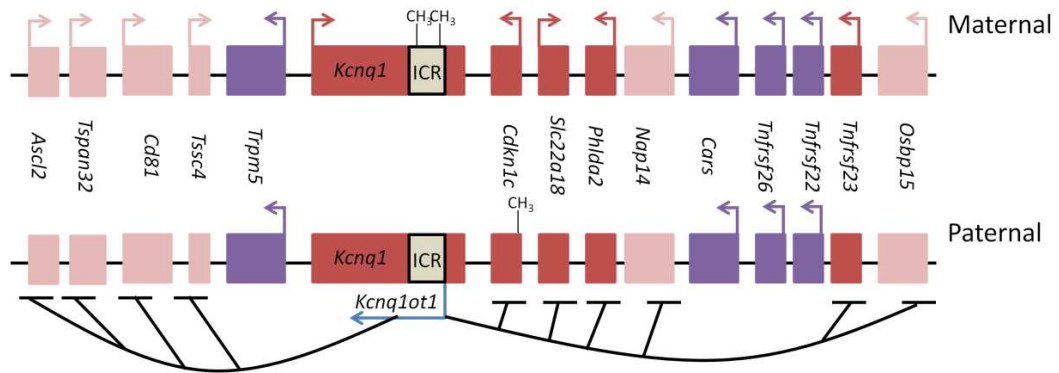


Figure 1.4 lncRNA model of imprinting at the mouse *Kcnq1* locus. Imprinting at this locus is regulated by paternal expression of the lncRNA *Kcnq1ot1* (blue arrow). The *Kcnq1ot1* promoter is contained within a maternally-methylated (CH₃) ICR (grey box). Expression of *Kcnq1ot1* is necessary to paternally repress neighboring genes in *cis*, (red and pink boxes) with many genes imprinted only in the placenta (pink boxes). Additionally, this locus harbors biallelically expressed genes (purple boxes). Expression is indicated by arrows. Parental origins of chromosome are indicated to the right and gene names are either indicated within the box or between the chromosomes.

deficiency, hypogonadism, mental deficiency and behavioral problems (Butler, 2009). Loss of function of the maternally expressed gene *UBE3A*, which is involved in early brain development, causes AS. AS is characterized by seizures, mental retardation, jerky arm movements, inappropriate laughter, lack of speech, among other symptoms (Butler, 2009). The majority of patients with BWS have abnormal methylation at 11p15, which harbors both the *H19* and *KCNQ1* clusters, resulting in the loss of maternal expression of the cell cycle inhibitor *CDKN1C* or increased expression of the paternally expressed growth factor *IGF2* (Choufani et al., 2010). This disease is characterized by macrosomia, macroglossia, prominent eyes with periorbital fullness and creased ears (Butler, 2009). Overexpression of *CDKN1C* or decreased expression of *IGF2* cause SRS, characterized by growth retardation (Shmela and Gicquel, 2013).

An increased risk of imprinting disorders has been described in children conceived by assisted reproductive technologies (ART), including *in vitro* fertilization and intracytoplasmic sperm injection (ICSI) (Owen and Segars, 2009). These procedures involve endocrine stimulation of the ovary, embryo culture, and transfer of preimplantation embryos, which have all been shown to cause alteration of DNA methylation and deregulation of imprinted genes in mice (de Waal et al., 2012b; Doherty et al., 2000; Fauque et al., 2007; Mann et al., 2004; Rivera et al., 2008; Sato et al., 2007). Whereas studies suggest an increased prevalence of imprinting disorders (particularly BWS and AS) (Owen and Segars, 2009) in children conceived from ART, it is unclear if this increased risk is due to ART procedures or the underlying infertility of the parents.

Additionally, these syndromes are rare making it difficult to pinpoint the underlying contributing factors for these disorders.

1.5 Epigenetic reprogramming in mammalian development

Although DNA methylation patterns in somatic-differentiated cells are generally stable and heritable, there are two waves of genome-wide DNA methylation reprogramming that takes place in mammalian development. These DNA demethylation and remethylation events occur in the germline and the preimplantation embryo (figures 1.5-1.6) (Reik et al., 2001). Whereas it has been well known that the *de novo* DNMTs are involved in resetting methylation marks (Abramowitz and Bartolomei, 2012), the mechanisms of DNA demethylation and the enzymes involved are just beginning to be elucidated. DNA demethylation can occur in two ways; (1) replication dependent (passive DNA demethylation) and (2) replication independent (active DNA demethylation). Recently, the discovery of 5-hydroxymethylcytosine (5hmC) and the enzymes that coordinate the conversion of 5mC to 5hmC, Ten-eleven translocation (TET) 1,2,3 proteins, has given us new insights into the mechanism of DNA demethylation (Ito et al., 2010; Kriaucionis and Heintz, 2009; Tahiliani et al., 2009) (Figure 1.7).

It is important to note that many of the techniques used to analyze DNA methylation differ in the ability to distinguish between 5mC and 5hmC. Bisulfite sequencing, for example, cannot distinguish between 5mC and 5hmC. However, antibodies specific to the different residues have been raised and verified. Additionally, there is ongoing effort to develop single base resolution techniques for distinguishing

between the two modifications, which include oxidative bisulfite sequencing (oxBS-seq) (Booth et al., 2012) and Tet-assisted bisulfite sequencing (TAB-seq) (Yu et al., 2012).

1.5.1 Erasure of DNA methylation in primordial germ cells

The resetting of methylation at imprinted loci in primordial germ cells (PGCs) is essential for sex-specific methylation patterns to be inherited in the next generation.

First, somatic patterns of DNA methylation need to be fully erased so that subsequent establishment of sex-specific marks can occur.

In mice PGCs are specified by external signals from the epiblast at E6.5 and arise from a small population of about 40 cells at E7.25 (Saitou, 2009). At E9.5 a small population of about 200 cells start to migrate through the hindgut endoderm and reach the genital ridges at ~E10.5 (Saitou, 2009). During this time, PGCs undergo widespread epigenetic changes including, loss of histone modifications, loss of DNA methylation and reactivation of the silent allele of imprinted genes (Hajkova et al., 2008; Hajkova et al., 2002; Szabo and Mann, 1995).

A number of recent studies suggests that demethylation of PGCs occur in two stages in the mouse; the first corresponding to the migration phase at ~E8.5 and the second with the gonadal stage at ~E10.5 (Guibert et al., 2012; Hackett et al., 2013; Kagiwada et al., 2013; Seisenberger et al., 2012). This first round of DNA demethylation is when the majority of sequences become demethylated, with ~30% of CpGs being methylated in E9.5 PGCs reduced from ~71% of CpGs methylated in E6.5 epiblasts (Seisenberger et al., 2012). Many studies suggest that this bulk demethylation occurs in a

passive/replication dependent manner, that is, the DNA is replicated with a failure of maintenance methylation by DNMT1. Despite the presence of DNMT1 (Hajkova et al., 2002) in PGCs, loss of methylation follows the kinetics of a replication dependent mechanism (Hackett et al., 2013). In PGCs, UHRF1 is detected as being excluded from the nucleus and no DNMT1 is detected at replication foci (Kagiwada et al., 2013). Furthermore, E9.5 PGCs have a high number of hemimethylated CpG sites, suggesting a loss of maintenance methylation (figure 1.5) (Seisenberger et al., 2012).

From E9.5 methylation levels drop gradually in the gonadal phase, to ~15% of CpGs methylated in E11.5 PGCs and again to ~14% and 7% in E13.5 male and female PGCs, respectively (Seisenberger et al., 2012). This second, gonadal phase is when imprint erasure is completed (figure 1.5) (Hackett et al., 2013; Hajkova et al., 2008; Seisenberger et al., 2012). A recent study that distinguished between 5mC and 5hmC reported conversion of ICR 5mC to 5hmC in PGCs. Interestingly, the timing of this conversion differed for individual imprinted loci. For example, in PGCs, ICRs at the *Kcnq1* and *Igf2r* clusters were enriched for 5hmC by E10.5, while ICRs at *Peg3* and *Peg10* loci were not enriched for 5hmC until day E11.5. This conversion corresponds with timing of when *Tet1* and *Tet2* expression peaks, at ~ E10.5-11.5 PGCs (with no detectable *Tet3*) (Hackett et al., 2013). How the 5hmC marks are removed still requires further investigation, though Hackett et al., 2013, found that the kinetics of 5hmC loss followed a replication dependent model at *Peg3* and *Peg10*. Additionally, various components of the base excision repair pathway, AID (a deaminase) and TDG (a

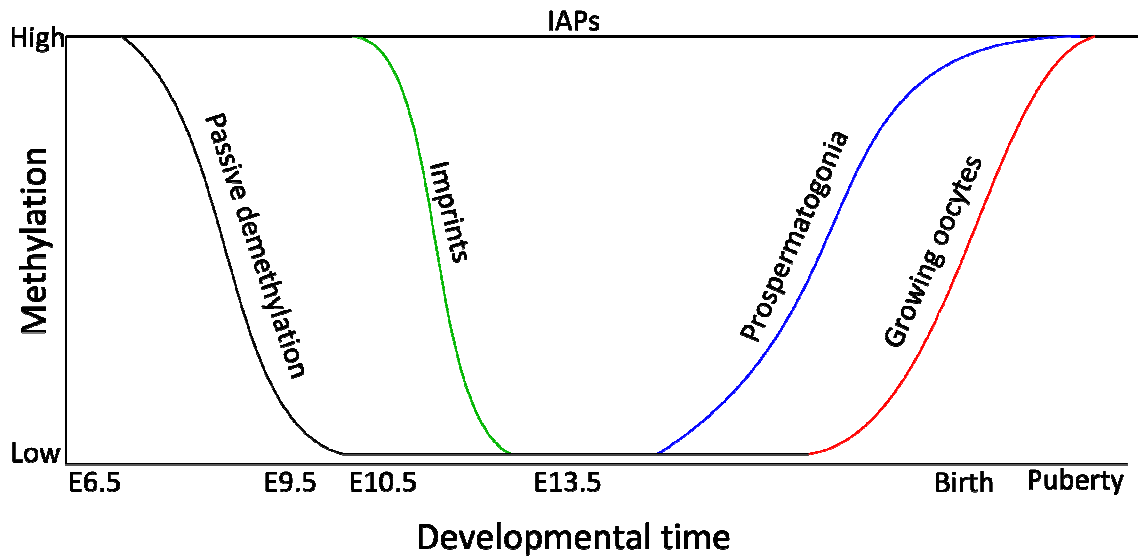


Figure 1.5 Epigenetic reprogramming in primordial germ cells. There are two rounds of DNA demethylation in PGCs; bulk DNA demethylation, which occurs in migrating PGCs (which is likely passive), and a second round in gonadal PGCs, when imprints (green line) are erased. IAPs are able to maintain methylation throughout PGC development. Remethylation occurs in prospermatogonia (blue line) or in growing oocytes (red line).

glycosylase), have been implicated in erasure of methylation in PGCs (figure 1.7) (Cortellino et al., 2011; Popp et al., 2010). AID deficient E13.5 PGCs have subtle global increases in methylation levels (Popp et al., 2010) and E11 PGCs lacking TDG had high levels of methylation at the *Igf2* promoter. However, these observations could be explained by developmental delay in the mutant PGCs, and methods used in both studies could not distinguish between 5mC and 5hmC. Therefore, further analysis is necessary to determine a definitive role of these BER components in reprogramming of PGCs.

Although the majority of the genome is demethylated in PGCs there are a few regions that escape erasure, for example, intracisternal-A-particles (IAPs) (figure 1.5) (Guibert et al., 2012; Hackett et al., 2013; Lane et al., 2003; Seisenberger et al., 2012). IAPs are evolutionarily the most recently acquired transposon family in the mouse genome, and thus potentially the most active (Qin et al., 2010). Methylation at IAPs may be required to suppress this potentially active element. Interestingly, maintenance of methylation at IAPs occurs even though UHFR1 is expressed only at very low levels and appears cytosolic, and DNMT1 is not detected at replication foci (Kagiwada et al., 2013). Therefore, it is unclear if methylation maintenance at IAPs in PGCs occurs using a novel mechanism, or if current technologies are not sensitive enough to detect these proteins acting in PGCs.

1.5.2 Establishment of DNA methylation in the germline

In female PGCs low levels of DNA methylation persist from E13.5 (Seisenberger et al., 2012), with *de novo* methylation occurring after birth in the growing oocyte (Bao et

al., 2000). Methylation of ICRs in growing oocytes is completed by the time oocytes arrest in metaphase II (figure 1.5) (Lucifero, 2004). Males, in contrast, exhibit robust *de novo* methylation in E16.5 PGCs (figure 1.5) (Seisenberger et al., 2012) with methylation at ICRs completed postnatally by the pachytene stage of meiosis (Davis et al., 2000).

Timing of methylation acquisition occurs in a locus-specific manner, with *Snrpn*, *Igf2r* and *Peg3* gaining significant methylation in oocytes by 10 days postpartum (dpp), and *Peg1* gaining methylation later, at ~25 dpp (Lucifero, 2004). Interestingly, acquisition of methylation at *Snrpn* occurs asymmetrically, with the maternal allele methylated earlier than the paternal (Lucifero, 2004). Asymmetric acquisition of methylation has also been observed at the *H19* locus, with the paternal allele methylated prior to the maternal (Davis et al., 2000). These observations suggest that an epigenetic marking exists at these loci carrying somatic memory. In the case of *H19*, CTCF sites have been implicated for somatic memory by coordinating allele-specific histone modifications that facilitate marking of the parental origin of each allele (Lee et al., 2010).

As previously mentioned, *de novo* methylation is deposited by DNMT3a, DNMT3b and the co-factor DNMT3L. Studies of conditional knockouts of *Dnmt3a* and *Dnmt3b* in germ cells provide evidence that DNMT3a is required for *de novo* methylation of all ICRs (both maternal and paternal) except for the paternally-methylated *Rasgrfl* ICR, which resembles repetitive DNA and requires both DNMT3a and DNMT3b (Kaneda et al., 2004; Kato et al., 2007). A defect in the establishment of methylation of germline DMRs was also observed in mice deficient for DNMT3L (Bourc'his and Bestor,

2004; Bourc'his et al., 2001). Oocytes deficient for DNMT3L lack methylation at maternal DMRs. Additionally, *Dnmt3L* null females exhibit a maternal lethal phenotype, in which embryos are hypomethylated at all maternally-methylated ICRs but global methylation is not reduced (Bourc'his et al., 2001). DNMT3L also plays a critical role in establishment of paternal methylation imprints. Whereas reports vary on the extent that paternal ICRs are affected in DNMT3L deficient male germ cells, ICRs at *H19/Igf2*, *Rasgrf1* and *Gtl2* (IG-DMR) require DNMT3L for full methylation (Bourc'his and Bestor, 2004; Kaneda et al., 2004; Kato et al., 2007; Webster, 2005).

Although the DNA methylation machinery is now well-established, it remains to be determined how this machinery is recruited to specific CpGs. Interestingly, a link has been found between histone methylation and DNA methylation. DNMT3L has binding affinity for nucleosomes containing unmethylated H3K4, which is abolished with the addition of methyl groups to this residue (Ooi et al., 2007). These results suggest that patterns of histone methylation could dictate patterns of DNA methylation, which could then be stably inherited. Furthermore, oocytes that lack lysine demethylase 1B (KDM1B), a H3K4 demethylase, are hypomethylated at a number of imprinted loci (Ciccone et al., 2009), suggesting that an unmethylated H3K4 is necessary for DNA methylation. Consistently, male germ cells assayed at the onset of *de novo* methylation reveal high levels of H3K4me3 at the maternally-methylated *Snrpn* and *Kcnq1* ICRs but absence of H3K4me3 at paternally-methylated *H19* ICR and IG-DMR, suggesting that H3K4me3 prevents maternally-methylated DMRs from acquiring DNA methylation in the male germline (Henckel et al., 2011). Interestingly, the association of DNA

methylation with an unmethylated H3K4 and the protection from DNA methylation with methylation of H3K4 is not limited to imprinted loci, but is also observed genome-wide (Meissner et al., 2008; Weber et al., 2007).

Even with the observation that DNA methylation requires a favorable histone environment, it is still unclear if there are any sequence signatures that distinguish ICRs from other CpG rich regions in the genome. One such signature has been proposed to be the spacing of CpGs at ICRs. Molecular modeling of the DNMT3a/DNMT3L complex indicates an optimal periodicity of CpGs for methylation at about 8-10 base pairs (Jia et al., 2007). Interestingly, this periodicity was reported at 12 maternal ICRs (Jia et al., 2007). However, recent studies were unable to detect this trend at ICRs in both oocytes and sperm (Tomizawa et al., 2011) and were unable to detect a difference in CpG spacing between methylated and unmethylated CpG islands in oocytes and sperm (Smallwood et al., 2011). Overall, the role of CpG spacing as a signature for ICRs remains unclear.

Many reports have uncovered a link between transcription and methylation establishment. For example, as described above, KDM1B is critical for establishment of methylation of many maternal ICRs (Ciccone et al., 2009). Interestingly, the human orthologue of KDM1B, LSD2, is associated with gene bodies of actively transcribed genes (Fang et al., 2010). Additionally, the PWWP domain of DNMT3a binds H3K36me₃, a mark of transcriptional elongation, which increases the methyltransferase activity of DNMT3a *in vitro* (Dhayalan et al., 2010). These observations suggest that *de novo* methylation is targeted to sites of active transcription.

In accordance, multiple imprinted loci have been shown to require transcription for establishment of DNA methylation, the first of these being the *Gnas* locus (Chotalia et al., 2009). This locus encodes multiple transcripts; the protein coding transcripts *Gnas*, *Gnasx1* and *Nesp* and the non-coding transcripts *Nespas* and *IA*. This region contains two maternally methylated DMRs, one that encompasses the *Gnasx1* and *Nespas* promoters, which acts as the ICR, and another that covers the *IA* promoter. A targeted mutation in the mouse that truncated the *Nesp* transcript, the furthest upstream transcript, and caused hypomethylation (in varying degrees) at all DMRs in mutant oocytes (Chotalia et al., 2009), suggesting a defect in methylation establishment. Interestingly, transcripts are also detected in growing oocytes at the maternally-methylated ICRs of the *Grb10*, *Igf2r*, *Impact*, *Kcnq1*, *Zac1* and *Snrpn* imprinted loci (Chotalia et al., 2009; Mapendano et al., 2006).

The imprinted *Rasgrf1* locus, which harbors a paternally-methylated ICR, also requires transcription for methylation establishment (Watanabe et al., 2011). In spermatogonia of mice mutant for various proteins in the piRNA pathway, including MILI, MIWI2 and MITOPLD, the *Rasgrf1* ICR, but not other paternally-methylated DMRs, exhibited reduced methylation. Further analysis revealed that a ncRNA (pit-RNA) transcribed from the *Rasgrf1* ICR was targeted by piRNAs, causing cleavage of this RNA. The authors propose a model in which targeting of piRNAs to pit-RNA is an important step in sequence specific methylation at the *Rasgrf1* locus (Watanabe et al., 2011).

Although paternal-specific methylation of the *H19* ICR and IG-DMR does not require the piRNA pathway (Watanabe et al., 2011), transcription is detected at both of these ICRs specifically in male PGCs at the onset of *de novo* methylation (Henckel et al., 2011). Together, these studies provide evidence suggesting the requirement of transcription at both maternally- and paternally-methylated ICRs. Nevertheless, additional experiments are necessary to prove the causality of this transcription in methylation establishment.

1.5.3 Reprogramming in the preimplantation embryo

Upon fertilization, two differentiated cell types with drastically different methylation levels, ~90% methylation in sperm and ~40% methylation in oocytes (Kobayashi et al., 2012), unite to form a zygote. The epigenetic signature of these gametes must be erased in order to regain developmental totipotency. However, throughout this reprogramming, imprints must be conserved in order to maintain the parental origin of each chromosome (figure 1.6).

After fertilization the maternal and paternal genomes are in separate pronuclei that undergo disparate mechanisms of epigenetic reprogramming. The maternal genome is passively demethylated over subsequent cleavage divisions with the exclusion of DNMT1 from the nucleus (Howell et al., 2001; Mayer et al., 2000). In contrast, the paternal pronucleus loses 5mC before the first cell division (Mayer et al., 2000; Oswald et al., 2000), suggesting an active mechanism of DNA demethylation (figure 1.6). Although a number of models for active DNA demethylation have been proposed, there

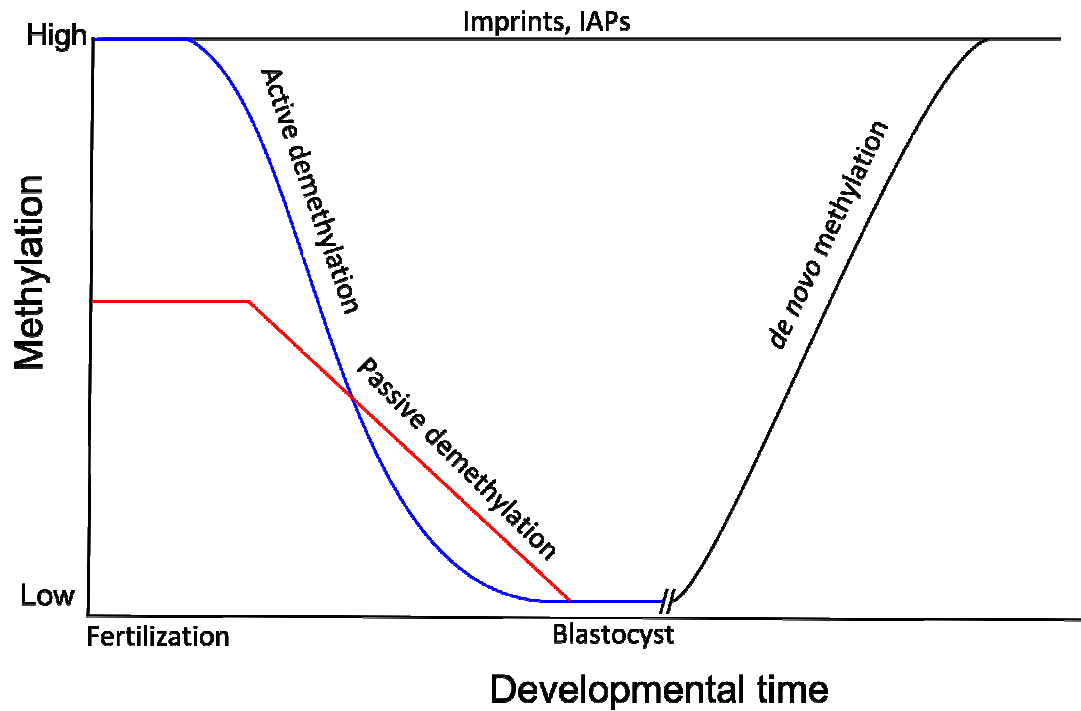


Figure 1.6 Epigenetic reprogramming in the preimplantation embryo. Genome-wide DNA demethylation after fertilization occurs with differing dynamics for the maternal and paternal genome. The maternal genome is passively demethylated (red line) whereas the paternal genome is actively demethylated (blue line) by conversion to 5hmC. Throughout this reprogramming, imprints and IAPs maintain DNA methylation. The majority of remethylation subsequently occurs shortly after implantation.

is increasing evidence that supports the conversion of 5mC to 5hmC as a route to demethylation.

Original studies indicating active DNA demethylation of the paternal genome used immunofluorescence with an antibody against 5mC, which detected a clear loss of 5mC signal (Mayer et al., 2000; Oswald et al., 2000). More recent studies reveal that concomitant with the loss of 5mC signal there is a strong increase in signal for 5hmC and the further oxidation products, 5-formylcytosine (5fC) and 5-carboxylcytosine (5caC) (Gu et al., 2011; Inoue et al., 2011; Inoue and Zhang, 2011; Iqbal et al., 2011; Wossidlo et al., 2011). TET3 is the enzyme required for these oxidation reactions. *Tet3* is highly expressed in preimplantation embryos and is enriched on the paternal pronucleus (Gu et al., 2011; Wossidlo et al., 2011). Analysis of 5hmC and 5mC by immunofluorescence in zygotes derived from *Tet3*^{-/-} oocytes revealed no 5hmC signals and retained 5mC signal on paternal pronuclei. Loss of 5hmC, 5fC and 5caC from the paternal genome occurs in a passive manner with gradual dilution over cleavage divisions (Gu et al., 2011; Inoue et al., 2011; Inoue and Zhang, 2011; Wossidlo et al., 2011). However, other pathways have been implicated in demethylation of the paternal pronucleus. For example, small molecule inhibition of BER pathway proteins PARP1 and APE1 result in increased methylation of the paternal genome (Hajkova et al., 2010). Whereas there is great evidence for passive loss of 5hmC, 5fC, and 5caC modifications of bulk DNA, other mechanisms might be employed at individual loci (figure 1.7).

Although the paternal and maternal genomes share the ooplasm, the maternal genome is not converted to 5hmC, and must be protected from this oxidation. The

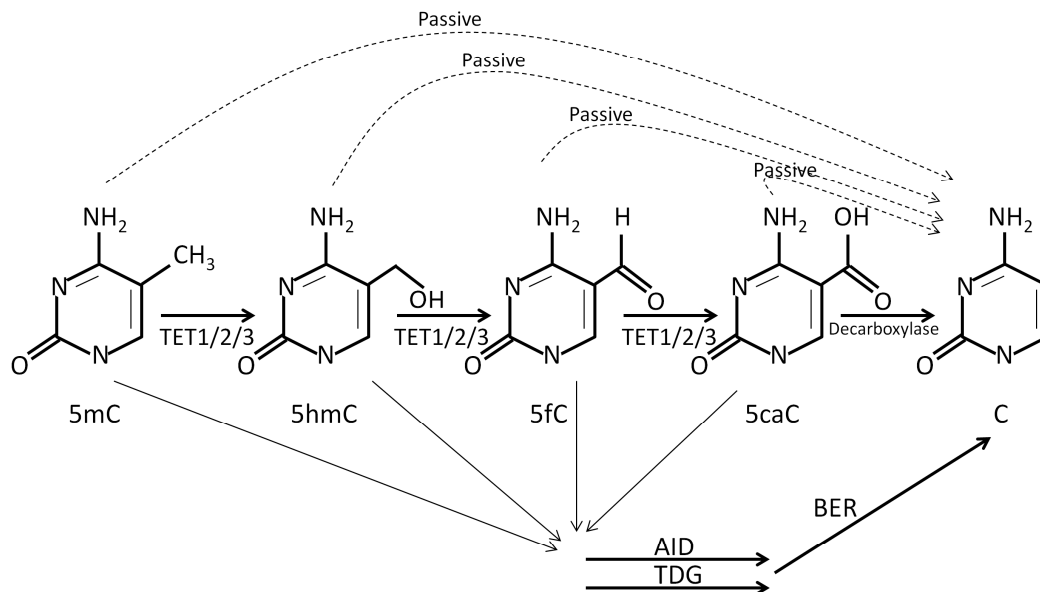


Figure 1.7 TET mediated oxidation of 5mC and models of DNA demethylation. Oxidation of 5mC to 5hmC and further derivatives 5fC and 5caC are mediated by TETs 1/2/3. Demethylation can occur either in a replication dependent (passive) manner or in an enzymatically driven manner. The base excision repair (BER) pathway and various enzymes involved (as indicated) have been implicated in DNA demethylation.

maternal factor STELLA (also known as DPP3a or PGC7) is critical for protection of both the maternal genome and paternally-methylated ICRs (as will be discussed) (Nakamura et al., 2007; Nakamura et al., 2012). STELLA is recruited to these regions by H3K9me2 and inhibits TET3 binding, thus preventing oxidation of 5mC (Nakamura et al., 2012).

Despite genome-wide reprogramming, there are several elements that maintain DNA methylation in the early embryo; ICRs, IAPs, as well as some CpG island promoters (figure 1.6) (Smallwood et al., 2011; Smith et al., 2012). DNA methylation is retained at imprinted loci by a combination of both DNMT1 and an oocyte-specific isoform, DNMT1o (Cirio et al., 2008; Hirasawa et al., 2008; Howell et al., 2001), and recruited by UHRF1 (Sharif et al., 2007).

Several *trans*-acting factors have been implicated in protecting ICRs from demethylation in a locus-specific manner. As mentioned, STELLA is implicated in retention of methylation at maternally-methylated (*Peg1*, *Peg3* and *Peg10*) as well as paternally-methylated ICRs (*H19* and *Rasgrf1*) (Nakamura et al., 2007), presumably by protection of conversion to 5hmC (Nakamura et al., 2012). MBD3, a member of the repressive nucleosomes remodeling and deacetylase (NuRD) complex, is required in the preimplantation embryo for maintaining methylation specifically at the *H19* locus (Reese et al., 2007). Furthermore, ZFP57, a KRAB zinc finger protein, is required for maintenance of methylation at a number of imprinted loci, including *Snrpn*, *Peg1*, *Peg3*, *Peg5* and *Dkl1* (Li et al., 2008), most likely through its interaction with KAP1 (Quenneville et al., 2011).

Not only does the methylated allele need to retain methylation at imprinted loci during embryonic reprogramming, but the unmethylated allele must maintain its hypomethylated status during subsequent remethylation. At the *H19* ICR maintenance of the hypomethylated maternal allele is accomplished by binding of CTCF. Embryos containing a mutant maternal allele that cannot bind CTCF gain methylation during embryogenesis (Engel et al., 2006; Pant et al., 2003; Szabo et al., 2004). In accordance with this model, mice with a mutant paternal allele that can bind CTCF, lose methylation during embryogenesis (Engel et al., 2004).

1.6 Models for DNA methylation dependent repression

Generally, DNA methylation is a repressive epigenetic mark, though reports have suggested an activating role at specific loci (Wu et al., 2010; Yu et al., 2013). Two models for DNA methylation dependent repression have been described. The first being a direct mechanism in which the presence of 5mC inhibits binding of transcription factors to DNA (figure 1.8). Many transcription factors have been identified that cannot bind to methylated DNA, such as E2f, CREB and, as described above, CTCF (Bell and Felsenfeld, 2000; Campanero et al., 2000; Hark et al., 2000; Iguchi-Arigo and Schaffner, 1989). Thus, expression would be silenced without transcription factor binding. The second model is an indirect mechanism that involves recruitment of proteins that bind methylated DNA and associate with chromatin modifiers (figure 1.8). Two families of proteins have been identified that fit into this second model, methyl-CpG-binding domain

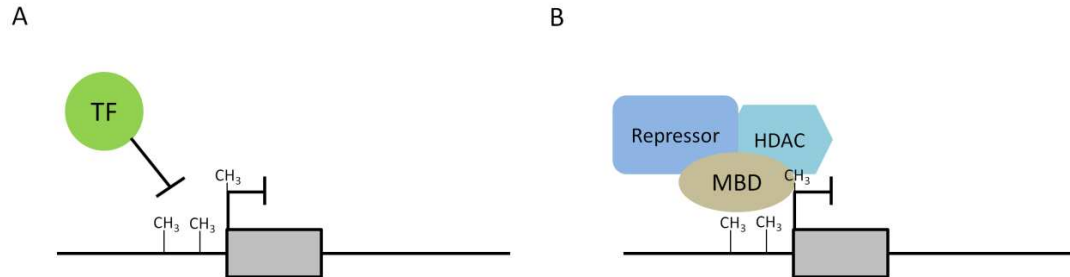


Figure 1.8 Models of DNA methylation dependent repression. Repression by DNA methylation can occur either directly (A) by inhibiting binding of transcription factors or indirectly (B) through binding of methyl-CpG- binding domain (MBD) proteins that interact with transcriptional repressors and chromatin modifiers to coordinate a repressive chromatin environment.

(MBD) proteins and Kaiso proteins. These models are not mutually exclusive and can work in concert (Klose and Bird, 2006).

In addition to these mechanisms, the DNMTs have been implicated in setting up a repressive chromatin state upon the deposition of methylation marks. DNMT1 has been shown to interact with chromatin modifiers and transcriptional repressors, for example, HDAC1/2, EZH2 and HP1 (Fuks et al., 2000; Robertson et al., 2000; Rountree et al., 2000; Smallwood et al., 2007; Vire et al., 2006). Association with these proteins would allow the establishment of a repressive chromatin environment throughout cell divisions. Furthermore, DNMT3b interacts with HDACs 1/2, HP1, Suv39h1 and the ATP dependent chromatin remodeler hSNF2H (Geiman et al., 2004).

1.6.1 MBD proteins and transcriptional repression

The MBD family of proteins includes 5 members; MECP2, MBD1, MBD2, MBD3 and MBD4. The MBD was initially identified as the minimal domain of MECP2 necessary for binding methylated DNA *in vitro* (Nan et al., 1993). A subsequent homology search led to the identification of MBD1, MBD2, MBD3 and MBD4 (Hendrich and Bird, 1998). With the exception of MBD3, which contains amino acid substitutions that prevent direct binding to methylated DNA (Ohki et al., 1999), the MBD family of proteins binds methylated DNA and interacts with transcriptional repressors (figure 1.9) (Bogdanović and Veenstra, 2009).

MECP2 was the first identified and is the most studied MBD family member. Mutations in human *MECP2*, an X-linked gene, cause the debilitating progressive

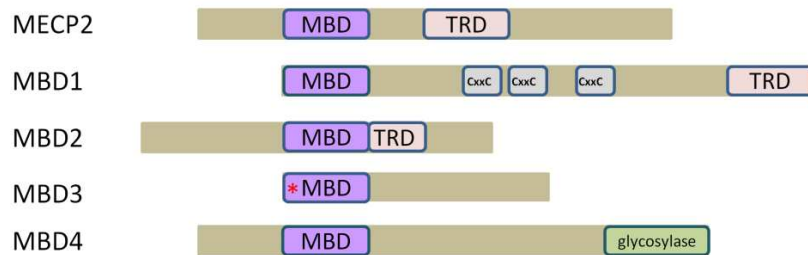


Figure 1.9 Methyl-CpG-binding domain proteins. There are 5 MBD family proteins in mammals, all of which can bind methylated DNA at the methyl binding domain (MBD, purple box), except MBD3 which has an amino acid substitution (red star) that does not allow direct binding to 5mC. MECP2, MBD1 and MBD2 all have a transcriptional repression domain (TRD, pink box), which interacts with co-repressors and chromatin modifiers. MBD1 also contains CxxC motifs (grey box) that allow binding to unmethylated DNA. MBD4, with a glycosylase domain (green box), is involved in DNA repair.

neurodevelopmental disorder Rett Syndrome (Amir et al., 1999). As with all X-linked disorders, Rett Syndrome more severely affects males, leading to death either prenatally or within the first two years of life (Schule et al., 2008). Thus, the vast majority of Rett patients are female. MECP2 associates with various co-repressor complexes such as Sin3a, NCoR and c-Ski through interaction with the transcriptional repression domain (TRD) (figure 1.9) (Jones et al., 1998; Kokura et al., 2001). *In vitro* experiments indicate that targeting MECP2 to promoter DNA causes transcriptional repression (Jones et al., 1998; Nan et al., 1998).

Mecp2 null mice have neurological defects resembling those of Rett Syndrome, as well as reduced brain size and body weight (Chen et al., 2001; Guy et al., 2001). There has been much effort in the field to identify targets of MECP2 as these genes could be causal in Rett Syndrome, however, transcriptional profiling of *Mecp2* null brains indicate few and subtle changes (Nuber et al., 2005; Tudor et al., 2002). Although deregulation of specific genes has not been identified, increased histone acetylation levels (Shahbazian et al., 2002) and increased transcription of transposable elements (Skene et al., 2010) have been detected in MECP2 deficient mouse brains. Recently, MECP2 was shown to bind 5hmC in the mouse brain, though the implications of this binding has yet to be determined (Mellen et al., 2012).

MECP2 has been detected as bound to the imprinted loci *U2af1-rs1*, *Ube3a*, *H19* and *Dlx5* *in vivo* (Fournier et al., 2002; Gregory et al., 2001; Horike et al., 2005; Kernohan et al., 2010; Samaco et al., 2005). Moreover, deregulation of *GNAS*, *IGF2* and *UBE3A* has been reported in Rett patient lymphocytes and postmortem brains (Ballestar

et al., 2005; Makedonski et al., 2005; Samaco et al., 2005). In accordance with these observations, *in vitro* analysis implicated MECP2 in the regulation of *H19* (Drewell et al., 2002). Surprisingly, when allele-specific expression analysis was performed in *Mecp2*^{-y} adult mouse brain normal imprinting was detected (Samaco et al., 2005).

In addition to the MBD, MBD1 also contains a TRD, as well as CxxC domains that allow binding to unmethylated DNA (figure 1.9) (Ohki et al., 1999). MBD1 has been shown to interact with repressive chromatin modifiers such as Suv39h1-HP1 (Fujita et al., 2003). The functional importance of MBD1 was demonstrated in HeLa cells, where MBD1 was shown to interact with SETDB1 during replication. This complex is recruited to chromatin by CAF1 to establish new repressive H3K9 methyl marks after replication, which was shown to be necessary for proper silencing of the *p53BP2* promoter (Sarraf and Stancheva, 2004).

Studies of patients with autism have identified mutations at *MBD1* as potentially causative (Li et al., 2005; O'Donnell et al., 2010). Similarly, *Mbd1*^{-/-} phenotypes manifest most prominently in the adult brain with deficits in adult neurogenesis and hippocampal function, as well as autism like behaviors (Allan et al., 2008; Zhao et al., 2003).

Analysis of *Mbd1*^{-/-} adult neural stem cells has uncovered a role for MBD1 in regulation of a number of miRNAs, which is likely methylation independent as methylated CpGs are not present in proximity to the miRNAs (Liu et al., 2013; Liu et al., 2010). MBD1 has been described bound to *U2af1-rs1* imprinted gene by ChIP analysis (Fournier et al., 2002). However, imprinting analysis in *Mbd1* null mice has not been reported.

MBD2 also binds methylated CpGs and confers transcriptional repression through its TRD (figure 1.9) (Boeke et al., 2000; Ng et al., 1999). MBD2 is a component of the NuRD complex. In accordance, repression established by MBD2 is sensitive to HDAC inhibitors (Zhang et al., 1999).

Mbd2 null mice are viable and develop normally but have abnormal maternal behaviors, decreased intestinal tumorigenesis and disordered T-cell differentiation (Hendrich, 2001; Hutchins et al., 2002; Sansom et al., 2003). Analysis of the *Mbd2* null mouse has revealed MBD2 dependent repression at specific genes. One such study reported leaky expression of IL-4 in T-cells (Hutchins et al., 2002). Additionally, deficiency of MBD2 on an APC (tumor suppressor) mutant background revealed elevated levels of known Wnt targets (Pesse et al., 2008) in the small intestine. However, it is unknown if MBD2 deficiency alone would cause this upregulation. Analysis of male *Mbd2*^{-/-} mice revealed proper repression of the *Xist* gene (involved in X-chromosome inactivation) (Hendrich, 2001), though analysis of male *Mbd2*^{-/-} fibroblasts revealed leaky *Xist* expression (Barr et al., 2007). It is therefore unclear if this leaky expression was due to cell culture conditions or loss of MBD2. Of interest, MBD2 has been reported bound to the imprinted gene *Peg3* in cyclophilin A knockdown P9 cells (Lu et al., 2006). However, early studies of the *Mbd2* null mice identified normal imprinting in adult brain, heart and spleen (Hendrich, 2001).

Unlike the other MBD family members, MBD3 cannot bind methylated DNA (figure 1.9) (Hendrich, 2001; Ohki et al., 1999). A recent study has indicated binding of MBD3 to 5hmC (Yildirim et al., 2011), however, other groups have been unable to

confirm this binding (Hashimoto et al., 2012). MBD3 is an essential member of the NuRD complex (Saito and Ishikawa, 2002; Zhang et al., 1999), though it is likely that MBD2 and MBD3 form mutually exclusive NuRD complexes (Le Guezennec et al., 2006) with distinct binding profiles (Baubec et al., 2013; Gunther et al., 2013).

MBD3 is essential for viability as *Mbd3*-null embryos die at ~E8.5 (Hendrich, 2001). Furthermore, *Mbd3*^{-/-} ES cells have a compromised ability to differentiate (Kaji et al., 2006; Kaji et al., 2007). Whereas MBD3 itself does not bind methylated DNA, it has been detected at *H19* and *U2af1-rs1* imprinted loci, which is likely indirect binding (Fournier et al., 2002; Reese et al., 2007). Additionally, as described above, MBD3 has been implicated in maintaining DNA methylation at the *H19* ICR throughout embryogenesis as blastocysts depleted of MBD3 lose methylation at the ICR and imprinted expression of *H19* (Reese et al., 2007).

MBD4, which binds methylated DNA but lacks a TRD, is a thymine glycosylase (figure 1.9). MBD4 acts as a DNA repair protein targeting sites of cytosine deamination (Hendrich et al., 1999). In accordance with MBD4 as a DNA repair protein, mutations in MBD4 have been found in cancers with microsatellite instability (Riccio et al., 1999). Moreover, mice deficient for MBD4 have increased cytosine to thymine transitions and an increased rate of tumorigenesis (Millar et al., 2002; Wong et al., 2002).

In this dissertation I have taken a two-fold approach to understanding mechanisms of imprinted regulation by (1) investigating the processes of how DNA methylation

marks and coordinates repression throughout normal mammalian development and (2) studying how these processes could be disrupted by environmental perturbations. In chapter 2, I focus on the *H19/Igf2* locus by defining a role for DNA methylation density in ICR mediated repression. I find that a CpG-depleted ICR is insufficient for paternal *H19* silencing *in vivo*. Chapter 3 focuses on the role of MBD1 and MBD2 as *trans*-factors mediating allele-specific repression at imprinted loci. Here, I show that these MBD proteins individually are dispensable for normal imprinting at several loci. In chapter 4, I describe work investigating factors involved in reprogramming imprints in the germline. In collaboration with the laboratory of Dr. Guo-Liang Xu at the Shanghai Institutes for Biological Sciences, Chinese Academy of Sciences, we identify a cooperative role for TET1 and TET2 in erasure of imprints in germ cells. In Chapter 5, I worked in collaboration with Dr. Ralph Brinster's laboratory at the University of Pennsylvania School of Veterinary Medicine, to investigate possible abnormalities in DNA methylation at imprinted loci in *in vivo* and *in vitro* aged spermatogonial stem cells, and ICSI derived offspring from spermatogonial stem cells frozen for ~14 years. We find that extreme aging, cryopreservation or ICSI does not significantly disrupt methylation at imprinted loci, suggesting that spermatogonial stem cells are resistant to these environmental perturbations.

Overall, this dissertation provides important insights into the *cis* and *trans* acting mechanisms involved in imprint establishment and maintenance. Understanding how DNA methylation regulates imprinted repression will further elucidate the etiology of imprinting disorders as well as other diseases caused by aberrant DNA methylation,

including cancer. Moreover, as reproductive technologies advance, we are faced by new challenges in human reproduction. Several ART procedures have been linked to disruption of imprinting. This work provides evidence that methylation imprints are in fact stable in spermatogonial stem cells that have undergone aging and cryopreservation, suggesting that these techniques can be valuable sources for male infertility treatment.

CHAPTER TWO

THE ROLE OF CpG CONTENT IN ICR-MEDIATED REPRESSION OF PATERNAL *H19*

Imprinted expression of *H19* and *Igf2* in the mouse is dependent upon a differentially methylated ICR (as described in chapter 1.3.1) (Srivastava et al., 2000; Thorvaldsen et al., 1998; Tremblay et al., 1997). Analysis of mutant mice has highlighted the importance of differential methylation at the ICR in both maternal *H19* expression and paternal *H19* repression. Studies clearly show that the unmethylated maternal ICR binds CTCF, which is required for insulation, maintenance of hypomethylation and activation of maternal *H19* expression (Engel et al., 2006; Schoenherr et al., 2002; Szabo et al., 2004). On the paternal allele, methylation at the ICR spreads to the *H19* promoter, repressing paternal *H19* expression (Srivastava et al., 2000; Thorvaldsen et al., 1998; Tremblay et al., 1997). Additionally, *in vitro* analysis indicated that location of CpGs within CTCF sites (but not outside of the CTCF sites) at the ICR was critical for repression of a reporter gene (Chen et al., 2008). While the ICR has been well defined to regulate imprinted expression of *H19*, our understanding of how methylation at the ICR acts to repress paternal *H19* remains incomplete.

Previously generated mutations at the endogenous *H19* ICR have suggested the presence of *cis*-acting elements necessary for paternal *H19* silencing. Aside from ICR deletion, which resulted in loss of imprinting upon both maternal and paternal inheritance (figure 2.1) (Srivastava et al., 2000; Thorvaldsen et al., 1998), there has been two mouse mutants described in which loss of imprinting occurred exclusively when the mutant

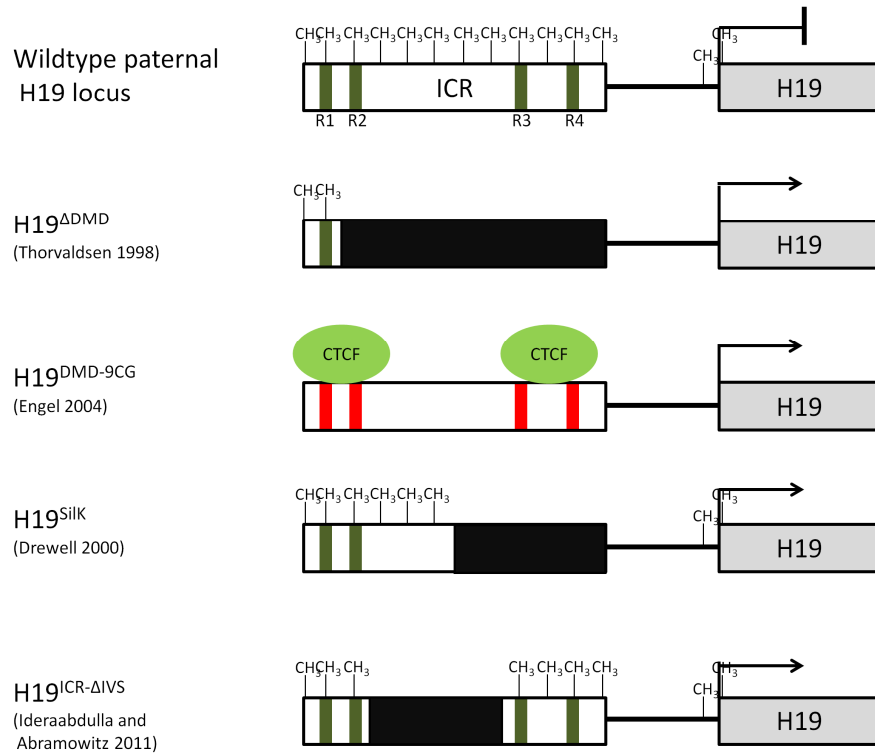


Figure 2.1 Mutant paternal ICRs and corresponding phenotypes. Wild type paternal ICR (top panel, white box) and published paternal mutant ICRs (references indicated) are drawn with corresponding phenotypes. Depicted are methylated CpGs (CH_3), wild type CTCF binding sites (R1-R4, as green rectangles), *H19* (grey box), mutant CTCF binding sites (red box), CTCF binding (green ovals), deleted sequence (black box). Expression is indicated with an arrow.

allele was paternally inherited. Upon paternal inheritance of a CpG-depleted ICR, in which 9 CpGs within CTCF binding sites had been mutated ($H19^{DMD-9CG}$), the mutant paternal allele was hypomethylated and paternal $H19$ expression was detected (figure 2.1). In mutant embryos, total $Igf2$ expression was decreased indicating the formation of an insulator, evidenced by a 40% decrease in size of the pups (Engel et al., 2004). Because CTCF was able to bind the mutant paternal ICR it remains unclear if paternal $H19$ expression was due to aberrant CTCF binding (resulting in hypomethylation and formation of an insulator) or because the allele had decreased CpG content. Additionally, paternal inheritance of a mutant allele in which half of the ICR had been deleted (including two CTCF binding sites and more than half of the CpGs ($H19^{Silk}$)), resulted in paternal $H19$ expression, though the mutant allele remained hypermethylated with normal $Igf2$ expression (figure 2.1) (Drewell et al., 2000). Again, it is unclear if paternal $H19$ expression was caused by deletion of CTCF sites, decreased size of the ICR or lowered number of CpGs.

Together, these studies (Drewell et al., 2000; Engel et al., 2004) implicate a *cis*-acting regulatory role for the ICR in $H19$ repression, but it remains elusive whether paternal $H19$ expression resulted from a decrease in CpG content at the ICR or manipulations/deletion of CTCF sites (figure 2.1). I addressed this question through analysis of a mouse mutant in which 8 CpGs within the ICR but outside of CTCF sites had been mutated ($H19^{ICR-8nrCG}$) (figure 2.2). Paternal inheritance of this allele resulted in paternal $H19$ expression, indicating that CpG density at the ICR is required for silencing $H19$. The target vector and targeting scheme was designed by Dr. Nora Engel. In

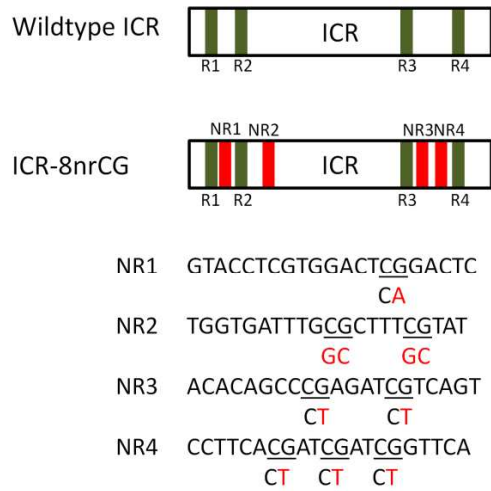


Figure 2.2 8nrCG mutant ICR. Point mutations were made to the endogenous ICR outside of CTCF binding sites (NR regions 1-4, red boxes). Mutated sequence is indicated in red lettering. Wild type ICR sequence is written in black lettering. Depiction of wild type ICR is drawn for comparison. CTCF binding sites (R1-R4) are also indicated (green boxes).

addition to Dr. Engel, Dr. Marisa Bartolomei, Dr. Joanne Thorvaldsen and Christopher Krapp contributed to the target vector construction and isolation of targeted alleles. I performed all of the breeding and analysis as well as all work for *in vitro* repressor assays. The results were combined with analysis of a mouse mutant in which the sequence between CTCF sites 2 and 3 had been deleted ($H19^{ICR-\Delta IVS}$) (Figure 2.1) and published in Ideraabdullah and Abramowitz et al. 2011.

2.1 Generation of the $H19^{ICR-8nrCG}$ allele and experimental design

To determine the role of CpG content at the ICR in $H19$ repression, mice carrying a mutant allele at the endogenous locus ($H19^{ICR-8nrCG}$) were generated by homologous recombination in mouse ES cells. This mutant decreased the number of CpGs at the ICR by 8 (~16% depletion) without changing the size of the ICR or disrupting CTCF binding sites (figure 2.2-2.3A). Germline transmission of the targeted clones and Cre mediated excision of the *neo^r* cassette in the mouse were confirmed by southern blot (figure 2.3B).

Mutant mice were bred onto a C57BL/6 (B6) strain and heterozygous mutants were crossed with wild type B6(CAST7) (C7) mice, which contained chromosome 7s from the *Mus musculus castaneus* (CAST) on a mostly B6 background (Mann, 2003). Tissues from F1 heterozygous mutant progeny were analyzed for imprinting defects as compared to wild type littermates. Analysis was performed for both paternal and maternal inheritance of the mutant $H19^{ICR-8nrCG}$ allele (figure 2.4).

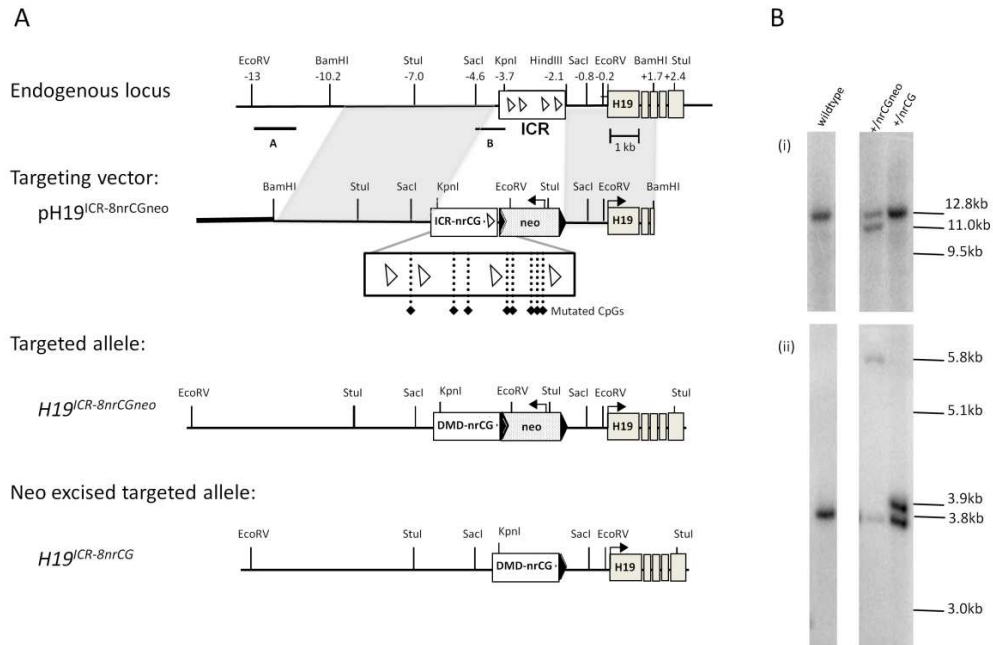


Figure 2.3 Generation of the $H19^{ICR-8nrCG}$ allele. (A) Illustration of the targeting scheme at the $H19$ locus. Positions (in kb) are relative to $H19$ transcription start site. Southern probes (A, B and C) indicated by horizontal lines below locus. The wild type endogenous $H19$ ICR (white rectangle) containing CTCF sites (white triangles), the $H19^{ICR-8nrCG}$ mutation (white box, dashed lines indicate mutated CpG sites), $H19$ exons (gray boxes), neo^r cassette (dotted box), $loxP$ sites (black arrowheads), 129/Sv $H19$ DNA (thin line) and pBluescript II KS (thick line) are shown. (B) Southern blots to confirm mice carrying correctly targeted alleles using external probe A - $EcoRV$ digest (i) and internal probe C- $SacI$ digest (ii).

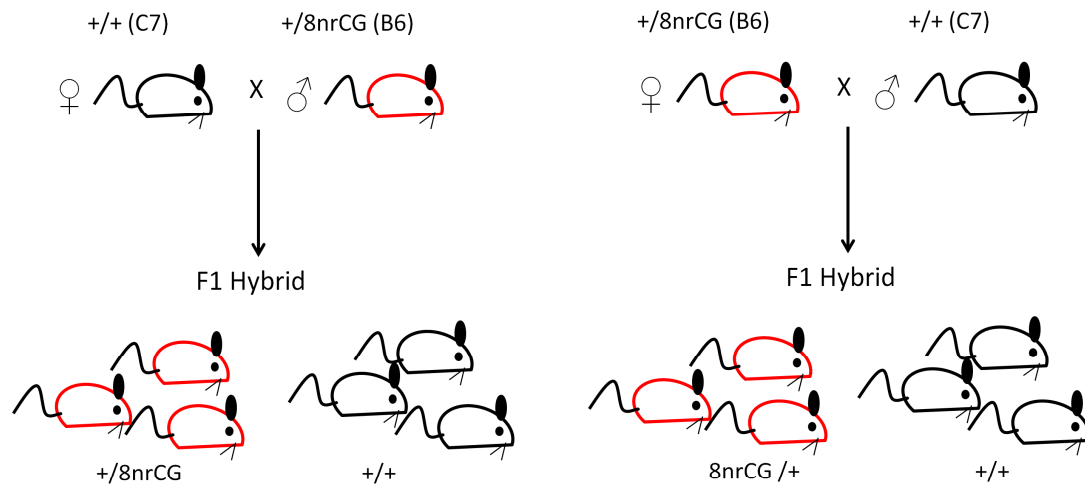


Figure 2.4 Mating schemes to analyze effect of $H19^{ICR-8nrCG}$ on imprinted $H19$ expression. Heterozygous mice carrying the $H19^{ICR-8nrCG}$ allele (red) on a B6 background were mated with wild type (black) C7 mice. F1 heterozygous progeny carrying the $H19^{ICR-8nrCG}$ allele were analyzed for imprinting defects at the $H19/Igf2$ locus as compared to wild type littermates. Analysis was performed on mice that either paternally (A) or maternally (B) inherited the $H19^{ICR-8nrCG}$ allele.

2.2 Aberrant *H19* expression from the paternal *H19*^{ICR-8nrCG} allele

To determine the effects of the 8nrCG mutation on imprinting at the *H19/Igf2* locus, allele-specific expression of heterozygous mutants that paternally inherited the mutant allele was analyzed. First, *H19* allelic expression was assayed in neonatal tissue by either an RNase protection assay in liver (figure 2.5A) or RT-PCR in tongue (figure 2.5B). Derepression of paternal *H19* was detected in both tissues. This aberrant paternal *H19* expression was detected as early as E6.5 in extra-embryonic tissues (figure 2.5C) and E13.5 in embryonic tissues (figure 2.7).

Biallelic *H19* expression in previously described mutants had also correlated with a decrease in size of the mutant mouse (Engel et al., 2004; Thorvaldsen et al., 1998). Here, despite biallelic *H19* expression, no size difference was observed between heterozygous mutants and wild type littermates (figure 2.6A). Additionally, no change in total *Igf2* was detected in neonatal livers of 8nrCG mutants compared to wild type littermates (figure 2.6B), suggesting that the loss of imprinting phenotype is specific to *H19* and that *Igf2* expression was not perturbed by the formation of an insulator on the mutant paternal allele.

2.3 Aberrant *H19* expression from the paternal *H19*^{ICR-8nrCG} correlates with developmental and tissue-specific expression of total *H19*

Aberrant paternal expression from the *H19*^{ICR-8nrCG} allele was not detectable at all developmental time points and tissues where *H19* is normally expressed, for example, E9.5 embryo (figure 2.5D). Analysis was therefore performed to assess whether

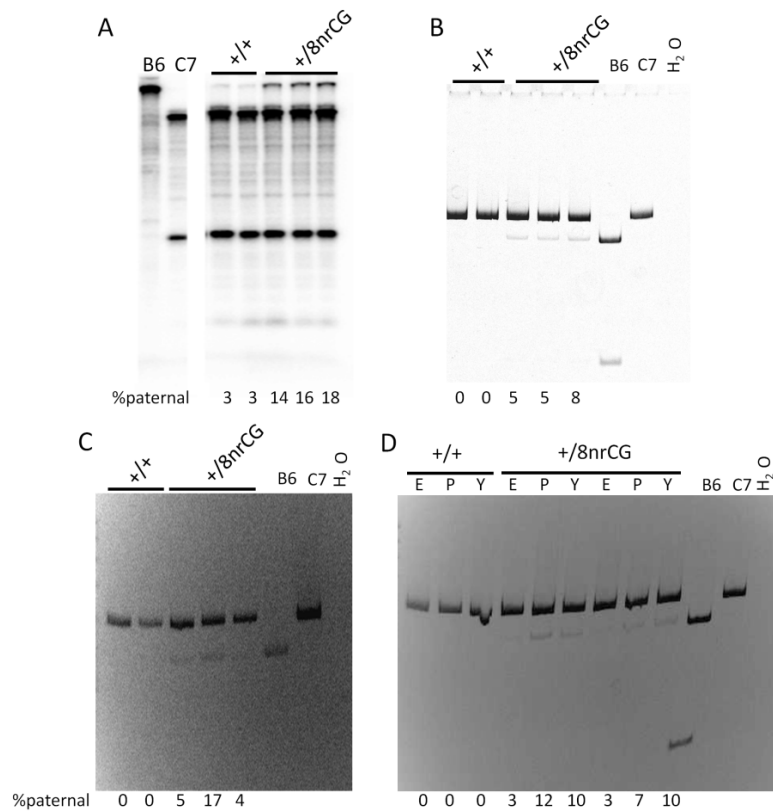


Figure 2.5 Aberrant *H19* expression from the paternal *H19*^{ICR-8nrCG} allele. (A) Allele-specific expression of *H19* was analyzed by an RNase protection assay on RNA from neonatal liver (A) or RT-PCR on cDNA (B-D) from (B) neonatal tongue, (C) E6.5 conceptuses or (D) E9.5 embryos (E), placentas (P) and yolk sacs (Y) from F1 hybrid heterozygous mutants (+/8nrCG) and wild type littermates (+/-). B6 and C7 controls are indicated. The percent *H19* expression derived from the paternal allele is shown below the panels.

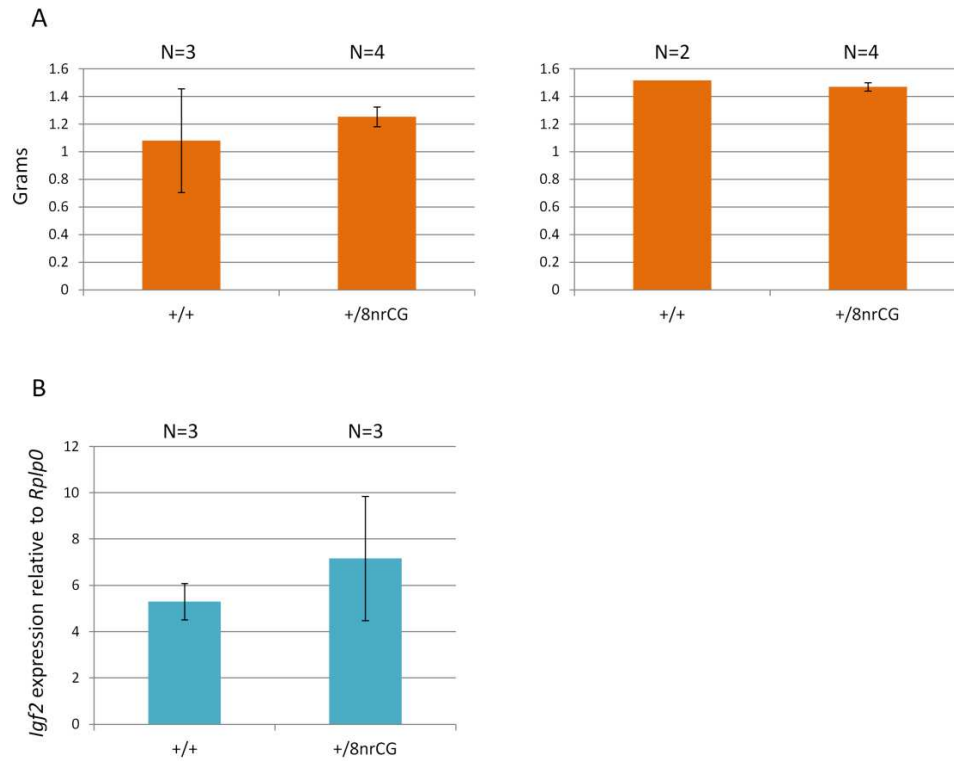


Figure 2.6 Mutants carrying a paternal *H19^{ICR-8nrCG}* allele have normal weights and *Igf2* expression. (A) Graph representing weights (orange bars) of heterozygous (+/8nrCG) and wild type littermates. Each graph represents a different litter. (B) qRT-PCR analysis of *Igf2* (blue bars) using neonatal liver cDNA from heterozygous (+/8nrCG) or wild type littermates (+/+). *Igf2* expression was normalized to *Rplp0*. Number of samples analyzed (N) is indicated above the graph. Error bars represent standard deviations.

derepression of paternal *H19* in the mutants followed the temporal and spatial pattern of total *H19* expression. *H19* is first detected in E3.5 trophectoderm and is not detectable in the embryo proper until E8.5 (Poirier et al., 1991). Levels steadily increase and peak in neonatal liver at about 3 days after birth where levels remain high until about day 9 when expression decreases to very low/basal levels by day 28 after birth (Pachnis et al., 1988).

Allele-specific *H19* expression was analyzed in the same tissue, liver, throughout development. Aberrant paternal *H19* expression levels in the 8nrCG mutant livers were highest in neonatal liver (figure 2.7), when total *H19* expression is at its highest (Pachnis et al., 1988). Derepression of paternal *H19* in the mutants was moderate in E13.5 liver and undetectable in liver from 4 week old mice (Figure 2.7), again corresponding with total *H19* levels (Pachnis et al., 1988). These data suggest that aberrant paternal expression detected from the *H19*^{ICR-8nrCG} allele is under the same temporal regulation as wild type *H19* expression rather than a novel regulatory mechanism created by the mutations.

In addition to analyzing derepression of *H19* throughout development, allele-specific *H19* expression in embryonic versus extraembryonic tissues at the same time point, E13.5, was examined (Figure 2.7). Paternal *H19* expression was detected in yolk sac, placenta and embryo, though derepression of paternal *H19* was more variable in extra-embryonic tissues than embryonic (Figure 2.7). These data confirm that the aberrant paternal expression from the *H19*^{ICR-8nrCG} allele correlates with the spatially restricted expression pattern of *H19*.

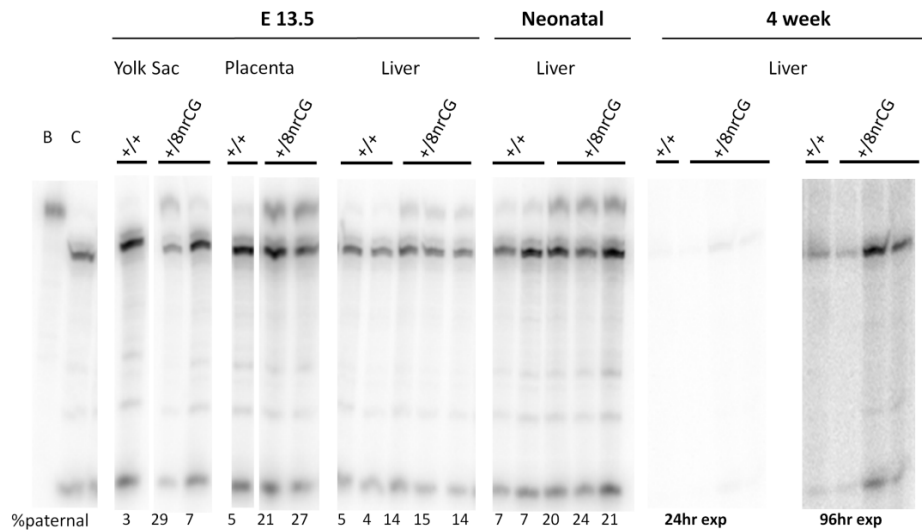


Figure 2.7 Aberrant paternal *H19* expression throughout development in *8nrCG* mutants. Allele-specific RNase protection assay was performed on RNA from tissues and time points indicated. RNA was collected from either F1 hybrid mutants carrying a paternal *H19*^{ICR-8nrCG} allele (+/8nrCG) or wild type littermates (+/+). Control B6 and C7 bands are indicated. The percent paternal *H19* expression is shown under the panels. Assay for 4 week liver is shown at normal (24 hour) exposure and overexposure (96 hours) due to low levels of expression in this tissue.

2.4 The paternal $H19^{ICR-8nrCG}$ allele remains hypermethylated despite paternal $H19$ expression

Expression of paternal $H19$ is often indicative of a loss of methylation at the paternal allele (Engel et al., 2004; Thorvaldsen et al., 1998). Therefore methylation at the mutant paternal ICR in neonatal liver, the tissue in which aberrant paternal $H19$ expression was at its highest, was assessed. Bisulfite sequencing throughout the ICR indicated that the mutant ICR maintained its hypermethylated status as compared to wild type littermates (figure 2.8A). Hypermethylation at the 8nrCG mutant ICR in neonatal liver was confirmed using non-allelic high throughput pyrosequencing. Methylation levels of the 8nrCG mutants were indistinguishable from their wild type littermates (figure 2.8B). In order to determine if methylation was properly established at the $H19^{ICR-8nrCG}$ allele, mature sperm was analyzed. Bisulfite sequencing analysis revealed that sperm from 8nrCG mutant mice properly established methylation at the mutant ICR (figure 2.8A).

It is possible that while the mutant ICR remained hypermethylated, spreading of methylation to the $H19$ promoter was disrupted, thus allowing aberrant paternal $H19$ expression. I therefore assessed methylation at the paternal $H19$ promoter proximal region by bisulfite sequencing (figure 2.9A) and the promoter by methylation sensitive restriction digestion and southern analysis (figure 2.9B). Interestingly, no loss of methylation was detected at the $H19^{ICR-8nrCG}$ allele as compared to wild type littermates. These data indicate an uncoupling of transcription and methylation, as aberrant $H19$ expression is detected from the mutant $H19^{ICR-8nrCG}$ allele despite maintaining full

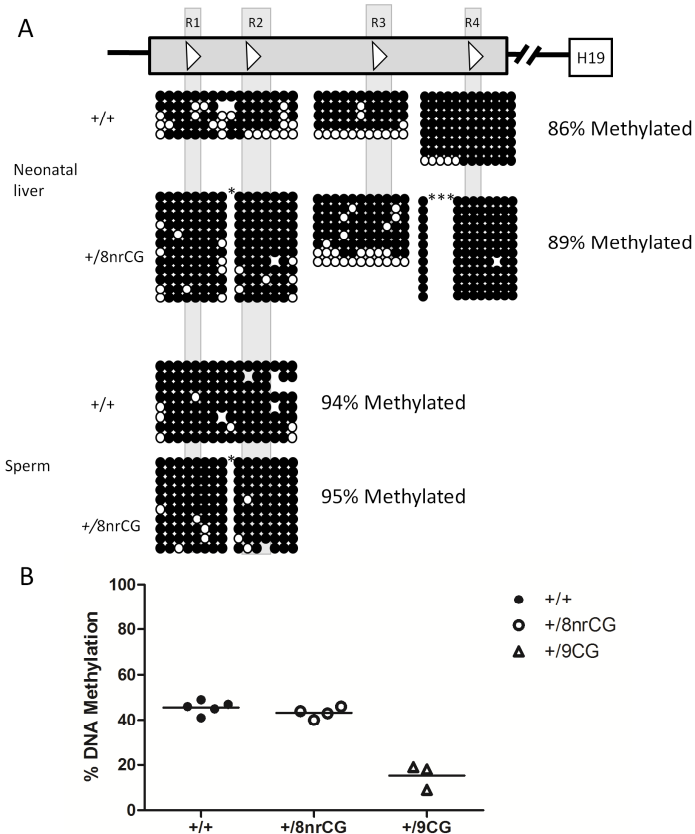


Figure 2.8 Hypermethylation throughout the paternal 8nrCG mutant ICR. (A) Schematic of the *H19* ICR. CTCF sites (triangles, R1–R4) at the ICR (horizontal grey rectangle) are depicted. Illustrated below is the methylation status of the mutant paternal *H19*^{ICR-8nrCG} and wild type paternal alleles as determined by bisulfite mutagenesis and sequencing performed with neonatal liver and mature sperm. Open and closed circles denote unmethylated and methylated cytosines, respectively, along a single horizontal strand of cloned DNA. Absent circles indicate undetermined sequence and asterisks (*) denote sequence mutated in the mutant allele. Shaded rectangles overlay cytosines assayed in CTCF sites. (B) Pyrosequencing was performed on bisulfite treated DNA from neonatal liver. Heterozygous 8nrCG mutants (+/8nrCG, open circles) were compared to wild type littermates (+/+, closed circles) as well as heterozygous 9CG mutants (+/9CG, open triangles) known to have a hypomethylated paternal ICR (Engel et al., 2004). Each circle or triangle represents an individual sample with the mean indicated by a horizontal black bar.

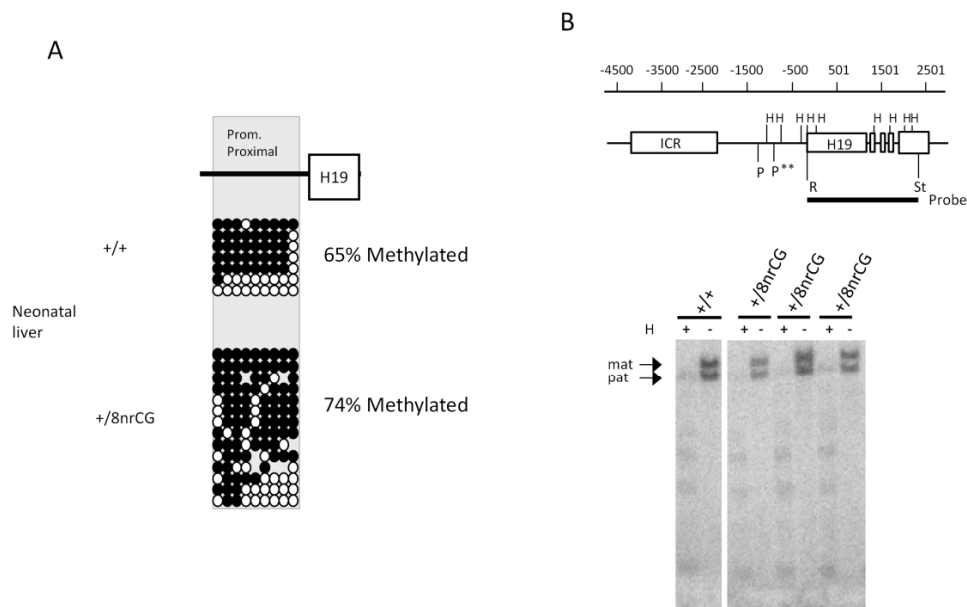


Figure 2.9 Hypermethylation at the promoter region of the paternal *H19*^{ICR-8nrCG} allele. (A) Schematic of the *H19* promoter proximal region. Illustrated below is the methylation status of the mutant *H19*^{ICR-8nrCG} and wild type paternal alleles as determined by bisulfite mutagenesis and sequencing performed with neonatal liver. Open and closed circles denote unmethylated and methylated cytosines, respectively, along a single horizontal strand of cloned DNA. Absent circles indicate undetermined sequence. Shaded rectangles overlay cytosines assayed the promoter proximal region. (B) Schematic of the *H19* region analyzed by methylation sensitive restriction digest and Southern blot. The position (in base pairs) relative to the start of transcription is depicted above. Illustrated are: the endogenous *H19* transcription unit and ICR (rectangles); *HpaII* (H) restriction sites; the polymorphic *PvuII* (P) site denoted by asterisks (**); and the probe used (bold line below *H19* transcription unit) - *EcoRI* (R) to *StuI* (St). Illustrated below, parental alleles were differentiated by digesting genomic DNA from neonatal liver with *PvuII*, *StuI* and *HpaII* (+) or with only *PvuII* and *StuI* (-). Genotypes of the sample and the presence (+) or absence (-) of *HpaII* (H) is marked above the panels. The maternal (mat) CAST allele is 3.4kb and the paternal (pat) B6 allele is 3.2kb.

methylation at the remaining CpGs. Therefore, decreasing the number of CpGs at the *H19* ICR by 8 (~16% depletion) rendered it unable to fully repress paternal *H19* expression even though the ability to maintain methylation remained intact.

2.5 Normal imprinting when the *H19*^{ICR-8nrCG} allele was maternally inherited

The effects of the 8nrCG mutation on the maternal allele were also assessed. Normal monoallelic *Igf2* expression was detected by RT-PCR (Figure 2.10A). Additionally, bisulfite sequencing analysis indicated that the maternal *H19*^{ICR-8nrCG} allele was properly hypomethylated in neonatal liver as compared to wild type littermates (figure 2.10B). These data suggest that maternal inheritance of the mutant allele does not disrupt imprinting at the *H19/Igf2* locus and that mutant phenotypes detected were specific to the paternal allele.

2.6 An *in vitro* repressor assay to assess contribution of methylation at the ICR on repression of a reporter gene

Although paternal *H19* expression from the mutant *H19*^{ICR-8nrCG} allele was clearly detected, it remains unclear if there is a specific CpG density necessary at the ICR for full repression of *H19*. In other words, is there a certain threshold of CpGs necessary for full repression or is repression additive, such that the level of repression is dependent on the amount of methylation? This question is difficult to assess at the endogenous locus as methylation at the *H19* promoter could mask subtle effects of the ICR. Additionally, multiple targeted mouse mutants would be costly. I therefore set up an *in vitro* system to quantify repression from the *H19* ICR. This system would allow easy assessment of various mutant ICR fragments in which differing amounts of CpGs had been mutated.

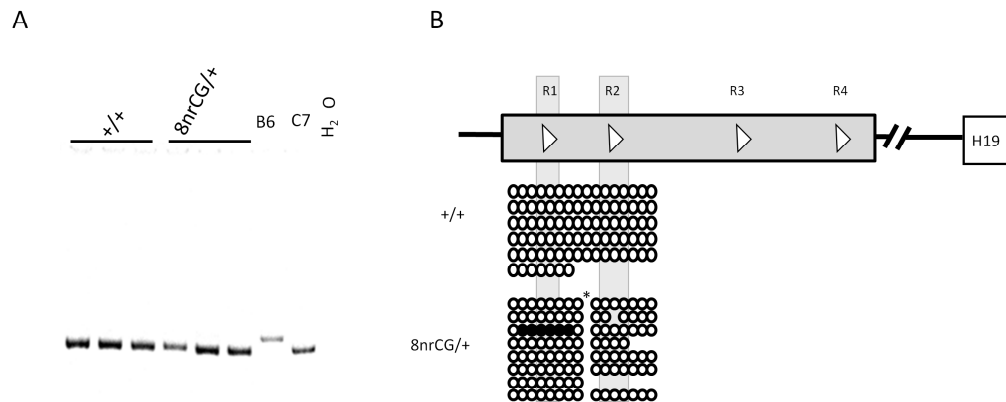


Figure 2.10 Imprinting analyses of the maternally inherited $H19^{ICR-8nrCG}$ allele. (A) Allele specific *Igf2* expression was analyzed by RT-PCR using neonatal liver cDNA from F1 hybrid mutants that inherited the $H19^{ICR-8nrCG}$ allele ($8nrCG/+$) maternally or wild type littermates ($+/+$). B6 and C7 controls are indicated. (B) Schematic of the *H19* ICR (above, not drawn to scale). CTCF sites (triangles, R1 –R4) at the ICR (horizontal grey rectangle) are depicted. Illustrated below is the methylation status of the mutant maternal $H19^{ICR-8nrCG}$ alleles and wild type maternal alleles as determined by bisulfite mutagenesis and sequencing performed with neonatal liver DNA. Open and closed circles denote unmethylated and methylated cytosines, respectively, along a single horizontal strand of cloned DNA. Absent circles indicate undetermined sequence and asterisks (*) denote sequence mutated in the mutant allele. Shaded rectangles overlay cytosines assayed in CTCF sites.

To quantify repression from the *H19* ICR, I set up a reporter system based on that used in Chen et al., 2008. To measure methylation dependent repression by the *H19* ICR, a reporter plasmid that has been depleted of CpGs (pCpGvitro-neo-lacZ, Invivogen) was used. Using a CpG-depleted reporter plasmid ensured that any repression measured was due to methylation at the ICR and not from elsewhere on the plasmid. This plasmid contains: a mouse CMV enhancer and human elongation factor 1 α driving expression of LacZ, an SV40 promoter to drive expression of *neo^r* and matrix attachment regions to form barriers between independent expression cassettes, all of which have been mutated such that there are no CpGs. Two different reporter plasmids to measure repression by the *H19* ICR were constructed; (1) a 1.8kb ICR fragment (spanning from *AatII* to *XhoI*) was cloned upstream of the CMV enhancer driving *LacZ* expression (CpGfree1) (Figure 2.11A) and (2) a 1.8kb ICR fragment (spanning from *AatII* to *XhoI*) replaced the CMV enhancer (CpGfree3) (figure 2.12A). β -Galactosidase (β -Gal) activity could then be compared between methylated and unmethylated plasmids to quantify repression by methylation at the ICR. CpGfree3 is almost identical to the reporter used in (Chen et al., 2008) except they used an *NcoI-BamHI* ICR fragment.

I first used the CpGfree1 reporter vector for my analysis, as this construct is most similar to the endogenous *H19* locus where enhancers are present to drive expression. The wild type (CpGfree1-wt) and 8nrCG (CpGfree1-8nrCG) ICR fragments were cloned upstream of the CMV enhancer. These plasmids were then either methylated or left unmethylated using the CpG methylase *M.SssI*. These constructs were transfected into Hep3b or F9 cells. Hep3b cells highly express *H19* and have been used previously to

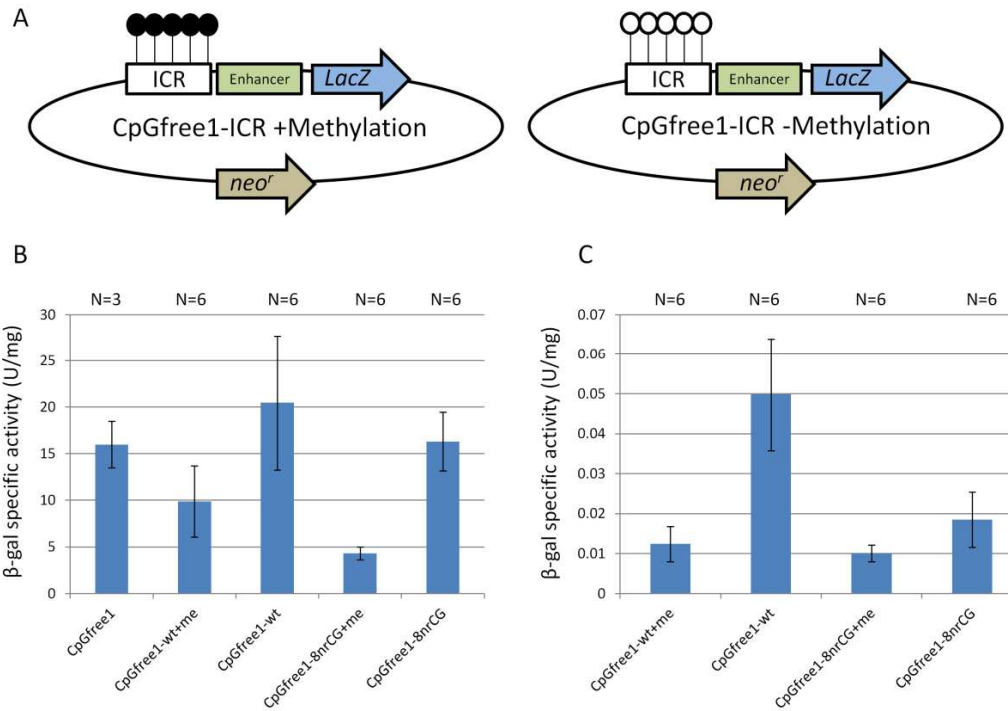


Figure 2.11 CpGfree1 repression assay. (A) Depiction of the CpGfree1 reporter plasmid with either a methylated (filled lollipops) or unmethylated (open lollipops) ICR fragment (white box) upstream of the CMV enhancer (green box), which drives LacZ expression (blue arrow). Also on the plasmid is *neo^r* (brown arrow), which allows selection for stable integration of the reporter plasmid. (B-C) Constructs containing either wild type (CpGfree1-wt) or 8nrCG (CpGfree1-8nrCG) fragments were methylated (+me) or left unmethylated and stably transfected into Hep3b (B) or F9 (C) cells. β -Gal activity was measured and normalized to total protein concentrations. Number of biological replicates performed for each construct is indicated above (N). Error bars represent standard deviations.

identify elements regulating *H19* expression (Hark et al., 2000; Holmgren et al., 2001). F9 cells do not express *H19*, and thus likely express repressors required for *H19* silencing. F9 cells were also used in Chen et al., 2008. Cells were stably transfected and β -Gal activity was assessed after ~10-14 days in selection. Significant decreases in β -Gal activity were detected from the methylated plasmids versus the unmethylated plasmids for both CpGfree1-wt and CpGfree1-8nrCG (P value < .05) in both cell lines (figure 2.11 B-C). However, loss of repression in *LacZ* expression with the methylated CpGfree-8nrCG versus the methylated CpGfree1-wt plasmids was not detected. This was surprising, as the assay did not mimic what had been seen *in vivo* where paternal *H19* was derepressed when the 8nrCG mutation was paternally inherited (Ideraabdullah et al., 2011). One possibility as to why derepression was not detected was that the strength of the CMV enhancer would not allow detection of subtle changes in repression.

Next, repression using the CpGfree3 reporter plasmids, where the wild type or 8nrCG ICR fragments replaced the CMV enhancer, were analyzed. The human elongation factor 1 α remained in place and still drove high levels of *LacZ* expression. Here, analysis was limited to F9 cells. Similar to the studies using the CpGfree1 reporters, the CpGfree3 plasmids containing either the wild type ICR fragment (CpGfree3-wt) or the 8nrCG mutant ICR fragment (CpGfree3-8nrCG) was methylated or left unmethylated. These reporter plasmids were stably transfected into F9 cells. β -Gal activity was assessed ~10-14 days after selection. Again, methylated CpGfree3-wt and CpGfree3-8nrCG reporters had decreased β -Gal activity as compared to unmethylated reporters (P value < .05) (figure 2.11B). However, I did not detect derepression of the

methylated CpGfree3-8nrCG reporter as compared to the CpGfree3-wt (figure 2.11B). Because this reporter plasmid was most similar to that used in Chen et al. 2008, analysis of the 9CG mutant ICR fragment (CpGfree3-9CG) was included. Using the same reporter system, Chen et al., 2008 reported that CpGs within CTCF sites are necessary for silencing the reporter gene. I therefore wanted to replicate their findings using a mutant ICR that mutated CpGs at CTCF sites. Again, I was unable to detect any derepression of *LacZ* expression with the methylated CpGfree3-9CG as compared to CpGfree3-wt (figure 2.12C). Because I was unable to reproduce the results reported in Chen et al., 2008 and the methylated mutant ICR plasmids (CpGfree3-8nrCG and CpGfree3-9CG) did not mimic the derepression of endogenous paternal *H19* as described in mutant mice (Engel et al., 2004; Ideraabdullah et al., 2011), I decided not to proceed forward with this assay.

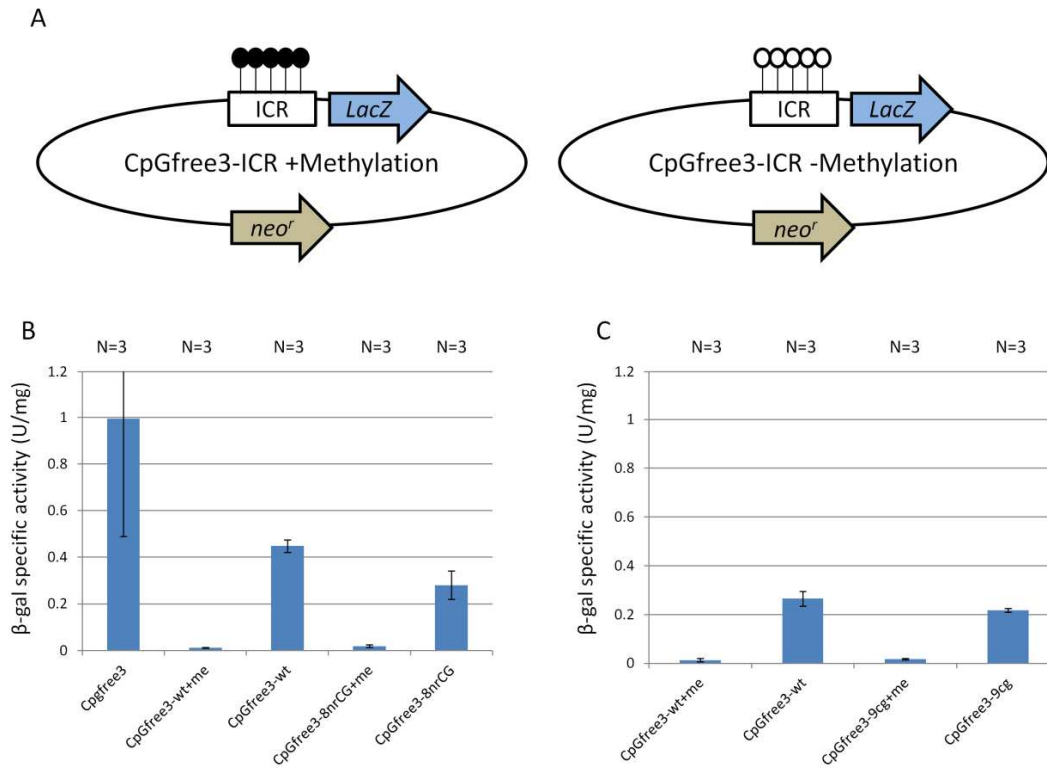


Figure 2.12 CpGfree3 repression assay. (A) Depiction of the CpGfree3 reporter plasmid with either a methylated (filled lollipops) or unmethylated (open lollipops) ICR fragment (white box) upstream of *LacZ* (blue arrow). Also on the plasmid is *neo^r* (brown arrow), which allows selection for stable integration of the reporter plasmid. (B-C) Constructs containing either wild type (CpGfree3-wt), 8nrCG (CpGfree3-8nrCG) or 9CG (CpGfree3-9CG) fragments were methylated (+me) or left unmethylated and stably transfected into F9 cells. β-Gal activity was measured and normalized to total protein concentrations. 3 biological replicates were performed for each construct (N). Error bars represent standard deviations.

CHAPTER THREE

THE ROLE OF METHYL-CPG-BINDING DOMAIN PROTEINS IN IMPRINTED GENE REPRESSION

Although it is clear that differential DNA methylation is necessary for marking parental alleles and regulating imprinted expression, *trans*-acting factors that are involved in conferring allelic repression remain unknown. Methyl-CpG-binding domain (MBD) proteins, which bind methylated DNA (Hendrich and Bird, 1998) and recruit repressive complexes (Bogdanović and Veenstra, 2009), are ideal candidates for interpreting allele-specific DNA methylation at imprinted loci and silencing the proper allele.

Previous studies have been unable to define a role for MBD proteins in genomic imprinting. Allele-specific analysis of imprinted genes in *Mbd2*^{-/-} adult mouse spleen, heart and brain as well as *Mecp2*^{-y} adult mouse brain showed normal imprinting (Hendrich, 2001; Samaco et al., 2005). However, many imprinted genes are involved in fetal growth and development with undetectable or very low levels of expression in adult tissues (Figure 3.1) (Pachnis et al., 1988; Poirier et al., 1991). Thus, it is possible that mechanisms for allele-specific repression may be different and more reliant on MBD proteins in tissues where imprinted genes are robustly expressed, as they are throughout embryogenesis. I therefore hypothesized that MBD proteins play a role in genomic imprinting specifically in tissues where imprinted genes are robustly expressed.

In support of this hypothesis, MECP2, MBD1, MBD2 and MBD3 have been shown to bind to imprinted loci by ChIP analysis (Fournier et al., 2002; Gregory et al.,

2001; Kernohan et al., 2010; Lu et al., 2006; Reese et al., 2007; Samaco et al., 2005). Additionally, depletion of NuRD complex (which contains MBD2) components, MBD3 (Reese et al., 2007) or MTA-2 (Ma et al., 2010), in mouse blastocysts caused loss of imprinting of *H19* (Ma et al., 2010; Reese et al., 2007) and *Peg3* (Ma et al., 2010). Furthermore, deregulation of *GNAS*, *IGF2* and *UBE3A* has been reported in Rett Syndrome patient lymphocytes and postmortem brains (Ballestar et al., 2005; Makedonski et al., 2005; Samaco et al., 2005).

To test my hypothesis, I analyzed allele-specific expression of imprinted genes in *Mbd1*^{-/-} or *Mbd2*^{-/-} E9.5-10.5 embryos, placentas, yolk sacs, and neonatal brains. Functional redundancy among the MBD proteins was assessed by employing cell culture systems in which siRNA and shRNA constructs were used to deplete trophoblast stem (TS) cells or mouse embryonic fibroblasts (MEFs) of MBD proteins. I have been unable to uncover a role for single MBD proteins in genomic imprinting, however, these proteins may be highly redundant.

3.1 Experimental design

To study the effects of loss of MBD1 or MBD2 on genomic imprinting I analyzed previously published mouse mutants (Hendrich, 2001; Zhao et al., 2003). *In vivo* studies focused on MBD1 and MBD2 because these proteins are least characterized at imprinted loci. The mutations were bred onto two strain backgrounds; B6 and C7. To ensure a CAST chromosome 7 (C7), 14 MIT markers spanning chromosome 7 were assayed. Heterozygous mutant mice on each strain (B6 or C7) were crossed to generate F1 hybrids

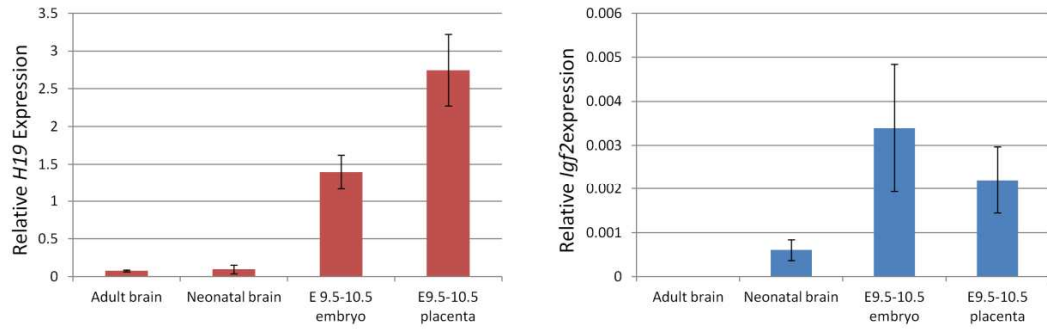


Figure 3.1 Expression of *H19* and *Igf2* in tissues used in the MBD study. qRT-PCR was performed on cDNA derived from adult brain (4 week), neonatal brain (day 0-4), E9.5-10.5 embryo and placenta to assay (A) *H19* (red bars) or (B) *Igf2* expression (blue bars). Expression levels were normalized to the geometric mean of *Rplp0* and *Gapdh*. Three individual mice were used for each tissue indicated. Error bars represent standard deviations.

for analysis. SNPs between the two strains of mice allowed assessment of allele-specific expression of imprinted genes along chromosome 7 (Weaver et al., 2010).

Because I was interested in defining a role for these proteins in genomic imprinting, tissues that very highly express imprinted genes; E9.5-10.5 embryos, placentas, and yolk sacs (figure 3.2A, 3.3A) were examined. Additionally, analysis in neonatal brain was included, as many imprinted genes are expressed in this tissue and MBD mutant phenotypes manifest most prominently in the brain. Although expression of *Mbd1* and *Mbd2* is highest in adult brain in wild type mice, transcripts are detectable in all the tissues analyzed (figure 3.2B, 3.3B). MBD1 protein is also detectable in E9.5 embryo and placenta (figure 3.2C). Unfortunately, there are no available reliable antibodies against MBD2 to measure protein.

3.2 Normal imprinting in *Mbd1* mutant mice

MBD1 has been reported to bind at imprinted genes (Fournier et al., 2002), however, imprinting analysis of *Mbd1* mutant mice had not been reported. B6 or C7 female *Mbd1*^{+/-} mice were mated with male *Mbd1*^{+/-} mice of the opposite strain. Five litters of F1 hybrid E9.5-10.5 embryos, placentas and yolk sacs were collected for imprinting analysis. I conducted allele-specific RT-PCR assays on paternally expressed *Snrpn*, *Peg3*, *Kcnq1ot1*, and *Igf2*, as well as maternally expressed *Zim1*, *Cdkn1c*, *H19*, *Kcnq1* in all tissues collected at this time point. Additionally, the maternally expressed gene *Ascl2* was analyzed in the placenta, as this gene exhibits placenta-specific expression. Normally, the level of RNA detected from the repressed allele is less than

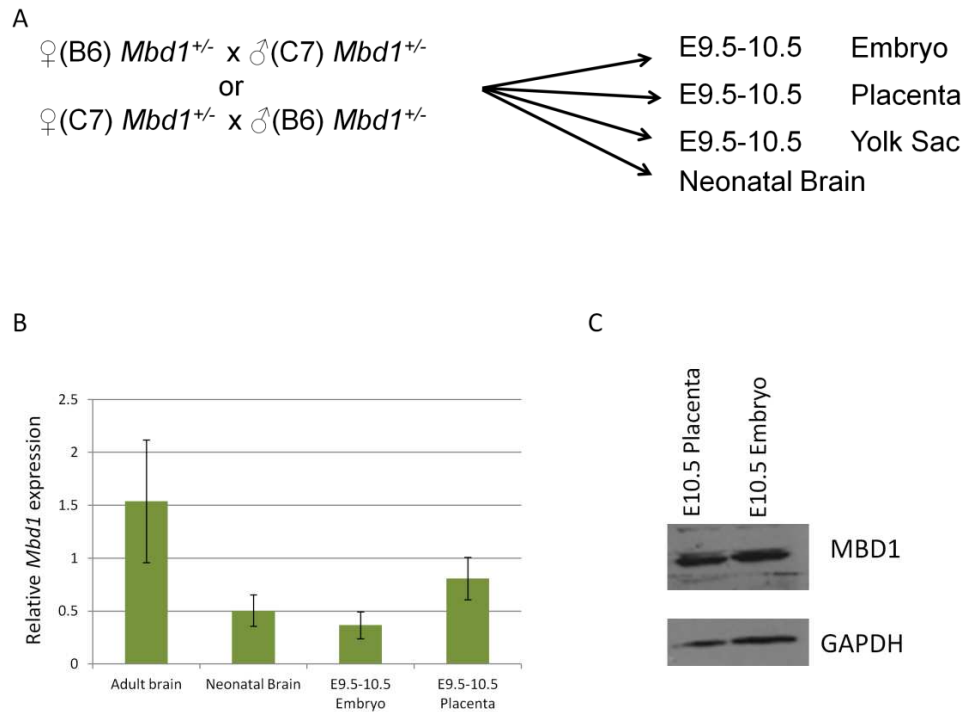


Figure 3.2 Experimental design and expression of *Mbd1* in wild type tissues. (A) Breeding scheme and tissues of offspring collected for analysis. Note that the female parent is written first in the crosses. (B) qRT-PCR analysis of *Mbd1* using cDNA prepared from wild type adult brains (4 weeks), neonatal brains (day 0-4), E9.5-10.5 embryos and placentas. Expression was normalized to the geometric mean of *Rplp0* and *Gapdh*. Tissues from three individual mice were used. Error bars represent standard deviations. (C) Western blot with antibodies against MBD1 or GAPDH. Protein lysates were prepared from E10.5 embryo and placenta.

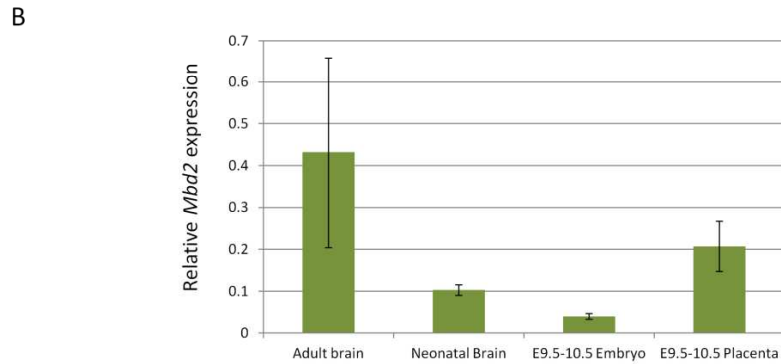
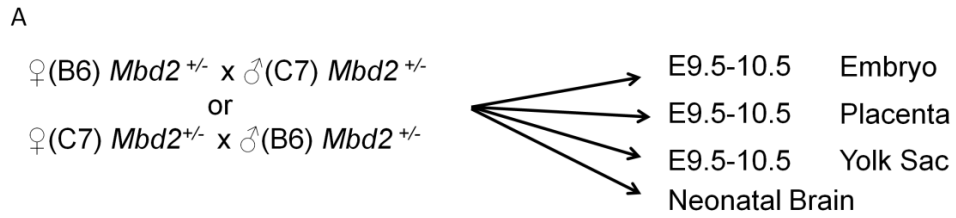


Figure 3.3 Experimental design and expression of *Mbd2* in wild type tissues. (A) Breeding scheme and tissues of offspring collected for analysis. Note that the female parent is written first in the crosses. (B) qRT-PCR analysis of *Mbd2* using cDNA prepared from wild type adult brains (4 weeks), neonatal brains (day 0-4), E9.5-10.5 embryos and placentas. Expression was normalized to the geometric mean of *Rplp0* and *Gapdh*. Tissues from three individual mice were used. Error bars represent standard deviations.

10% of total expression (though higher levels can be detected in placenta). To control for this, expression levels of mutants were compared to wild type littermates. Imprinting was maintained in 4 *Mbd1*^{-/-} E9.5-10.5 tissues when compared to 16 *Mbd1*^{+/-} and 12 wild type littermates (table 3.1) (P value > .05 in all cases). Because MBD1 was reported to play a role in brain function, neonatal brain was also tested for loss of imprinting. Here, analysis was performed on the same genes as the E9.5-10.5 litters except for *Igf2* (not imprinted in the brain), *Kcnq1* (not expressed in this tissue) and *Ascl2* (not expressed in this tissue). Allele-specific expression was assessed using cDNA from neonatal brains from 4 litters containing 5 *Mbd1*^{-/-} and compared to 7 *Mbd1*^{+/-} and 9 wild type littermates. Normal imprinting was detected in all neonatal brain samples (table 3.1) (P value > .05 in all cases). I therefore conclude that MBD1 alone is not required for allele-specific repression at imprinted loci.

3.3 Normal imprinting in *Mbd2* mutant mice

Next, analysis was extended to *Mbd2* mutant mice. *Mbd2* null mice exhibit phenotypes most similar to mice harboring a mutation for the imprinted gene *Peg3* (Hendrich, 2001; Lefebvre et al., 1998; Li et al., 1999). Moreover, MBD2 has been reported bound to *Peg3* in cyclophilin A knockdown P9 cells (Lu et al., 2006). However, early studies of *Mbd2* null mice identified normal imprinting in adult brain, heart and spleen (Hendrich, 2001). Similar to the *Mbd1* mutant analysis, either B6 or C7 *Mbd2*^{+/-} females were mated with *Mbd2*^{+/-} males of the opposite strain. Again imprinting at paternally expressed *Snrpn*, *Peg3*, *Kcnqlot1*, and *Igf2*, as well as maternally expressed

Table 3.1 Allele-specific expression analysis of imprinted genes in F1 hybrid *Mbd1* mutant samples

	E9.5-10.5									Neonatal		
	Embryo			Placenta			Yolk Sac			Brain		
	+/+	+/-	-/-	+/+	+/-	-/-	+/+	+/-	-/-	+/+	+/-	-/-
<i>Surpn</i>	0.0±0	0.0±0	0.0±0	0.0±0	0.0±0	0.0±0	0.0±0	0.0±0	0.0±0	0.0±0	0.0±0	0.0±0
<i>Peg3</i>	0.0±0	0.0±0	0.0±0	0.0±0	0.0±0	0.0±0	0.0±0	0.0±0	0.0±0	0.0±0	0.0±0	0.0±0
<i>Zim1</i>	0.0±0	0.0±0	0.0±0	0.0±0	0.0±0	0.0±0	0.0±0	0.0±0	0.0±0	0.0±0	0.0±0	0.0±0
<i>Kcnq1ot1</i>	0.0±0	0.0±0	0.0±0	8.9±11.3	14.8±20	8.3±14.4	0.0±0	0.0±0	0.0±0	0.0±0	0.0±0	0.0±0
<i>Cdkn1c</i>	0.0±0	0.7±1.0	2.2±2.5	4.4±5.8	7.3±6.3	6.4±6.7	0.0±0	0.0±0	1.0±2.0	.8±2.4	0.0±0	0.0±0
<i>H19</i>	0.0±0	0.0±0	0.0±0	6.4±11.6	4.0±4.1	1.6±2.0	0.0±0	0.0±0	0.0±0	0.0±0	0.0±0	0.0±0
<i>Igf2</i>	0.0±0	0.0±0	0.0±0	0.0±0	0.0±0	0.0±0	0.0±0	0.0±0	0.0±0	NI	NI	NI
<i>Kcnq1</i>	0.0±0	0.0±0	0.0±0	0.0±0	0.0±0	0.0±0	0.0±0	0.0±0	0.0±0	NE	NE	NE
<i>Ascl2</i>	NE	NE	NE	1.4±2.7	2.6±8.6	1.0±1.7	NE	NE	NE	NE	NE	NE

Percent total expression from the normally repressed allele with standard deviations is indicated for each respective tissue and genotype. Maternally expressed genes are designated in red. Paternally expressed genes are designated in blue.

Mbd1^{+/+} (+/+): N=12 for E9.5-10.5 tissues and 9 for neonatal brain.

Mbd1^{+/-} (+/-): N=16 for E9.5-10.5 tissues and 7 for neonatal brain.

Mbd1^{-/-} (-/-): N=4 for E9.5-10.5 tissues and 5 for neonatal brain.

NE not expressed in this tissue.

NI not imprinted in this tissue.

Zim1, *Cdkn1c*, *H19*, *Kcnq1* and *Ascl2* were assessed. Allele-specific RT-PCR analysis performed on cDNA from E9.5-10.5 embryos, placentas and yolk sacs from 2 F1 hybrid litters did not detect any loss of imprinting in the 6 *Mbd2*^{-/-} tissues as compared to 7 *Mbd2*^{+/-} and 2 wild type littermates (table 3.2) (P value > .05). Similarly, normal imprinting was observed in neonatal brains collected from 3 litters with 4 *Mbd2*^{-/-} as compared to 10 *Mbd2*^{+/-} and 3 wild type littermates (table 3.2) (P value > .05). Because previously published studies most implicated MBD2 in the regulation of *Peg3* expression, analysis of the *Peg3* DMR in *Mbd2* mutants was performed. High throughput pyrosequencing on bisulfite mutagenized DNA from neonatal brains indicated that methylation levels of the *Peg3* DMR in *Mbd2* null mutants were indistinguishable from heterozygous and wild type littermates (~45% methylation) (figure 3.4). Therefore, I conclude that MBD2 is dispensable for allele-specific repression at imprinted loci.

3.4 Loss of MBD1 or MBD2 is not compensated by upregulation of transcripts from other MBD proteins

There are multiple MBD family proteins involved in DNA methylation dependent repression. Thus, it is possible that the lack of imprinting phenotypes in the *Mbd1* and *Mbd2* mutant mice were due to compensation by the other MBD proteins. One way compensation can occur is through transcriptional upregulation of the other MBD proteins in the mutants. To test this, I analyzed expression of *Mbd2* and *Mecp2* in *Mbd1* mutant embryos by qRT-PCR, but was unable to detect increased expression (figure 3.5A). Similarly, *Mbd2* mutant embryos also did not upregulate *Mecp2* or *Mbd1* (figure 3.5B). However, these results do not rule out the possibilities that the other MBD

Table 3.2 Allele-specific expression analysis of imprinted genes in F1 hybrid *Mbd2* mutant samples

	E9.5-10.5									Neonatal		
	Embryo			Placenta			Yolk Sac			Brain		
	+/+	+/-	-/-	+/+	+/-	-/-	+/+	+/-	-/-	+/+	+/-	-/-
<i>Snrpn</i>	0.0	0.0±0	0.0±0	0.0	0.0±0	0.0±0	0.0	0.0±0	0.0±0	0.0±0	0.0±0	0.0±0
<i>Peg3</i>	0.0	0.0±0	0.0±0	0.0	0.0±0	0.0±0	0.0	0.0±0	0.0±0	0.0±0	0.0±0	0.0±0
<i>Zim1</i>	0.0	0.0±0	0.0±0	0.0	0.0±0	0.0±0	0.0	0.0±0	0.0±0	0.0±0	0.0±0	0.0±0
<i>Kcnq1ot1</i>	0.0	0.0±0	0.0±0	0.0	5.7±11.3	0.0±0	0.0	0.0±0	0.0±0	0.0±0	0.0±0	0.0±0
<i>Cdkn1c</i>	0.0	0.0±0	0.0±0	14.4	8.0±3.5	13.9±4.4	0.0	0.0±0	0.0±0	0.0±0	0.0±0	0.0±0
<i>H19</i>	0.0	0.0±0	0.0±0	0.0	0.0±0	0.0±0	0.0	0.0±0	0.0±0	0.0±0	0.0±0	0.0±0
<i>Igf2</i>	0.0	0.0±0	0.0±0	6.8	3.5±6.4	6.5±5.5	0.0	0.0±0	0.0±0	NI	NI	NI
<i>Kcnq1</i>	0.0	0.0±0	0.0±0	0.0	0.0±0	0.0±0	0.0	0.0±0	0.0±0	NE	NE	NE
<i>Ascl2</i>	NE	NE	NE	0.0	0.0±0	0.0±0	NE	NE	NE	NE	NE	NE

Percent total expression from the normally repressed allele with standard deviations is indicated for each respective tissue and genotype. Maternally expressed genes are designated in red. Paternally expressed genes are designated in blue.

Mbd2^{+/+} (+/+): N=2 for E9.5-10.5 tissues and 3 for neonatal brain.

Mbd2^{+/-} (+/-): N=7 for E9.5-10.5 tissues and 10 for neonatal brain.

Mbd2^{-/-} (-/-): N=6 for E9.5-10.5 tissues and 4 for neonatal brain.

NE not expressed in this tissue.

NI not imprinted in this tissue.

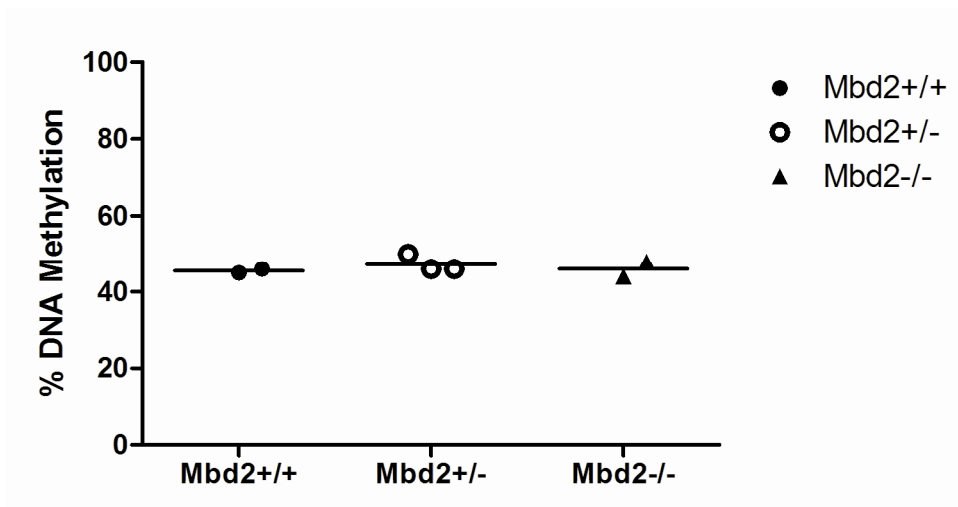


Figure 3.4 Normal Methylation at the *Peg3* DMR in *Mbd2* mutants. Methylation levels at the *Peg3* DMR were determined by pyrosequencing. Bisulfite mutagenized DNA from neonatal brain was analyzed from the genotypes indicated. Each circle or triangle represents an individual sample with the mean indicated by a black horizontal bar.

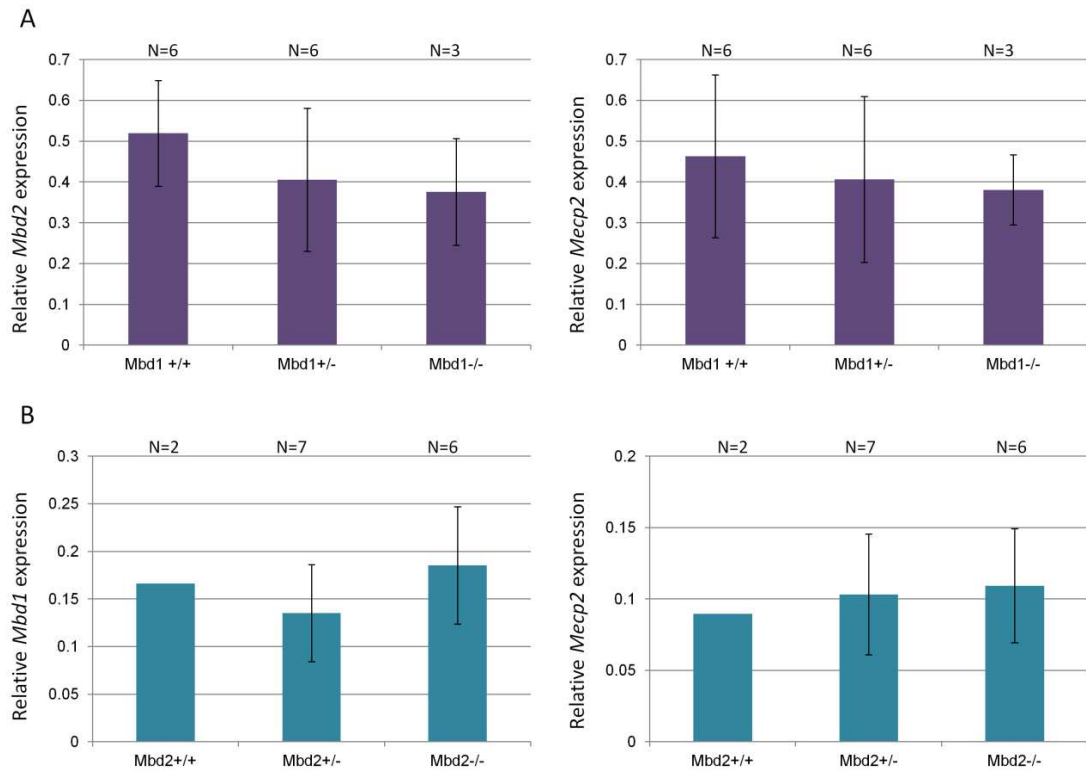


Figure 3.5 Expression of other MBD family members in *Mbd1* and *Mbd2* mutant embryos. (A) Expression levels of *Mbd2* and *Mecp2* in *Mbd1*^{+/+}, *Mbd1*^{+/-} and *Mbd1*^{-/-} E9.5-10.5 embryos (purple bars). Expression was normalized to the geometric mean of *Rplp0* and *Gapdh*. (B) Expression levels of *Mbd1* and *Mecp2* in *Mbd2*^{+/+}, *Mbd2*^{+/-} and *Mbd2*^{-/-} E9.5-10.5 embryos (blue bars). Expression was normalized to *Rplp0* and *Gapdh*. Number of individual samples analyzed is indicated (N). Error bars represent standard deviations.

proteins could be upregulated at the protein level, or that they have redundant function with overlapping binding sites, as has been recently reported (Baubec et al., 2013).

3.5 Assessing functional redundancy among the MBD proteins

To assess compensation and redundancy between MBD proteins I used cell culture systems in which MBD proteins were depleted by RNAi-based knockdown. Experiments were performed using F1 hybrid MEFs and TS cells. MEFs exhibit imprinted expression of many genes and have also been used in similar RNAi based experiments to identify factors involved in regulation of imprinting (Lin et al., 2011; Yao et al., 2010). TS cells exhibit imprinted expression of many genes with total expression of these genes being greater than in MEFs (Lin, 2011).

3.5.1 Transient siRNA depletion of MBD proteins in MEFs and TS cells

I first analyzed depletion of MBD proteins by transient siRNA experiments. siRNAs directed against *Mbd1* (siMbd1), *Mbd2* (siMbd2), *Mbd3* (siMbd3) and a control sequence that does not target any known transcripts in the mouse genome (siControl) were transfected into MEFs or TS cells. 48 hours after initial transfections another round of transfections with the siRNAs was performed. Cells were collected ~72 hours after initial transfection for analysis. I was unsuccessful at finding reliable antibodies against MBD2 or MBD3, and therefore could only measure levels of depletion of transcripts by qRT-PCR. Depletion of MBD1 was confirmed by western blot and ~89% depletion was detected in these cells (figure 3.6A). qRT-PCR indicated ~51% decrease in transcription of *Mbd2* (figure 3.6B), and ~63% decrease in transcription of *Mbd3* (figure 3.6C).

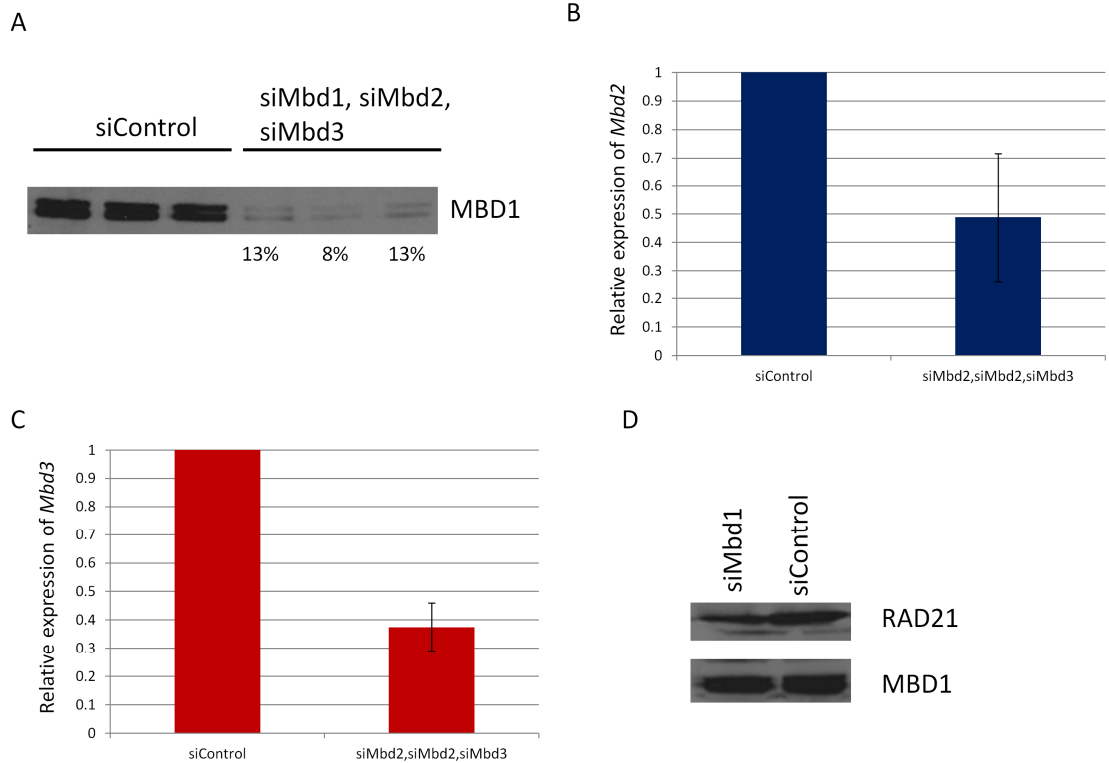


Figure 3.6 Depletion of MBD1, MBD2 and MBD3 in MEFs or TS cells. (A) Western blot to detect MBD1 in MEF lysates from cells transfected with siControl or MEF lysates from cells transfected with siMbd1, siMbd2, and siMbd3. Percent protein levels as compared to siControl cells is indicated below. (B-C) qRT-PCR to analyze (B) *Mbd2* (blue bars) or (C) *Mbd3* (red bars) expression was performed in siControl transfected and siMbd1, siMbd2 and siMbd3 transfected cells. *Mbd2* or *Mbd3* expression was normalized to *Rplp0*. Expression levels for *Mbd2* and *Mbd3* in the triple transfected cells are graphed relative to expression in siControls. Error bars represent standard deviations. Three biological replicates were used. (D) Western blot to detect MBD1 in TS cell lysates from cells transfected with siControl or lysates from TS cells transfected with siMbd1. RAD21 was used as a loading control.

Table 3.3 Allele-specific expression analysis of imprinted genes in F1 hybrid MEFS transiently depleted of MBD1, MBD2, MBD3 or MBD1, MBD2 and MBD3

	MEFS					
	WT	siControl	siMbd1	siMbd2	siMbd3	siMbd1, siMbd2, siMbd3
<i>Surpn</i>	0.0±0	0.0±0	0.0	0.0	0.0	0.0±0
<i>Peg3</i>	0.0±0	0.0±0	0.0	0.0	0.0	0.0±0
<i>Zim1</i>	0.0±0	0.0±0	0.0	0.0	0.0	0.0±0
<i>Kcnq1ot1</i>	0.0±0	0.0±0	0.0	0.0	0.0	0.0±0
<i>Cdkn1c</i>	0.0±0	0.0±0	0.0	0.0	0.0	0.0±0
<i>H19</i>	0.0±0	0.0±0	0.0	0.0	0.0	0.0±0
<i>Igf2</i>	0.0±0	0.0±0	0.0	0.0	0.0	0.0±0

Percent total expression from the normally repressed allele with standard deviations is indicated for each siRNA experiment. Maternally expressed genes are designated in red. Paternally expressed genes are designated in blue.

WT N=3

siControl: N=3

siMbd1: N=1

siMbd2: N=1

siMbd3: N=1

siMbd1,siMbd2,siMbd3: N=3

Allele-specific expression analysis performed on paternally expressed *Snrpn*, *Peg3*, *Kcnq1ot1*, and *Igf2*, as well as maternally expressed *Zim1*, *Cdkn1c* and *H19* indicated normal imprinting at all loci (table 3.3). For analysis in TS cells only the siRNA towards *Mbd1* was tested because the MBD1 antibody was the most reliable. Transfection efficiency (as determined using a fluorescent RNA) in TS cells was only ~10% (data not shown). Unsurprisingly, I was unable to deplete MBD1 in these cells (figure 3.6D).

3.5.2 Stable shRNA depletion of MBD proteins in *Mbd2*^{-/-} MEFs and TS cells

Because I was interested in defining transcriptional changes that resulted from a change in epigenetic landscape after depletion of MBD proteins (which could take longer than a transient assay would allow), I pursued stable depletion of these factors. Here, efforts were focused on MECP2, MBD1 and MBD2 as these are the three MBD proteins that both bind methylated DNA and repress transcription. Therefore, these proteins are most likely to exhibit redundant functions. The siRNA sequences against *Mbd1* and *Mbd2*, and a published sequence against *Mecp2* (Zhou et al., 2006) were converted into short hairpin sequences that were cloned into the PLKO.1 lentiviral vector (Addgene). F1 hybrid MEFs were prepared from F1 hybrid *Mbd2*^{-/-} embryos. This allowed experiments to be performed in cells that had no functional MBD2, and therefore no MBD2 antibody was necessary. shRNAs targeting a control sequence (shControl), *Mbd1* (shMbd1), *Mecp2* (shMecp2) or *Mbd1* and *Mecp2* were stably expressed in *Mbd2*^{-/-} MEFs. Cells were collected at ~7 days and 2 passages after initial infection, for protein and RNA analysis. On average, there was ~72% depletion of MECP2 (figure 3.7A,C) and ~84% depletion of MBD1 (figure 3.7B,C) as determined by western blot.

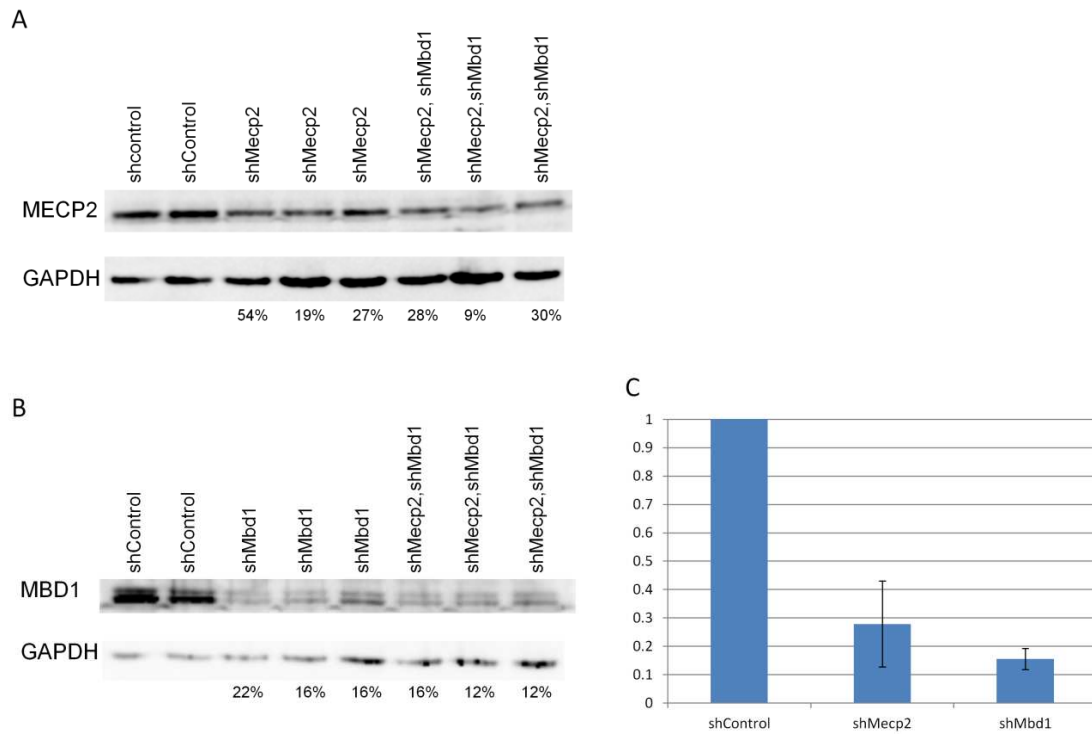


Figure 3.7 Stable depletion of MBD1 and MECP2 in *Mbd2*^{-/-} MEFs. (A-B) Western blot to detect (A) MECP2 or (B) MBD1 in *Mbd2*^{-/-} MEF lysates from cells expressing shControl, shMbd1, ShMecp2, or both shMecp2 and shMbd1 (as indicated). GAPDH was used as a loading control. Percent protein expression as compared to shControl is indicated. (C) Graphic representation of protein levels compared to shControl.

Table 3.4 Allele-specific expression analysis of imprinted genes in F1 hybrid *Mbd2*^{-/-} MEFs depleted of MBD1, MECP2 or MBD1 and MECP2

	MEFS				
	WT	<i>Mbd2</i> ^{-/-} ; shControl	<i>Mbd2</i> ^{-/-} ; shMbd1	<i>Mbd2</i> ^{-/-} ; shMecp2	<i>Mbd2</i> ^{-/-} ; shMbd1, shMecp2
<i>Snrpn</i>	0.0±0	0.0±0	0.0±0	0.0±0	0.0±0
<i>Peg3</i>	0.0±0	0.0±0	0.0±0	0.0±0	.7±1.3
<i>Zim1</i>	0.0±0	2.6±2.3	2.0±2.1	0.8±1.4	2.4±2.1
<i>Kcnq1ot1</i>	0.0±0	0.0±0	0.0±0	0.0±0	0.0±0
<i>Cdkn1c</i>	0.0±0	0.0±0	0.0±0	0.0±0	0.0±0
<i>H19</i>	0.0±0	0.0±0	0.0±0	0.0±0	0.0±0
<i>Igf2</i>	0.0±0	0.0±0	0.0±0	0.0±0	0.0±0

Percent total expression from the normally repressed allele with standard deviations is shown for MEFs expressing the indicated shRNA. Maternally expressed genes are designated in red. Paternally expressed genes are designated in blue. N=3 for all experiments.

Allele-specific expression analysis was performed on paternally expressed *Snrpn*, *Peg3*, *Kcnq1ot1*, and *Igf2*, as well as maternally expressed *Zim1*, *Cdkn1c* and *H19*. Loss of imprinting was not detected in either the *Mbd2*^{-/-} MEFs depleted of MBD1, *Mbd2*^{-/-} MEFs depleted of MECP2 or *Mbd2*^{-/-} MEFs depleted of both MBD1 and MECP2 (table 3.4). Because substantial amounts of MBD1 and MECP2 remained, no conclusions on the redundancy between these proteins can be made, but reduced levels of MBD family members did not disrupt imprinted expression.

Stable shRNA knockdown experiments were also performed in TS cells. Again, cells stably expressed an shRNA targeting a control sequence (shControl), *Mbd1* (shMbd1), *Mecp2* (shMecp2) or both *Mbd1* and *Mecp2*. TS cells were collected at ~7 days, and 2 passages after initial infection for analysis. I was unable to deplete MBD1 or MECP2 in TS cells (figure 3.8), which was consistent with previous studies indicating that shRNA knockdown has low efficiency in TS cells (Golding and Mann, 2011). Additionally, expression of TS cell pluripotency markers (*mEomes*, *Fgfr2*, *Esrrb*) and a marker of differentiated giant cells (*Ascl2*) were analyzed. I observed high levels of expression of pluripotency markers (figure 3.9A), but in the samples which stably expressed shRNAs, transcription of *Ascl2* (figure 3.9B) was detected. Giant cells are tetraploid (Tanaka et al., 1998) and may exhibit different patterns of imprinted gene expression. Although levels of *Ascl2* are low, expression indicated that a subset of cells were undergoing differentiation. Biallelic expression from even a few cells could make analysis of imprinting difficult. Therefore I did not continue to pursue knockdown experiments in TS cells.

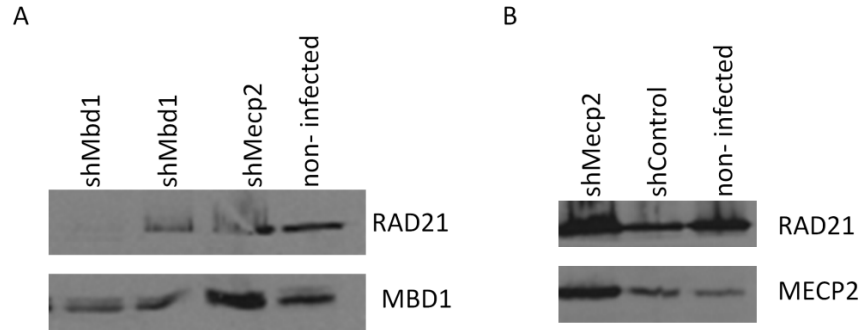


Figure 3.8 Infection of shRNA constructs in TS cells. (A-B) Western blots to detect (A) MBD1 or (B) MECP2 in lysates from TS cells expressing the indicated shRNA. RAD21 was used as a loading control.

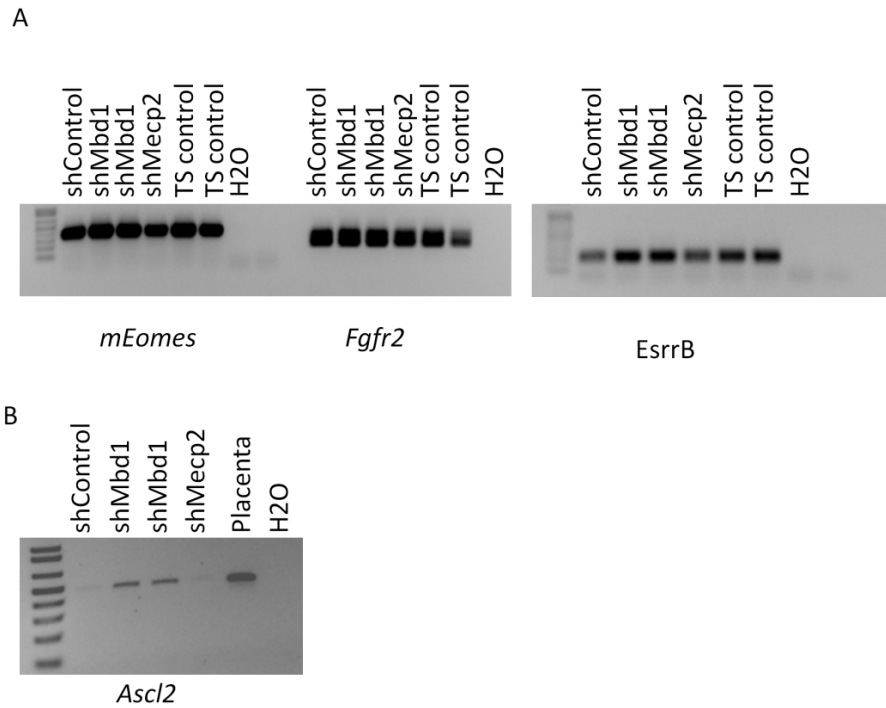


Figure 3.9 Expression of pluripotency and differentiation markers in TS cells. (A) RT-PCR to detect expression of TS cell pluripotency markers (as indicated below gel) in TS cells stably expressing shRNAs (as indicated above gel). (B) RT-PCR to detect expression of *Ascl2*, a marker of differentiated giant cells in cells stably expressing shRNAs (as indicated).

3.5.3 Overexpression of the MBD in MEFs

Due to the limitations of knockdown studies, I decided to assess the issue of compensation using a different approach. The prevailing model of repression by MBD proteins suggests that the proteins bind to methylated DNA through the MBD and other regions of the protein (particularly the TRD) interact with transcriptional repressors and chromatin modifiers. Based on this model, overexpression of the MBD alone could displace binding of endogenous MBD proteins and lead to a loss of repression. I could therefore overexpress the MBD in F1 hybrid MEFs and analyze allele-specific imprinted expression. cDNA from wild type brain was used to amplify the MBD domain of *Mecp2*, as deletion studies have defined the boundaries of the MECP2 MBD (Nan et al., 1993). Primers were designed to include amino acid 76 through amino acid 160 of MECP2. The MBD was modified to include a C-terminal flag-tag and an N-terminal SV40 nuclear localization signal. This modified MBD was then cloned into the retroviral pBABE-puro vector (pBABE-MBD), which expresses the puromycin resistance gene and promotes high levels of protein expression in mammalian cells (Morgenstern and Land, 1990).

F1 hybrid MEFs were infected with either an empty vector (pBABE) or the pBABE-MBD construct. Cells were collected ~7 days and 1 passage after initial infection for expression and protein analysis. On average, a 9.25 fold increase in *Mecp2* MBD expression was detected from the cells expressing pBABE-MBD (figure 3.10A).

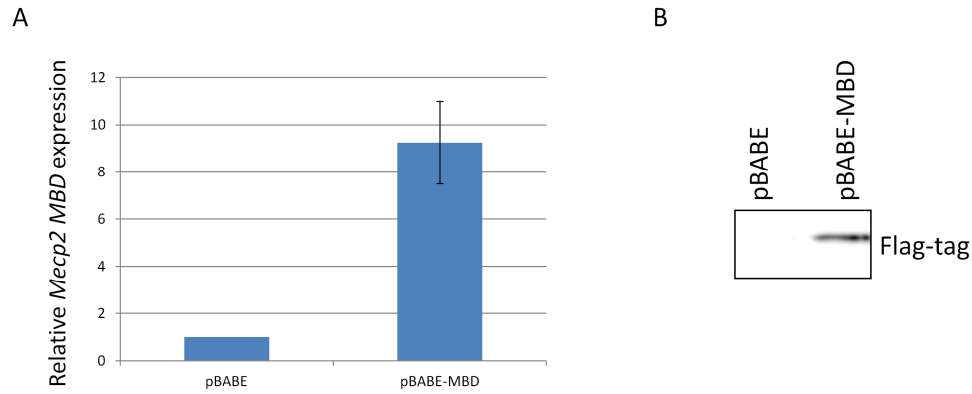


Figure 3.10 Overexpression of the MBD in F1 hybrid MEFs. (A) qRT-PCR to analyze expression *Mecp2 MBD* was performed in F1 hybrid MEFs infected with empty vector (pBABE) or pBABE-MBD. *Mecp2 MBD* expression was normalized to *Rplp0*. Expression levels are graphed relative to expression in pBABE control cells. Error bars represent standard deviations. Three biological replicates were used. (B) Western blot to detect the flag-tagged-MBD in cells that stably express pBABE-MBD.

Table 3.5 Allele-specific expression analysis of imprinted genes in F1 hybrid MEFs which overexpress the MBD

	MEFS	
	pBABE	pBABE-MBD
<i>Snrpn</i>	0.0±0	0.0±0
<i>Peg3</i>	0.0±0	0.0±0
<i>Zim1</i>	0.0±0	0.0±0
<i>Kenq1ot1</i>	0.0±0	0.0±0
<i>Cdkn1c</i>	0.0±0	0.0±0
<i>H19</i>	0.0±0	0.0±0
<i>Igf2</i>	0.0±0	0.0±0

Percent total expression from the normally repressed allele with standard deviations is shown for MEFs expressing the indicated shRNA. Maternally expressed genes are designated in red. Paternally expressed genes are designated in blue. N=3 for all experiments.

Translation of the MBD was confirmed by western blot using an antibody against the flag-tag (figure 3.10B).

Allele-specific expression analysis was performed on paternally expressed *Snrpn*, *Peg3*, *Kcnq1ot1*, and *Igf2*, as well as maternally expressed *Zim1*, *Cdkn1c* and *H19* with normal imprinting detected in all samples (table 3.5). However, the level of overexpression necessary to displace endogenous MBD proteins remains unknown and the poor quality of antibodies against the MBD proteins does not allow quantification of the loss of binding. Therefore, it remains possible that levels of overexpression in this experiment were insufficient to displace endogenous MBD proteins from their targets.

3.6 Breeding to generate *Mbd1*^{-/-}*Mbd2*^{-/-} mice

Of most interest would be to genetically test for redundancy between MBD1 and MBD2 through analysis of *Mbd1*^{-/-}*Mbd2*^{-/-} mice. Previous studies have assessed redundancy between MECP2 and MBD2 through analysis of *Mecp2*^{-y}*Mbd2*^{-/-} mice. These double mutant mice had the same phenotypes as the *Mecp2*^{-y} mouse, suggesting these two proteins are not redundant (Guy et al., 2001). However, the possibility remains that the strong phenotype of the *Mecp2* null mouse masked slightly different phenotypes in the *Mecp2*^{-y}*Mbd2*^{-/-} mouse. Therefore analysis of *Mbd1*^{-/-}*Mbd2*^{-/-} would be most ideal for uncovering functional redundancy, as the *Mbd1* null and *Mbd2* null phenotypes are more subtle. Analysis of these double mutant mice could uncover imprinting defects that were not detected in single mutants.

One complicating factor in generating an *Mbd1*^{-/-}*Mbd2*^{-/-} mouse mutant, is that these two genes are located ~4 megabases apart on mouse chromosome 18. The genetic distance between these genes is ~5 centimorgans, meaning there is ~1/20 chance of recombination between the two genes during meiosis. I have been breeding *Mbd1*^{+/-}*Mbd2*^{+/-} x *Mbd1*^{-/-} (breeding is set up in both directions). *Mbd2*^{-/-} mothers do not nurture their offspring (Hendrich, 2001), therefore, all matings were set up to get the recombination on a *Mbd1* null background. An *Mbd1*^{-/-}*Mbd2*^{+/-} recombinant mouse has been obtained, and breeding is currently ongoing to increase the numbers of the double mutant recombinants.

CHAPTER FOUR

TET-MEDIATED ERASURE OF IMPRINTS IN THE MAMMALIAN GERMLINE

DNA methylation at imprinted loci must be erased in the germline to allow re-setting of sex-specific marks for the next generation. Until recently, the mechanism of this demethylation remained unknown. With increased sensitivity of methylation analysis and the discovery of 5hmC, however, these mechanisms are beginning to be elucidated. Recent studies have indicated two waves of demethylation in PGCs; (1) the majority of DNA is passively demethylated in migrating PGCs (Kagiwada et al., 2013; Seisenberger et al., 2012) and (2) imprints, as well as other sequences, are demethylated after the PGCs reach the genital ridge (Hackett et al., 2013; Hajkova et al., 2010; Seisenberger et al., 2012). Interestingly, enrichment of 5hmC has been detected in PGCs at imprinted loci at the onset of demethylation (Hackett et al., 2013; Yamaguchi et al., 2013).

Presence of 5hmC in PGCs indicates activity of the TET proteins. PGCs express both *Tet1* and *Tet2* (*Tet1* at much higher levels), with no detectable *Tet3* expression (Hackett et al., 2013; Hajkova et al., 2010; Kagiwada et al., 2013). Mice deficient in TET1 or TET2 have been analyzed, with very subtle defects. Some *Tet1* null mice had a small body size at birth and *Tet1* null females had compromised fertility (Dawlaty et al., 2011; Yamaguchi et al., 2012). *Tet2* null adult mice had an increased likelihood of developing myeloid malignancies (Ko et al., 2011; Li et al., 2011; Moran-Crusio et al., 2011; Quivoron et al., 2011). Because of the subtle phenotypes of individual *Tet1*^{-/-} or

Tet2^{-/-} mutants, and the similar expression patterns exhibited by these proteins, we hypothesized that TET1 and TET2 have a cooperative role in DNA demethylation at imprint loci in PGCs.

To test this hypothesis, we analyzed germ cells of mice deficient for TET1 and TET2 (double knockout, DKO). We found that PGCs lacking TET1 and TET2 retain DNA methylation at some imprinted loci. Importantly, this aberrant retention of DNA methylation was also observed in mature male gametes and fetuses from DKO females. This study was done in collaboration with Dr. Guo-Liang Xu's laboratory at the Institute of Biochemistry and Cell Biology, Chinese Academy of Sciences in Shanghai China. The mutant mice were targeted in Dr. Xu's laboratory. Dr. Xu's graduate student Bang-An Wang performed all analyses in PGCs. I performed methylation analysis of DKO sperm, kidney and embryos from DKO females. It is important to note that after initiation of this project, an independent study analyzing *Tet1*^{-/-}*Tet2*^{-/-} mice was published (Dawlaty et al., 2013). A comparison of our work with that in Dawlaty et al., 2013 can be found in chapter 6.11.

4.1 TET1 and TET2 deficient PGCs lack 5hmC

To determine the role of TET-mediated DNA demethylation in PGCs, mutations targeting *Tet1* or *Tet2* were made in the mouse. Double heterozygous (*Tet1*^{+/-}*Tet2*^{+/-}) male and female mice were mated to produce *Tet1/Tet2* DKO mice for analysis (figure 4.1A). The DKO mice had grossly normal prenatal and postnatal growth and development.

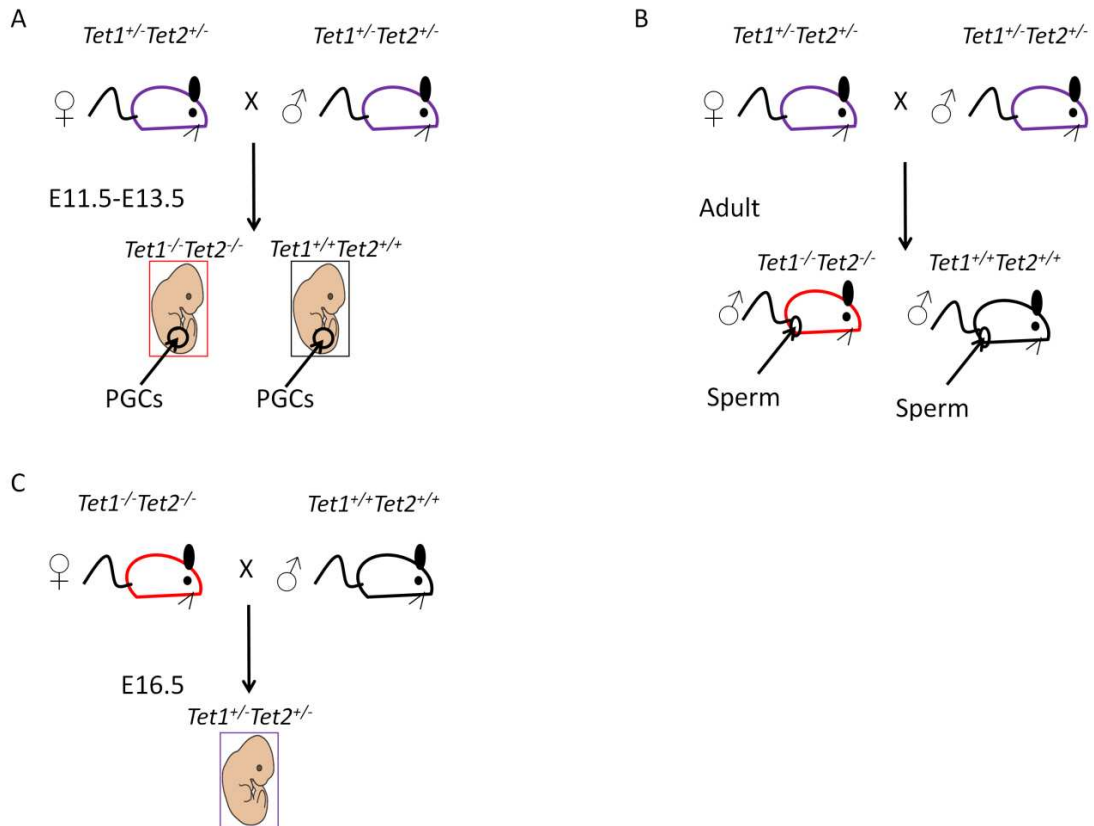


Figure 4.1 Mating schemes for analysis of TET1/TET2 deficiency in imprint erasure. (A-B) *Tet1/Tet2* double heterozygous mice (purple) were mated to produce DKO (red) or wild type (black) offspring. (A) DKO and wild type embryos were collected at E11.5 or E13.5 and PGCs were isolated for analysis. (B) Adult males born from double heterozygous parents were used for analysis of mature gametes and somatic tissues. (C) DKO females were mated to wild type males and E16.5 double heterozygous embryos were collected for analysis.

Because we were interested in understanding 5hmC conversion and demethylation at imprinted loci in PGCs, we examined DNA modifications in gonadal PGCs as erasure of DNA methylation at imprinted genes is known to occur after PGCs reach the genital ridge (Seisenberger et al., 2012). Immunostaining of genital ridge sections detected presence of 5hmC in wild type PGCs at E11.5. In contrast, 5hmC was barely detectable in E11.5 PGCs from DKO mice (figure 4.2). Therefore, TET1 and TET2 are required for conversion of 5mC to 5hmC in PGCs.

4.2 TET1 and TET2 deficient PGCs retained DNA methylation at imprinted loci

We next assessed whether demethylation at imprinted loci was impaired in PGCs that lacked TET1 and TET2, and thus could not oxidize 5mC to 5hmC. Again, double heterozygous (*Tet1*^{+/-}*Tet2*^{+/-}) male and female mice were mated to produce *Tet1/Tet2* DKO mice for analysis (figure 4.1A). Bisulfite mutagenesis and sequencing was performed on DNA from male and female PGCs at E13.5. Normally, at this stage, methylation at imprinted loci has been erased (Seisenberger et al., 2012). We analyzed a paternally-methylated DMR, *H19*, and a maternally-methylated DMR, *Mest* (also known as *Peg1*). Considerable amounts of methylation were detected at both DMRs in DKO male and female E13.5 PGCs, whereas very little methylation was detected in wild type PGCs (figure 4.3). These data indicated the requirement of 5mC to 5hmC conversion for imprint erasure as abnormal retention of DNA methylation at imprinted loci was observed in DKO E13.5 PGCs.

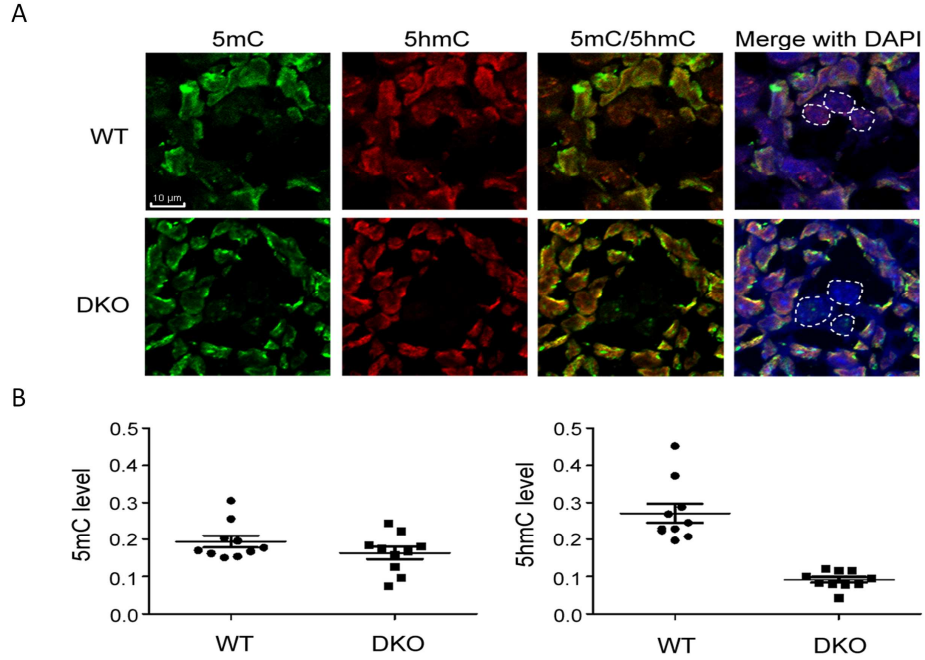


Figure 4.2 Reduction of 5hmC in TET1/TET2 deficient PGCs. Immunofluorescence images of 5mC (green) and 5hmC (red) of cryosections of genital ridges from E11.5 wild type (WT) and DKO littermates. DNA is stained with DAPI (blue). PGCs are outlined with dashed lines. Bar, 10 μ m. (B) Quantification of the relative levels of 5mC and 5hmC from (A). Each data point is based on the level of the 5mC or 5hmC signal relative to the DAPI staining intensity of the same cell. Error bars indicate standard error. Figure courtesy of Dr. Guo-Liang Xu and Bang-An Wang.

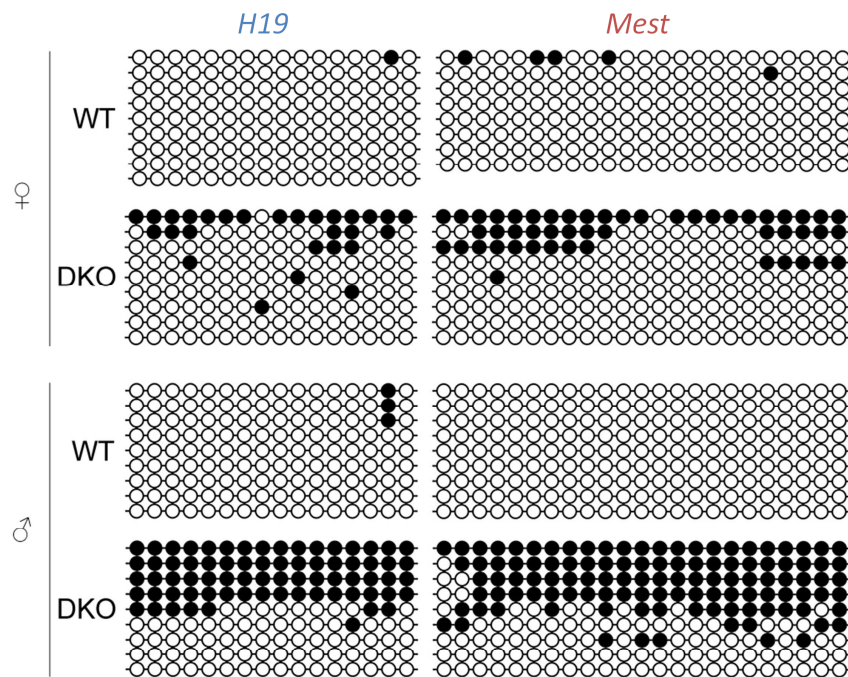


Figure 4.3 Retention of methylation at imprinted loci in TET1/TET2 deficient E13.5 PGCs. Bisulfite mutagenesis and sequencing was performed on DNA isolated from either wild type (WT) or DKO, male (♂) and female (♀) E13.5 PGCs. DMRs at paternally-methylated *H19* (designated in blue) and maternally-methylated *Mest* (designated in red) were analyzed. Open and closed circles denote unmethylated and methylated cytosines, respectively, along a single horizontal strand of cloned DNA. Figure courtesy of Dr. Guo-Liang Xu and Bang-An Wang.

4.3 Abnormal methylation at imprinted loci in TET1/TET2 deficient sperm

It is possible that aberrant retention of DNA methylation observed in DKO E13.5 PGCs could be erased later in gametogenesis. We therefore analyzed methylation at imprinted DMRs in mature sperm. The TET1/TET2 deficient mice used for analysis were conceived from mating double heterozygous males and females (*Tet1*^{+/-}*Tet2*^{+/-} x *Tet1*^{+/-}*Tet2*^{+/-}) (figure 4.1B). Wild type mice used for comparisons were not necessarily littermates of the DKO mice, due to the difficulty of obtaining both genotypes in a single litter (1/16 chance of getting each genotype). Pyrosequencing was performed on bisulfite mutagenized DNA from mature sperm from DKO or wild type males. We analyzed the paternally-methylated *H19* ICR and IG-DMR (*Gtl2*) and the maternally-methylated DMRs at *Snrpn*, *Peg3*, *Mest*, *Kcnq1ot1* and *Grb10*. Interestingly, we found that the levels of methylation at these DMRs were quite variable, with significant retention of DNA methylation detected at *Mest* (P value < .05), *Kcnq1ot1* and *Grb10* (P value < .01) (figure 4.4). We therefore conclude that TET-mediated DNA demethylation is locus specific, with some loci more susceptible to aberrant methylation patterns in the absence of TET1 and TET2. It is important to note that although conversion to 5hmC is blocked in DKO germ cells, UHFR1 levels are very low and DNMT1 is not detectable at replication foci in PGCs (Kagiwada et al., 2013). Thus, passive DNA demethylation could act as a back-up mechanism to demethylate imprinted loci in the absence of 5hmC conversion. Passive demethylation could also explain the variability in methylation levels and the locus-specificity of aberrant methylation in DKO sperm.

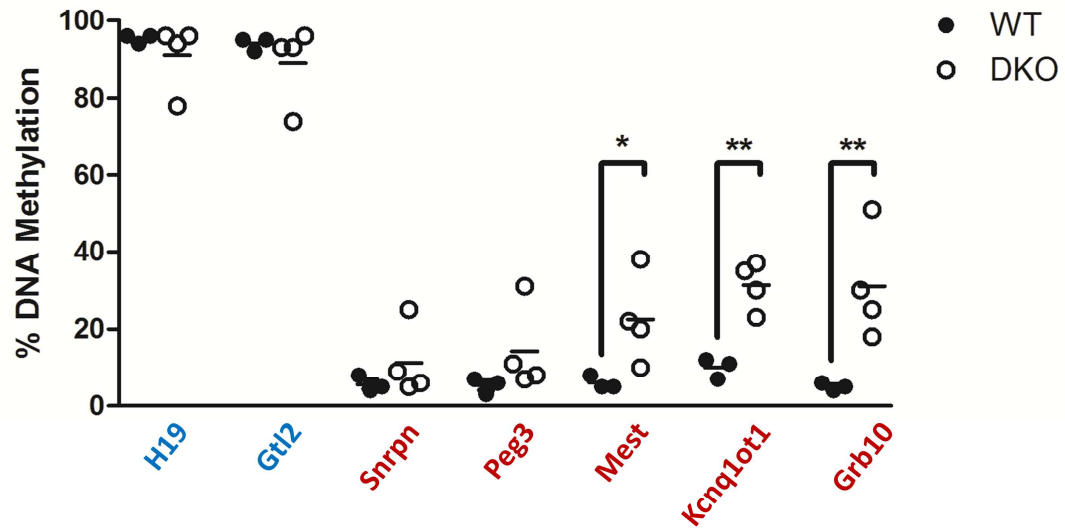


Figure 4.4 Retention of methylation at imprinted loci in TET1/TET2 deficient mature sperm. Percent DNA methylation at imprinted DMRs for wild type (WT, closed circles) and DKO (open circles) sperm DNA as determined by pyrosequencing. Paternally-methylated DMRs are designated in blue and maternally-methylated DMRs are designated in red. Each circle represents an individual sample with the mean of each genotype indicated by a horizontal black bar. *P < .05, **P < .01.

Recent studies indicate that the majority of DNA methylation, including methylation at repetitive elements, is passively lost as PGCs migrate to the genital ridge (Kagiwada et al., 2013; Seisenberger et al., 2012). We performed the LUMinometric Methylation Assay (LUMA) on adult testes to assess genome-wide DNA methylation levels in mature germ cells. This assay quantifies genomic cutting of a methylation sensitive restriction enzyme (*HpaII*) and methylation insensitive restriction enzyme (*MspI*) with each normalized to cutting of *EcoRI*. The ratio of cuts between the two enzymes gives levels of global DNA methylation (Karimi et al., 2006). LUMA analysis performed on DNA from DKO adult testes indicated normal levels of DNA methylation at ~70% of CpGs methylated (figure 4.5). Our data supports the model that passive DNA demethylation is responsible for erasure of genome-wide methylation as TET1 and TET2 were dispensable for normal genomic methylation patterns.

Additionally, we assessed methylation at imprinted DMRs in somatic tissues of mice deficient for TET1 and TET2. Because we generated these mice from *Tet1*^{+/-}*Tet2*^{+/-} parents, the parental germline giving rise to DKO mice had both TET1 and TET2 proteins. Additionally, TET3, the enzyme necessary for demethylation of the paternal genome after fertilization (Gu et al., 2011; Iqbal et al., 2011; Wossidlo et al., 2011), remained unperturbed. We pyrosequenced bisulfite mutagenized DNA from DKO and wild type kidneys to assess DNA methylation at *H19*, *Gtl2*, *Snrpn*, *Peg3*, *Kcnq1ot1* and *Mest* DMRs (figure 4.6). We detected normal levels of methylation (~50%) at all imprinted DMRs, indicating that TET1 and TET2 deficiency predominantly affects germ cells.

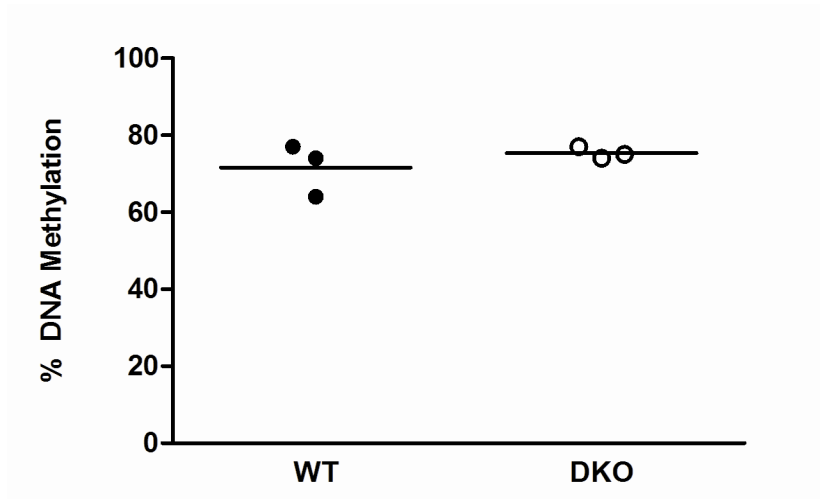


Figure 4.5 Normal genomic methylation levels of adult TET1/TET2 deficient testes. Methylation levels of adult (4 months of age) testis DNA were determined by the LUMinometric Methylation Assay (LUMA) for wild type (WT, closed circle) and DKO (open circle) males. Each circle represents an individual sample with the mean methylation for each genotype indicated by a horizontal bar.

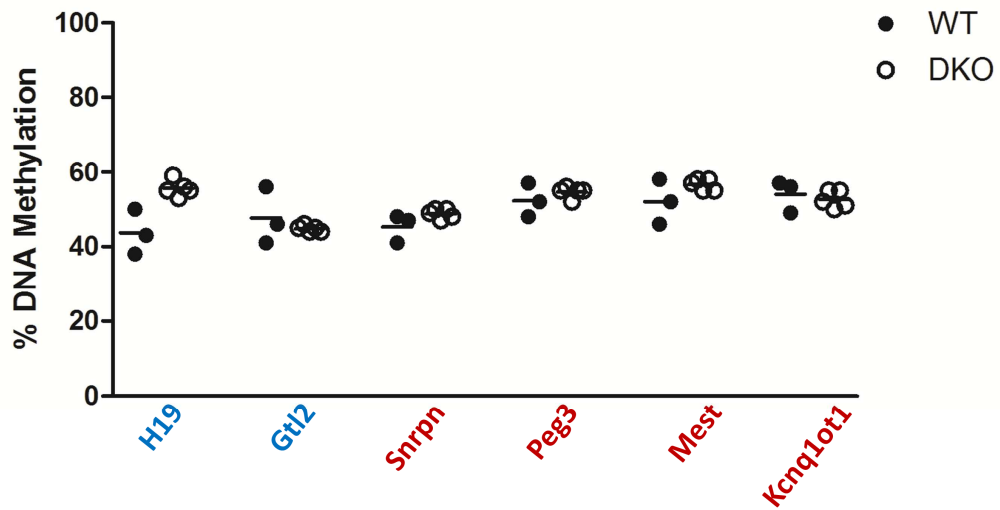


Figure 4.6 Normal methylation levels at imprinted loci in kidneys of TET1/TET2 deficient mice. Percent DNA methylation at imprinted DMRs for wild type (WT, closed circles) and DKO (open circles) kidney DNA as determined by pyrosequencing. Paternally-methylated DMRs are designated in blue and maternally-methylated DMRs are designated in red. Each circle represents an individual sample with the mean of each genotype indicated by a horizontal black bar.

4.4 Aberrant methylation in fetuses from TET1/TET2 deficient females

While male reproduction was largely unaffected by TET1/TET2 deficiency, female DKO mice were subfertile with increased frequency of pregnancy loss. To assess methylation defects in offspring from DKO females, we mated *Tet1*^{-/-}*Tet2*^{-/-} females with wild type males (figure 4.1C). We were able to recover 2 late stage (~E16.5) embryos from a pregnant DKO female. Pyrosequencing was performed on bisulfite treated DNA from the 2 fetuses for analysis of methylation at imprinted loci. Interestingly, we detected increased levels of DNA methylation specifically at paternally-methylated DMRs, *H19* and *Gtl2*, with methylation levels of ~77% and 69%, respectively (figure 4.7). This suggests that the DKO maternal germline was unable to properly erase methylation at paternally-methylated loci. These unerased imprints were then inherited in offspring. Therefore, we conclude that TET-mediated DNA demethylation is required for erasure of methylation at some imprinted loci in PGCs, and without TET proteins (TET1 and TET2) aberrant retention of methylation occurs in the germline that could be inherited in the next generation.

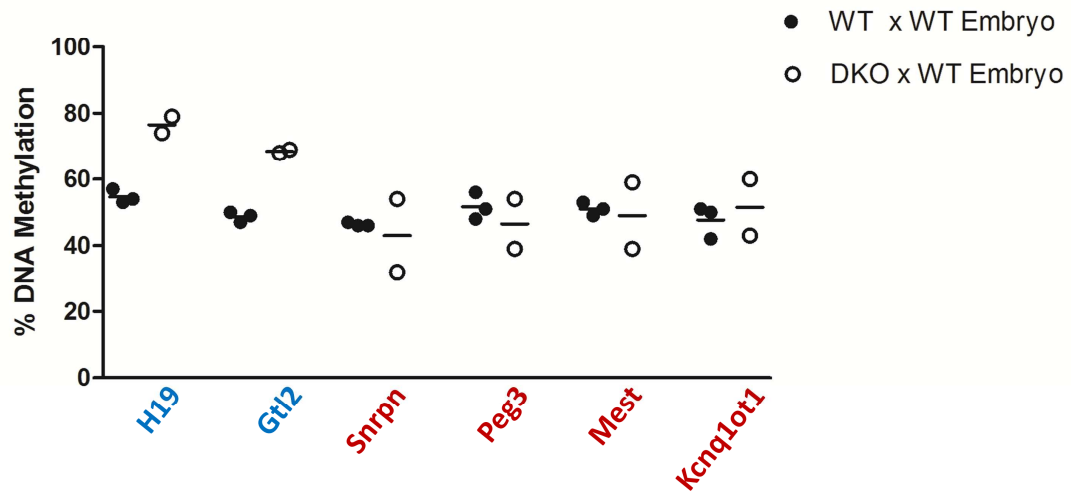


Figure 4.7 Retention of methylation at paternally-methylated DMRs in offspring of a TET1/TET2 deficient female. Percent DNA methylation at imprinted DMRs for embryos from wild type (WT) females mated with WT males (closed circles) and embryos from a DKO female mated with a WT male (open circles) as determined by pyrosequencing. Paternally-methylated DMRs are designated in blue and maternally-methylated DMRs are designated in red. Females are listed first in crosses. Each circle represents an individual sample with the mean of each genotype indicated by a horizontal black bar.

CHAPTER FIVE

STABILITY OF DNA METHYLATION IN SPERMATOGENIAL STEM CELLS DESPITE ENVIRONMENTAL PERTURBATIONS

The reversibility of epigenetic marks makes the epigenome particularly susceptible to disruptions by environmental influences (McCarrey, 2012). For example, manipulations associated with ART procedures occur during times of epigenetic reprogramming, and have been associated with aberrant DNA methylation (Eroglu and Layman, 2012). Specifically, endocrine stimulation of the ovary, embryo culture, or transfer of preimplantation embryos, have all been shown to cause alteration of DNA methylation and deregulation of imprinted genes in mice (de Waal et al., 2012b; Doherty et al., 2000; Fauque et al., 2007; Mann et al., 2004; Rivera et al., 2008; Sato et al., 2007).

Recent advances in understanding male germline stem cells, spermatogonial stem cells (SSCs), have allowed development of techniques with great potential for male infertility treatment. SSCs reside within a specific microenvironment of the seminiferous tubule called the niche, and serve as the foundation of spermatogenesis. SSCs can either undergo self-renewal or differentiate into mature sperm. These fate decisions are tightly regulated by growth factors and extracellular signals secreted by Sertoli cells within the niche (Brinster, 2007). In 1994 Dr. Ralph Brinster described an SSC transplantation assay in which he displayed the ability of cultured SSCs to generate a colony of spermatogenesis after transplantation to the seminiferous tubules of a recipient male (Brinster and Avarbock, 1994). Additionally, advances in cell culture techniques allow

for long-term *in vitro* culture of SSCs (Kanatsu-Shinohara et al., 2005). These technologies allow preservation of the male germline, which has utility in species continuity and perpetuating valuable livestock. Importantly, there are great medical applications of these technologies including preserving the germline of prepubertal boys undergoing radiation or chemotherapy causing infertility.

For application of these techniques in fertility treatment, it will be necessary to not only cryopreserve, culture and transplant SSCs, but intracytoplasmic sperm injection (ICSI) will likely be used to ensure fertilization and obtain pregnancies. The ICSI procedure itself involves many steps that coincide with times of epigenetic reprogramming, which could disrupt imprint establishment and maintenance. First, gonadotropin stimulation of the ovary is used to obtain large numbers of oocytes. Oocytes are then cultured and injected with a single sperm. Embryos are cultured until blastocyst stage and transferred into a recipient female. All of these manipulations take place during periods of epigenetic reprogramming and have been reported to cause methylation and expression abnormalities in mice (de Waal et al., 2012b; Doherty et al., 2000; Fauque et al., 2007; Mann et al., 2004; Rivera et al., 2008; Sato et al., 2007). Knowing that a wide variety of environmental influences could induce epigenetic perturbations, we were interested in determining the stability of DNA methylation at imprinted loci throughout long-term SSC culture, transplantation, cryopreservation and ICSI. These studies were performed in collaboration with Dr. Ralph Brinster's laboratory at the University of Pennsylvania School of Veterinary Medicine. I worked with Dr. Jonathan Schmidt to assess whether *in vivo* and *in vitro* aging was detrimental to SSC

function. I performed methylation analysis on SSCs and an ICSI-derived pup, with all cell culture work, mouse work and gene expression analysis performed by the Brinster Laboratory and published in (Schmidt et al., 2011). I worked with Dr. Xin Wu and Dr. Shaun Goodyear to characterize offspring derived from SSCs cryopreserved for more than 14 years. For these studies I performed methylation analysis, with all cell culture work, mouse work and genetic analysis performed by the Brinster Laboratory and published in (Wu et al., 2012). Despite environmental perturbations we detected normal methylation at ICRs, confirming the stability of epigenetic modifications in cultured, frozen or serially transplanted SSCs.

5.1 Analysis of aged SSCs

Currently, SSCs can be cultured *in vitro* indefinitely. Because of the potential utilization of culture techniques to maintain human SSCs for fertility treatments, it is imperative to characterize the stability of epigenetic marks in SSCs after long-term culture or extreme aging. We did this by analyzing DNA methylation profiles at imprinted DMRs in both *in vivo* aged SSCs (figure 5.1) and *in vitro* aged SSCs (figure 5.2).

5.1.1 Normal methylation detected in *in vivo* aged SSCs

To determine the effect of *in vivo* aging on SSC function, SSC cultures were initiated when the SSCs were 8, 300 or ~1500 days of age. SSCs were isolated from 8 day old pups, or 10 month old adults for the 8 days (young) or 300 days (aged) SSC

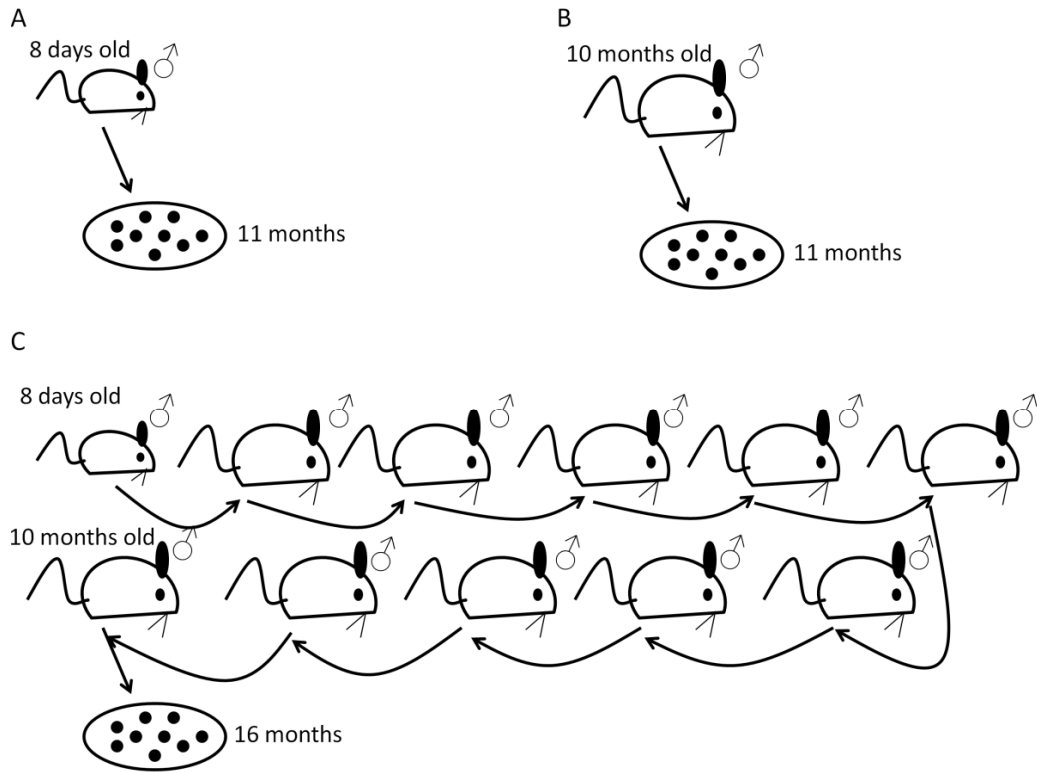


Figure 5.1 Experimental design for *in vivo* aging analysis. (A) SSCs were isolated from 8 day old male pups (young) and cultured for 11 months (n=3). (B) SSCs were isolated from 10 month old male mice (aged) and cultured for 11 months (n=3). (C) SSCs were isolated from the 10th recipient of a serial transplantation experiment in which SSCs were serially transplanted every 3 months into young testes. SSCs were isolated from the final recipients at 10 months after transplantation (ST-aged) and cultured for 16 months (n=3).

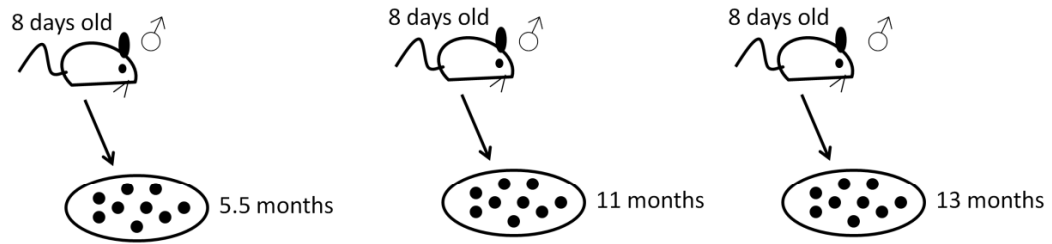


Figure 5.2 Experimental design for *in vitro* aging analysis. SSCs were isolated from 8 day old male mice (young) and cultured for 5.5, 11 or 13 months (n=3 for all).

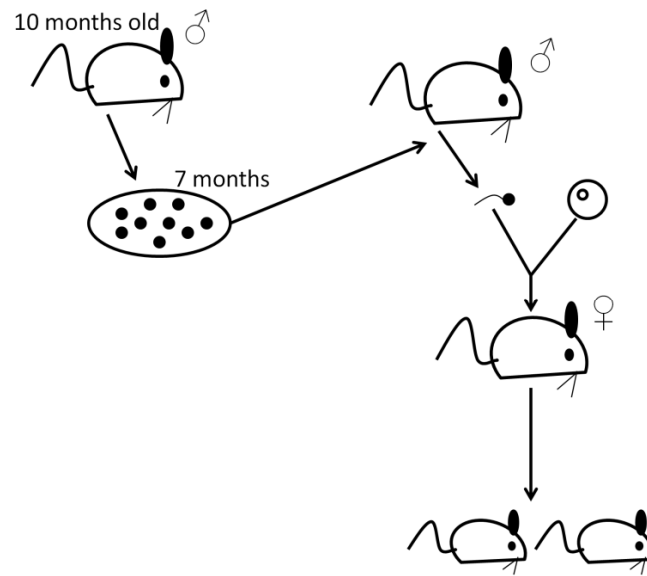


Figure 5.3 Experimental design for analysis of offspring derived from aged SSCs, transplantation and ICSI. SSCs were isolated from 10 month old male mice and cultured for 7 months and subsequently transplanted into a recipient male. Sperm isolated from the recipient male 6 months after transplantation was used for ICSI. Analysis was performed on the ICSI-derived offspring.

experimental groups, respectively (n=3 for both groups) (figure 5.1A-B). For the third treatment group, SSCs were isolated from the 10th recipient of a serial transplantation (ST) experiment in which SSCs were serially transplanted every 3 months into young testes. SSCs were isolated and cultured from the final recipients at 10 months after transplantation to generate the 1500 days of age (ST-aged) group (n=3) (figure 5.1C).

To identify possible deficiencies of the aged stem cells we analyzed DNA methylation at multiple imprinted DMRs. We focused on the *H19* ICR and IG-DMR because these loci are methylated during spermatogenesis. Using COmbined Bisulfite Restriction Analysis (COBRA) we were able to determine the methylation status of these regions. Bisulfite mutagenesis followed by PCR amplification converts unmethylated cytosines to thymines, while methylated cytosines remain. This process creates restriction sites that are unique to methylated sequences. Thus, with PCR amplification of bisulfite treated DNA and subsequent digestion with restriction enzymes unique to the methylated sequence, we were able to determine the methylation status of these paternally-methylated DMRs. In order to evaluate the effects of donor age on methylation at the *H19* ICR and IG-DMR, we compared young, ST-aged, and aged SSCs after 11, 16 and 11 months in culture, respectively. No differences in methylation patterns were observed between young, ST-aged and aged donor cultures, with ~100% methylation detected in all samples (figure 5.4 lanes 7-9). Therefore, *in vivo* aging of SSCs did not disrupt methylation patterns at paternally-methylated DMRs.

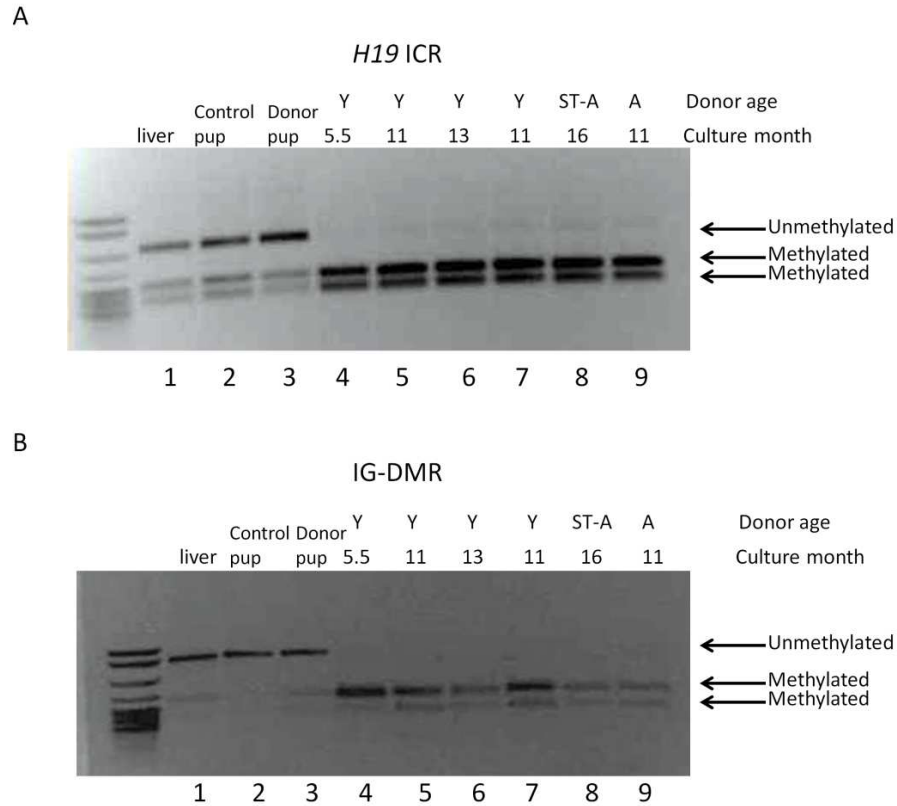


Figure 5.4 Maintenance of DNA methylation at paternally-methylated DMRs. COBRA was performed on bisulfite mutagenized DNA to analyze (A) the *H19* ICR or (B) IG-DMR and run out on a 1% agarose gel. Digested/ methylated fragments and undigested/unmethylated fragments are indicated to the right of panel. Shown here are representative gels displaying one sample from each experimental group. Lane 1, adult liver; lane 2, control day 0 pup somatic tissue; lane 3, ICSI-derived day 0 pup from donor sperm from SSCs that was cultured for 7 months prior to transplantation and maintained in the recipient mouse for 6 months before sperm isolation; lane 4, young (Y) donor cultured for 5.5 months; lane 5, young (Y) donor cultured for 11 months; lane 6, young (Y) donor cultured for 13 months; lane 7, young (Y) donor cultured for 11 months; lane 8, ST-aged (ST-A) donor cultured for 16 months; lane 9, aged (A) donor cultured for 11 months. Modified from Schmidt et al., 2011.

5.1.2 Normal methylation detected in *in vitro* aged SSCs

To determine the effect of *in vitro* aging on SSCs, SSCs were isolated from 8 day old mice and cultured for 5.5, 11 or 13 months (n=3 for each group) (figure 5.2).

COBRA was performed to assess methylation at the *H19* ICR and IG-DMR in these samples. No difference in methylation was observed among the *in vitro* aged groups, with ~100% methylation detected in all samples (figure 5.4 lanes 4-6). These data confirmed a previous report indicating stability of epigenetic modifications over long-term culture of SSCs (Kanatsu-Shinohara et al., 2005).

5.1.3 Normal methylation in offspring derived from aged SSCs, transplantation and ICSI

In vitro and *in vivo* aging did not appear to induce any methylation defects at the *H19* ICR or IG-DMR. However, because ICSI would likely be used in application of these techniques, we wanted to assess whether the combination of SSC aging followed by transplantation and ICSI would alter DNA methylation patterns in offspring. SSCs were isolated from 10 month old mice and cultured for 7 months. After 7 months in culture the SSCs were transplanted into a recipient male. Sperm was isolated from the recipient male 6 months after transplantation and used for ICSI (figure 5.3). Two offspring were generated from this procedure. COBRA was performed to analyze methylation at the *H19* ICR and IG-DMR of an ICSI derived pup (figure 5.4, lane 3) and a naturally sired control pup (figure 5.4, lane 2). Methylation at the *H19* ICR and IG-DMR in the ICSI derived pup was indistinguishable from control (figure 5.4, lanes 2-3). We therefore

conclude that methylation at imprinted loci in SSCs were stable throughout aging either *in vivo*, *in vitro* or combined SSC aging, transplantation and ICSI.

5.1.4 Aged SSCs have decreased stem cell function

Whereas epigenetic analysis indicated normal methylation at paternally-methylated DMRs, stem cell deficiencies were observed in the aged SSCs. Notably, the ST-aged SSCs had a decreased proliferation rate *in vitro*, and the *in vitro* aged SSCs had compromised ability to colonize the seminiferous tubule upon transplantation (Schmidt et al., 2011). Microarray analysis of *in vitro* aged SSCs (cultured greater than 14 months) identified a number of gene expression changes involved in SSC function. Long-term cultured SSCs had decreased expression of genes important for SSC self-renewal, such as *Bcl6b* and *Lhx1*, and increased expression of genes implicated in SSC differentiation, *Stra8* and *Kit* (Schmidt et al., 2011). This suggests that as an SSC ages, the decision to differentiate or self-renew shifts from self-renewal in younger SSCs to differentiation in aged SSCs. Therefore, SSCs will likely not be able to be cultured and maintain their stemness indefinitely.

5.2 Analysis in mice derived from SSCs cryopreserved for ~14 years

The findings that aged SSCs maintained expected DNA methylation levels at imprinted DMRs provided preliminary evidence that these techniques could be used for medical applications. Nevertheless, of great importance for human infertility would be the ability of SSCs to maintain proper epigenetic modifications despite long-term

cryopreservation. Chemotherapy or radiation treatment can result in infertility. Adult males can produce sperm for cryopreservation, whereas prepubertal boys cannot.

Cryopreservation of testicular tissue from boys may allow for future transplantation of SSCs to re-establish fertility in adulthood (Brinster, 2007). Therefore, we wanted to characterize DNA methylation profiles from mice derived from cryopreserved SSCs.

5.2.1 Normal methylation profiles in mice derived from SSCs cryopreserved for ~14 years

Testis cells from mouse pups (aged 6-14 days) that were frozen for ~14 years, were thawed and transplanted into recipient testes of mice in which endogenous spermatogenesis had been destroyed by busulfan treatment. Sperm from these recipient males were isolated and used for ICSI. A total of 5 pups were born from the ICSI procedure that appeared grossly normal (Wu et al., 2012) (figure 5.5). To assess the possibility that epigenetic defects occurred as a result of these procedures, we analyzed DNA methylation in these pups.

LUMA was performed on genomic liver DNA (as described in chapter 4.3) to assess genome-wide DNA methylation. Methylation levels of 5 control livers (sired from natural matings) and 4 ICSI derived livers were assessed. Genomic methylation levels in the ICSI derived mice were indistinguishable from control mice at ~72% CpGs methylated (figure 5.6). Therefore, repetitive elements appeared to be properly methylated in mice derived from ICSI using sperm from cryopreserved SSCs.

Next, we asked if imprinted DMRs have abnormal levels of methylation. Previous studies have demonstrated that ICSI, as well as other environmental influences,

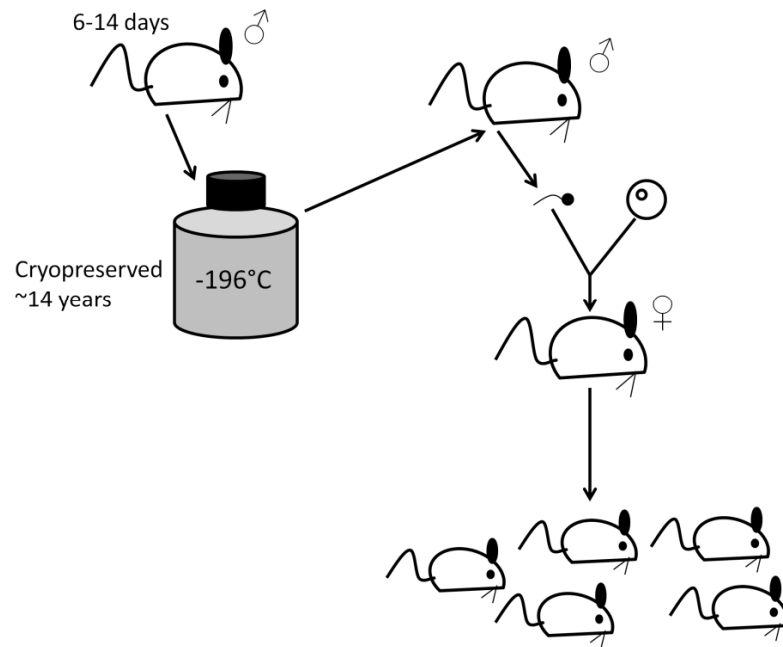


Figure 5.5 Experimental design to analyze offspring derived from SSCs cryopreserved ~14 years. Testis cells from mouse pups (aged 6-14 days) that were frozen for ~14 years, were thawed and transplanted into recipient testes of mice in which endogenous spermatogenesis had been destroyed. Sperm from these recipient males were used for ICSI. A total of 5 pups were born from the ICSI procedure.

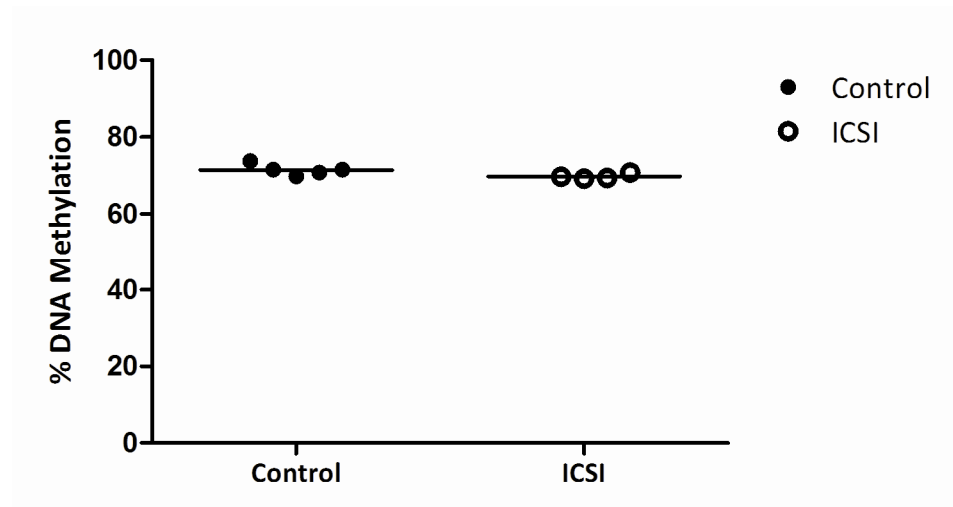


Figure 5.6 Normal genome-wide DNA methylation detected in offspring derived from ICSI using sperm from cryopreserved SSCs. Methylation levels of liver DNA were determined by the Luminometric Methylation Assay (LUMA) for naturally sired mice (control, closed circles) and ICSI-derived mice using sperm from cryopreserved SSCs (ICSI, open circle). Each circle represents an individual sample with the mean methylation for each group indicated by a horizontal bar.

can induce abnormal methylation and expression of imprinted genes (de Waal et al., 2012a). We analyzed two paternally-methylated DMRs; *H19* ICR and IG-DMR. Pyrosequencing of bisulfite treated liver DNA indicated normal levels of methylation at the *H19* ICR in ICSI derived as compared to control mice (figure 5.7A). COBRA was performed to analyze methylation at the IG-DMR. Using this assay, levels of methylation detected in the ICSI mice were indistinguishable from controls (figure 5.7B). Therefore, methylation at these paternally-methylated DMRs was maintained in SSCs after long-term cryopreservation, and properly inherited in the next generation despite the use of ICSI.

Additionally, we analyzed methylation at maternally-methylated DMRs; *Snrpn* and *Peg3*. Pyrosequencing analysis of bisulfite treated liver DNA did not uncover any significant difference between methylation levels at the *Snrpn* DMR in ICSI derived mice and control mice (figure 5.8A). COBRA analysis of the *Peg3* DMR also indicated normal levels of methylation in the ICSI derived mice when compared to control mice (figure 5.8B). We therefore conclude that mice derived by ICSI using sperm from SSCs cryopreserved for ~14 years had normal levels of methylation both genome-wide and at imprinted loci. These data confirms the prospect of using these procedures to restore fertility in males who had undergone gonadotoxic treatment as boys.

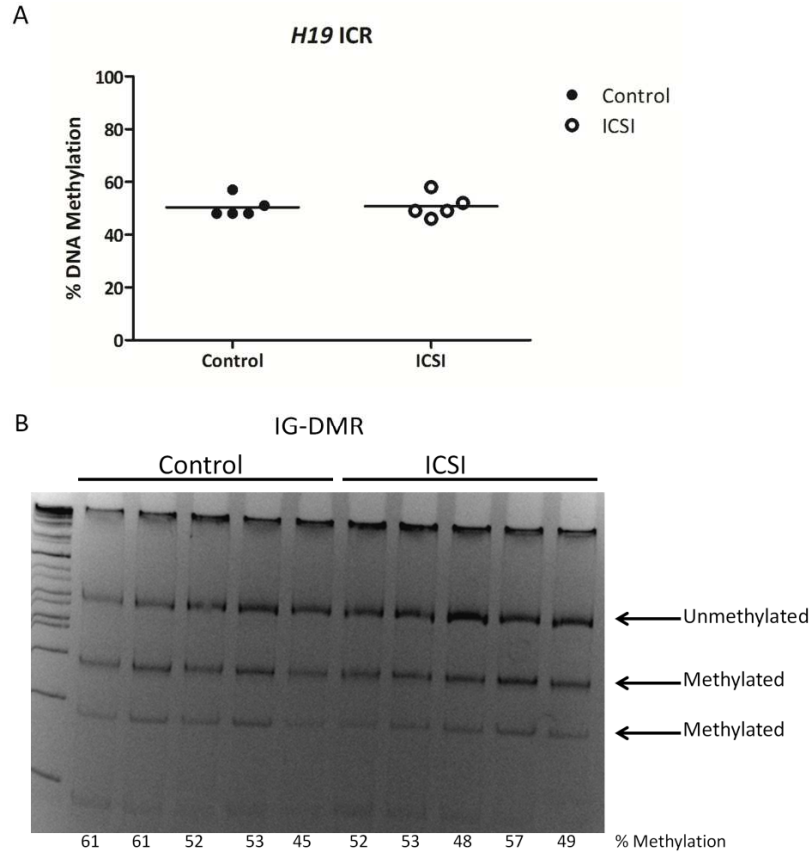


Figure 5.7 Normal methylation at paternally-methylated DMRs in mice derived from ICSI using sperm from cryopreserved SSCs. (A) Pyrosequencing was performed on bisulfite mutagenized liver DNA from naturally sired (control, closed circles) mice and ICSI- derived mice using sperm from cryopreserved SSCs (ICSI, open circles) to determine DNA methylation levels at the *H19* ICR. Mean methylation for each experimental group is represented with a black horizontal line. Each circle represents an individual sample. (B) COBRA was performed on bisulfite mutagenized DNA to analyze methylation at the IG-DMR and run out on a 12% acrylamide gel. Percent methylation as quantified by comparing band intensities of methylated to unmethylated fragments (indicated to the right) is written below panel.

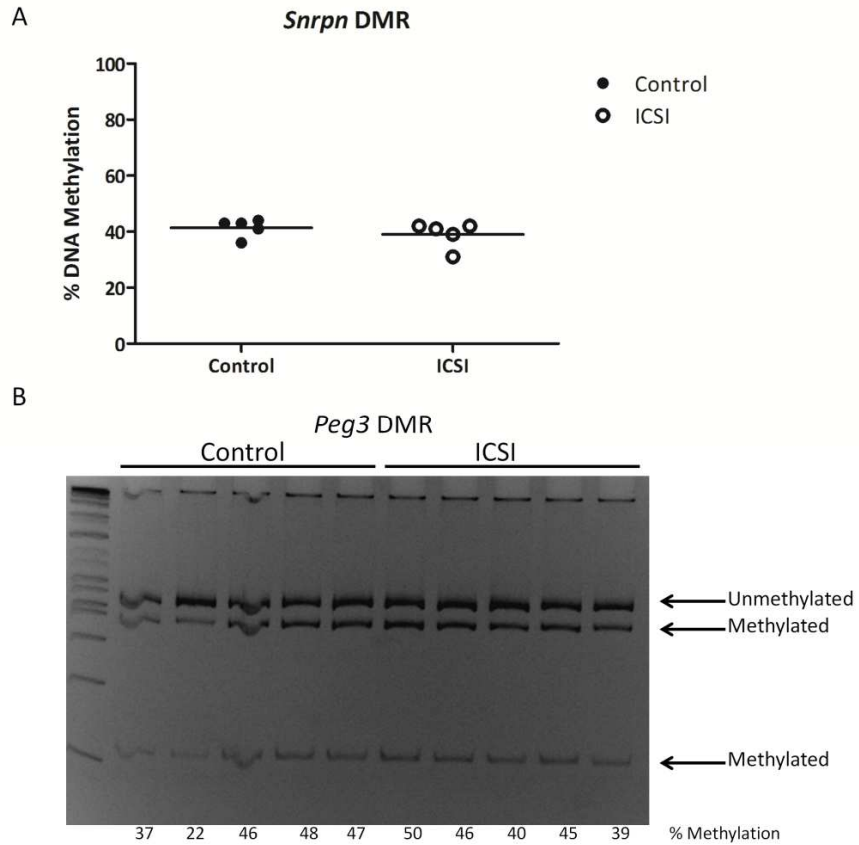


Figure 5.8 Normal methylation at maternally-methylated DMRs in mice derived from ICSI using sperm from cryopreserved SSCs. (A) Pyrosequencing was performed on bisulfite mutagenized liver DNA from naturally sired (control, closed circles) mice and mice derived from ICSI using sperm from cryopreserved SSCs (ICSI, open circles) to determine DNA methylation levels at the *Snrpn* DMR. Mean methylation for each experimental group is represented with a black horizontal line. Each circle represents an individual sample. (B) COBRA was performed on bisulfite mutagenized DNA to analyze methylation at the *Peg3* DMR and run out on a 12% acrylamide gel. Percent methylation as quantified by comparing band intensities of methylated to unmethylated fragments (indicated to the right) is written below panel.

CHAPTER SIX

DISCUSSION AND FUTURE DIRECTIONS

Genomic imprinting is a complex epigenetic phenomenon required for normal mammalian development. Imprinted expression requires marking the parental origin of the chromosome so that a specific parental allele is stably repressed or stably expressed. DNA methylation is essential for marking and silencing imprinted genes. These DNA methylation imprints and allele-specific expression patterns must be maintained throughout early development and in differentiated somatic tissues. Additionally, marking of the alleles must be reset in the germline to allow for establishment of sex-specific marks in the mature gamete, which will be transmitted to the next generation. These processes are critical for normal imprinting, and can be disrupted by environmental stress. This dissertation focused on identifying both *cis* and *trans* mechanisms by which DNA methylation confers imprints and how environmental stresses can disrupt imprinted regulation. We have defined a novel regulatory role for CpG content at the *H19* ICR in silencing paternal *H19*. We have also identified TET1 and TET2 as *trans* factors involved in resetting imprints in the germline and have provided evidence that individual MBD proteins are dispensable for normal imprinting. Moreover, we have demonstrated that methylation imprints are in fact stable in spermatogonial stem cells that have undergone aging and cryopreservation, suggesting that these techniques can be valuable sources for male infertility treatment.

6. 1 Non-promoter methylation in gene silencing

Whereas DNA methylation at the *H19* ICR is established in sperm and maintained in the zygote, methylation at the paternal *H19* promoter region is not detected until midgestation (Tremblay et al., 1997; Tremblay et al., 1995). Intriguingly, mice that paternally inherited an allele in which the *H19* ICR had been deleted did not gain methylation at the *H19* promoter region (Srivastava et al., 2000; Thorvaldsen et al., 2006). It was proposed that the paternal ICR acts as a center for spreading of methylation to the paternal *H19* promoter, indicating a *cis*-regulatory role for the ICR in paternal repression. This had been the prevailing model for how the ICR silences paternal *H19* in *cis*. Our data indicates a novel regulatory role for DNA methylation at the *H19* ICR in repression of *H19* directly. In mice that inherited a mutant paternal allele in which 8 CpGs within the ICR but outside of CTCF binding sites had been deleted, *H19*^{ICR-8nrCG} allele, significant levels of paternal *H19* expression were detected despite maintaining a hypermethylated ICR and promoter (figures 2.5, 2.7-2.9). Therefore, we conclude that while *H19* promoter methylation is necessary for repression, it is clearly not sufficient. This is particularly the case when total *H19* is expressed very highly. In these tissues, the silent *H19* allele is in an environment that is conducive to expression, with all the proper transcriptional machinery actively transcribing the normally active allele. Therefore, multiple levels of repression may be necessary to ensure silencing. Our data highlights the importance of non-promoter methylation as a means of repression when promoter methylation alone is insufficient.

One remaining question is how does methylation at the *H19* ICR act from a distance to silence *H19*? The repressive NuRD complex has been implicated in regulation of paternal *H19* repression. Depletion of NuRD components MTA-2 or MBD3 resulted in biallelic *H19* expression in blastocysts (Ma et al., 2010; Reese et al., 2007). It is possible that DNA methylation at the *H19* ICR recruits the NuRD complex, resulting in a repressive chromatin environment and *H19* silencing. With depletion of methylation at the ICR, there might be a decrease in NuRD recruitment resulting in a more permissive chromatin environment. Of note, MBD2 also is a NuRD complex component, although MBD2 and MBD3 form mutually exclusive complexes (Baubec et al., 2013; Gunther et al., 2013; Le Guezennec et al., 2006). Because we did not detect any loss of imprinting in *Mbd2* null mice, it is likely that MBD3-NuRD complexes exclusively act at *H19* in preimplantation embryos and cannot be compensated for by MBD2-NuRD complexes. However, this hypothesis is difficult to confirm biochemically due to the low amounts of material that can be collected from preimplantation embryos.

6.2 CpG content mediates paternal *H19* repression

It can be argued that the mutations made to the 8nrCG ICR disrupted a binding site for a repressor or generated a binding site for an activator. We do not believe this to be the case for three reasons. First, other than the presence of CTCF sites, the ICR is poorly conserved among species (Frevel et al., 1999; Stadnick et al., 1999). Secondly, DNase footprinting of the paternal methylated *H19* ICR had not detected any footprints (Szabo et al., 2000). Lastly, there have been two other mouse mutants reported to have

similar phenotypes to the $H19^{ICR-8nrCG}$ allele when paternally inherited; the $H19^{ICR-\Delta IVS}$ (Ideraabdullah et al., 2011) and $H19^{SilK}$ (Drewell et al., 2000) alleles. The ΔIVS mutant ICR has a deletion of the intervening sequence between CTCF sites 2 and 3, deleting 873 base pairs of the ICR (figure 2.1). The SilK mutant ICR deleted 1.2 kilobases of sequence, overlapping with the distal half of the ICR (figure 2.1). When paternally inherited, both of these mutant ICRs maintained methylation but paternal $H19$ was detected. The sequence deleted in the $H19^{SilK}$ allele had been described as a silencer in *Drosophila* when introduced as a transgene (Lyko et al., 1997). Later it was found that silencing in *Drosophila* was mediated by the *Drosophila* specific factor Su(Hw) (Schoenfelder and Paro, 2004). These three disparate mutants with similar phenotypes contain no sequence mutations common to all mutants. The one common feature is that they have lowered CpG content at the ICR. We therefore posit that decreased CpG content, rather than disruption of a specific element resulted in paternal $H19$ expression from the mutant alleles.

6.3 CpG content does not have a role in methylation maintenance

Studies at the endogenous locus in mice have indicated that the ICR harbors *cis*-elements essential for maintaining paternal DNA methylation. The $H19^{DMD-9CG}$ allele (mutated 9 CpGs within CTCF sites, figure 2.1) properly acquired methylation in sperm, but upon paternal inheritance, became hypomethylated during embryogenesis. Loss of methylation associated with the paternal $H19^{DMD-9CG}$ allele could have been the result of either (1) CTCF aberrantly binding to CpG-depleted binding sites causing

hypomethylation of the entire allele, or (2) decreased CpG density rendered the ICR unable to be recognized for maintenance. Because paternal inheritance of the *H19*^{ICR-8nrCG} allele maintained methylation we conclude that CpG content at the ICR does not coordinate methylation maintenance in the preimplantation embryo. Therefore, it is likely that in mice with a paternal *H19*^{DMD-9CG} allele, CTCF bound the mutant allele resulting in hypomethylation.

6.4 Further elucidation of the mechanism for paternal repression of *H19*

Here, we have shown significant levels of paternal *H19* expression when the number of CpGs at the ICR was decreased by 8 (~16% depletion). What remains unclear, is if there is a specific threshold of DNA methylation density necessary for silencing, or if repression is additive, with increased repression correlated with increased number of CpGs. Unfortunately, we were unable to investigate this question using an *in vitro* repressor assay described in chapter 2.6. Using this assay we were unable to reproduce derepression that was observed in mice. One potential problem with the repressor assay could be that at the endogenous locus there is interaction between the ICR and the *H19* promoter. A different promoter may not interact with the ICR in the same manner. Therefore, it would be of interest to establish an *in vitro* repressor assay using the *H19* promoter. If insertion of mutant ICRs upstream of the *H19* promoter driving reporter expression could recapitulate derepression seen in the mouse, this assay could be used to better define how many CpGs are necessary at the ICR to maintain silencing.

Furthermore, by performing this assay in various cell-types we can determine tissue-specificity for repression.

There are still remaining questions regarding how ICR DNA methylation represses expression in *cis*; (1) is DNA methylation at the ICR critical for establishing methylation at the *H19* promoter and (2) is all DNA methylation equally as effective in repressing? Comparison of mice that have paternally inherited the *H19*^{ICR-8nrCG} or *H19*^{DMD-9CG} alleles indicates that CpGs within (but not outside) CTCF binding sites are critical to prevent full activation of paternal *H19*. To address these questions one could make a targeted mouse mutant in which all CpGs within the ICR but outside of CTCF binding sites are mutated. Allele-specific expression analysis in mice that paternally inherit the mutant allele would indicate whether methylation exclusively at CTCF binding sites (which should still inhibit CTCF binding) is sufficient to prevent full activation of paternal *H19*. Methylation analysis at the paternal *H19* promoter region would indicate if the promoter gains methylation despite the fact that the ICR is hypomethylated. These experiments would further define ICR-mediated paternal *H19* repression.

6.5 *H19*^{ICR-8nrCG} allele and implications for human disease

In addition to defining mechanisms of imprinted repression, these studies highlight the importance of studying subtle genetic perturbations for disease etiology. Reports have identified epimutations at the *H19/Igf2* locus in SRS patients associated with biallelic *H19* expression (Bartholdi et al., 2009; Begemann et al., 2010; Gicquel et

al., 2005). The 8nrCG mutant, presented here, suggests that single base pair mutations play key roles in deregulation of the *H19/Igf2* locus. Although disease phenotypes were not identified in our analysis, it is possible that the *H19^{ICR-8nrCG}* allele is sensitized to secondary genetic/epigenetic mutations or exposure to environmental factors that could result in SRS-like features. Further studies that combine mutant models or include environmental perturbation may be necessary to generate a mouse model of SRS.

We have shown how subtle changes in non-promoter DNA methylation could disrupt gene-regulation. This finding is of particular concern for studying human cancers. The cancer epigenome is characterized by global hypomethylation and local promoter hypermethylation (Baylin and Jones, 2011). Research has predominantly focused on hypermethylation at promoters of tumor suppressor genes and has resulted in FDA approval of demethylating agents in the management of myelodysplasia and acute myelogenous leukaemia (Azad et al., 2013). We have shown that hypomethylation in regions flanking genes could play an essential regulatory role in gene expression. Non-promoter hypomethylation could cause upregulation of oncogenes driving cancer progression. It will therefore be important for future studies to focus on the global hypomethylation in cancers and analyze the potential off-target effects that demethylating agents used in treatments have on these regions.

6.6 Individual MBD proteins are dispensable for normal imprinting in the mouse

Studies have clearly indicated a role for DNA methylation in allele-specific marking and repression of imprinted loci (Bourc'his et al., 2001; Kaneda et al., 2004;

Kato et al., 2007; Li et al., 1993; Weaver et al., 2010). However, *trans*-acting factors required for DNA methylation dependent repression remain unclear. Here, we investigated the role that MBD family proteins, specifically MBD1 and MBD2, have in allele-specific repression at imprinted loci. Surprisingly, we find that mouse tissues that highly express many imprinted genes (embryos, placentas, yolk sacs and neonatal brains) retained proper imprinting without any functional MBD1 or MBD2 (tables 3.1-3.2). We have therefore confirmed studies performed on adult tissues indicating that MBD2 is dispensable for proper imprinting, and have shown for the first time that MBD1 also is dispensable for imprinted repression.

There remains the possibility that the MBD proteins have redundant functions. Initial phenotyping of the *Mbd1*^{-/-} and *Mbd2*^{-/-} mutant mice revealed somewhat subtle, but distinct phenotypes, suggesting that these proteins regulate discrete sets of genes. Recent ChIP-seq analysis in which tagged-MBD proteins were expressed in mouse ES cells indicate that the MBD proteins that bind methylated DNA (MECP2, MBD1, MBD2 and MBD4) have overlapping enrichment profiles with strongest interaction detected at methylated, CpG-dense, and inactive regulatory regions (Baubec et al., 2013). Although it is unclear if MBD proteins are involved in regulation of imprinted repression, it is likely that multiple MBD proteins bind and are able to compensate for deficiency of a single protein.

Our attempts to test redundancy using RNAi-based knockdown have been unable to show definitively whether these proteins have compensatory functions. We have been able to severely decrease overall levels of MBD1 and MECP2 in *Mbd2* null MEFs, but

substantial amounts of protein still remained (figure 3.7). Thus, it is unclear if remaining protein was enough to confer proper allele-specific repression, or if these proteins have no role in imprinting. It is therefore of utmost importance to test genetically for compensation. As described in chapter 3.6 we are currently breeding to obtain *Mbd1*^{-/-} *Mbd2*^{-/-} mice. Analysis of these double mutant mice would be ideal to uncover functional redundancy, as the *Mbd1* null and *Mbd2* null phenotypes are quite subtle. Once we have obtained the *Mbd1*^{-/-} *Mbd2*^{-/-} mutant (which requires recombination as described in chapter 3.6) we can easily breed for triple *Mbd1*^{-/-} *Mbd2*^{-/-} *Mecp2*^{-y} mutants.

6.7 MBD2 and MBD3 form functionally distinct NuRD complexes *in vivo*

Intriguingly, the MBD protein that does not bind methylated DNA, MBD3 (Ohki 1999), has been implicated in allele-specific repression at *H19* (Reese et al., 2007). MBD3 and MBD2 are the most similar of the MBD proteins with 77% sequence conservation outside of the MBD domain (Clouaire and Stancheva, 2008) and both are members of the NuRD complex. Purification and analysis of NuRD complexes indicates that MBD2 and MBD3 are mutually exclusive components (Le Guezennec et al., 2006). Recent ChIP-seq analysis reveals differential genome-wide binding for MBD3- NuRD and MBD2- NuRD complexes (Baubec et al., 2013; Gunther et al., 2013), which would suggest functional differences between the two complexes. Whereas blastocysts depleted of MBD3 exhibit biallelic *H19* expression and loss of methylation at the *H19* ICR (Reese et al., 2007), *Mbd2* null mice do not display imprinting defects. Our work supports the

idea that MBD2 and MBD3 containing NuRD complexes have functional differences in regulating gene expression *in vivo*.

6.8 MBD proteins: gene-specific or global regulators of repression

Questions still remain as to how these proteins function *in vivo* and why phenotypes predominantly manifest in the brain even though expression is ubiquitous. Overall, our data are in concert with other *in vivo* studies that have been unable to define specific genes regulated by individual MBD proteins. As opposed to early *in vitro* studies in which overexpression of MBD proteins caused repression of a methylated reporter gene (Boeke et al., 2000; Jones et al., 1998; Nan et al., 1997; Nan et al., 1998; Ng et al., 1999), studies of the null mice have produced a very small number of genes that are regulated by MBD proteins (Hutchins et al., 2002; Liu et al., 2013; Liu et al., 2010; Phesse et al., 2008). Again, if these proteins are highly redundant, changes in expression would not be expected.

There has been great interest in defining genes that are regulated by MECP2 as these could cause symptoms of Rett Syndrome and would be therapeutic targets. Numerous studies have investigated changes in gene expression in *Mecp2* null mouse brains, however, few and subtle changes in gene expression have been identified (Guy et al., 2011). Interestingly, increased transcription of repetitive elements and increased global levels of histone acetylation have been detected in *Mecp2* null mouse brains, suggesting that MECP2 might be playing a more global regulatory role to subtly fine-tune expression (Guy et al., 2011; Shahbazian et al., 2002; Skene et al., 2010). Moreover,

ChIP-seq analysis indicated that MBD proteins binding profiles tract with DNA methylation levels, supporting the idea that MBD proteins act globally rather than at specific loci (Baubec et al., 2013).

It remains unknown as to why deficiencies of these proteins cause predominantly brain-specific phenotypes despite being ubiquitously expressed. One potential mechanism is that DNMT1 (rather than the MBD proteins) is the critical factor for setting up repressive chromatin as it deposits DNA methylation during replication. Like the MBD proteins, DNMT1 has been shown to interact with chromatin modifiers and transcriptional repressors, for example; HDAC1/2 (Fuks et al., 2000; Robertson et al., 2000; Rountree et al., 2000), EZH2 (Vire et al., 2006) and HP1 (Smallwood et al., 2007). The MBD proteins could be playing a reinforcement role to maintain chromatin state when cells are not replicating. It is possible that in most tissues, where replication is ongoing, MBD proteins are not critical, as DNMT1 is sufficient for repression. However, in the brain where neurons are post mitotic, MBD proteins have a greater role in reading DNA methylation marks and maintaining chromatin state in the absence of replication. If this is the case, it is not surprising that the most striking phenotypes manifest in the adult brain and that global/subtle changes are detected rather than regulation at specific genes, including imprinted loci.

6.9 TET1 and TET2 mediate DNA demethylation at imprinted loci in PGCs

Recent reports suggest that DNA demethylation is mediated by 5mC oxidation to 5hmC in the zygote and PGCs (Gu et al., 2011; Hackett et al., 2013; Inoue and Zhang,

2011; Iqbal et al., 2011; Wossidlo et al., 2011; Yamaguchi et al., 2013). Our analysis in the germline of *Tet1^{-/-}Tet2^{-/-}* mice indicates that, indeed, demethylation at imprinted loci requires 5mC oxidation to 5hmC, which is mediated by TET1 and TET2. The mechanism by which demethylation occurs after conversion to 5hmC and if this mechanism is the same for all imprinted loci remains unclear. However, our analysis in *Tet1/Tet2* DKO sperm indicates a locus-specific sensitivity to TET1 and TET2 deficiency.

Various models for how DNA demethylation can occur after conversion to 5hmC have been proposed (figure 1.7). Components of the BER pathway, such as the glycosylase, TDG, and deaminase, AID, have been implicated in erasure of methylation in the germline. AID expression, however, in E9.5-13.5 PGCs is very low (Kagiwada et al., 2013) and unlike TET deficiency, AID deficiency in PGCs does not lead to profound demethylation defects (Popp et al., 2010). TDG, on the other hand, has relatively high levels of expression in PGCs (Kagiwada et al., 2013) and TDG deficient E13.5 PGCs retained methylation at the *Igf2* promoter (Cortellino et al., 2011). Accordingly, in TDG-deficient ES cells, accumulation of 5fC and 5caC were detected, suggesting that TDG is required for active demethylation of 5hmC (Shen et al., 2013). Another potential model for demethylation is that 5hmC is passively demethylated in a replication dependent manner, which has been reported in PGCs for the imprinted genes *Peg3* and *Peg10*. Moreover, bisulfite sequencing (which cannot distinguish between 5mC and 5hmC) analysis revealed that *H19*, *Nnat*, *Peg3*, *Snrpn*, *Kcnq1ot1* and *Peg10* DMRs follow slower or close to expected kinetics for purely passive demethylation in PGCs (Kagiwada

et al., 2013). In studying PGCs deficient in TET1 and TET2, we impeded 5mC conversion to 5hmC and detected retention of methylation at imprinted loci, but cannot conclude whether other enzymes might be necessary for normal DNA demethylation.

6.10 Locus-specific susceptibility to TET deficiency

Methylation analysis of TET1 and TET2 deficient sperm indicate that some maternally-methylated DMRs were fully erased in the male germline, while others were not (figure 4.4). Therefore, some loci are more sensitive to loss of TET function. In PGCs, timing of 5mC oxidation to 5hmC varies between DMRs. For example, 5hmC is detected earlier for *Kcnq1ot1* and *Igf2r* than it is for *Peg3* and *Peg10* (Hackett et al., 2013). Interestingly, in our studies, *Kcnq1ot1* exhibited aberrant methylation in DKO sperm whereas *Peg3* did not. It is possible that the variability in timing of 5hmC conversion is indicative of different mechanisms of erasure used at these loci, some being more dependent on TET function.

Many reports indicate that passive demethylation is responsible for bulk DNA demethylation in PGCs, supported by the fact that UHFR1 is very lowly expressed and DNMT1 is excluded from replication foci in these cells (Kagiwada et al., 2013; Seisenberger et al., 2012). It is likely that passive DNA demethylation could occur at imprinted loci in the absence of 5hmC conversion. We propose this to be the case because we do detect full erasure of methylation at some imprinted DMRs in DKO sperm. Moreover, at loci where we do detect retention of methylation, levels are reduced from the expected 50% (if no erasure occurred) (figure 4.4). Furthermore, levels of

aberrant methylation were quite variable between samples. We therefore hypothesize that passive DNA demethylation can occur irrespective of 5mC oxidation, though at some loci this mechanism is not sufficient for complete erasure.

6.11 Comparison of two independent *Tet1*^{-/-}*Tet2*^{-/-} mutant mice

After initiation of our studies investigating the role of TET1 and TET2 in imprint erasure, the Jaenisch laboratory published analysis of an independent *Tet1*^{-/-}*Tet2*^{-/-} mutant (Dawlaty et al., 2013). Whereas we find normal development of mice deficient for TET1 and TET2 that were conceived from double heterozygous parents, Dawlaty and colleagues report that the *Tet1*^{-/-}*Tet2*^{-/-} mice were detected at a 3-fold reduced frequency. This perinatal lethality phenotype was only partially penetrant with some DKO mice developing normally (Dawlaty et al., 2013). Seemingly, this is a major discrepancy, but we did not have the number of litters necessary to detect incomplete penetrance of lethality of DKO mice. Because we set up double heterozygous mice for our matings, there was only a 1/16 chance of obtaining a *Tet1*^{-/-}*Tet2*^{-/-} mouse. Mice were genotyped at weaning, and when a *Tet1*^{-/-}*Tet2*^{-/-} mouse was identified it looked grossly normal. For this reason, we did not pursue potential perinatal lethality. Dawlaty and colleagues also identified defects in midgestation embryos and malformations in pups deficient in TET1 and TET2. However, these analyses were performed in litters conceived from mating *Tet1*^{+/-}*Tet2*^{+/-} females with *Tet1*^{-/-}*Tet2*^{-/-} males (Dawlaty et al., 2011). Therefore, these abnormalities could have resulted from the combination of having a TET1/TET2

deficient father and a TET1/TET2 depleted mother. Because we did not set up similar crosses we cannot make a comparison with our mutant mice.

Dawlaty et al. analyzed DNA methylation in one TET1/TET2 deficient sperm sample, and similar to our results, reported increased methylation at *Mest*, normal methylation at *H19* and *Peg3*, and no changes in global methylation levels (figure 4.4-4.5). Likewise, we both find subfertility of DKO females and increased levels of methylation at *H19* in progeny from these females. Dawlaty et al. additionally detected aberrant methylation at a number of imprinted loci in progeny of DKO males. We have not done this analysis, although such studies are planned in the future.

Overall, our studies are in agreement with those published by the Jaenisch laboratory. However, direct comparison is somewhat difficult as different matings were typically used to obtain *Tet1^{-/-}Tet2^{-/-}* or a small sample size does not allow proper statistical analysis.

6.12 Future directions for analysis of TET-mediated erasure of imprints

We have clearly shown that erasure of imprints in the germline was compromised without functional TET1 and TET2. Furthermore, aberrant methylation was heritable. Nevertheless, numerous experiments are required to fully characterize the effects that loss of TET1 and TET2 have on imprint erasure. Firstly, our analysis in DKO sperm indicated that some DMRs properly erase methylation. These DMRs need to be analyzed in DKO E13.5 PGCs. Presence of methylation at these DMRs in DKO E13.5 PGCs

would indicate that there was a delay in erasure, whereas absence of methylation would indicate that erasure of these DMRs is independent of TET proteins.

Additionally, analysis needs to be performed for retention of methylation in mature oocytes. Because we do detect increased methylation at paternally-methylated DMRs in offspring of DKO females, we expect that oocytes from TET1/TET2 deficient females would similarly retain methylation. To this end, we also need to analyze methylation in progeny of DKO males. Based on our sperm data, we expect to detect high levels of methylation on specific maternally-methylated loci, namely, *Mest*, *Grb10* and *Kcnqlot1*. Whereas our initial observations indicate that TET1/TET2 deficient males are fertile and offspring appear normal, it is possible that retention of methylation at imprinted loci is associated with tissue-specific expression changes, which may exert more subtle phenotypes such as growth defects or behavioral abnormalities, as observed with *Grb10*, *Mest* and *Peg3* mutant mice (Garfield et al., 2011; Lefebvre et al., 1998; Li et al., 1999).

Moreover, although aberrant methylation in DKO mice is inherited in progeny, it is unknown if this results in expression abnormalities. Allele-specific expression analysis can be performed in progeny of *Tet1^{-/-}Tet2^{-/-}* females mated with wild type C7 males, or vice-versa. This would allow us to determine if increased methylation detected in progeny results in biallelic expression of the corresponding genes.

Furthermore, we would like to ensure that compromised erasure of imprints detected in DKO mice were intrinsic to PGCs. That is, retention of methylation was not

due to overall abnormal development of PGCs or lack of TET1 and TET2 in the inner cell mass as these embryos developed. In order to do this, we have been breeding for conditional germline-specific knockouts of *Tet1* and *Tet2*.

6.13 Stability of methylation imprints in spermatogonial stem cells

The reversibility of epigenetic marks make them particularly susceptible to environmental influences that act to disrupt the epigenome (McCarrey, 2012). Specifically, manipulations associated with ART procedures, which occur during times of epigenetic reprogramming, have been associated with aberrant DNA methylation (Eroglu and Layman, 2012). We therefore wanted to assess how the establishment and maintenance of imprints could be disrupted in a system experiencing environmental perturbations. To this end, we analyzed imprints in spermatogonial stem cells (SSCs) subject to varying environmental insults. Recent advances in understanding SSCs have lead to a variety of techniques with great potential for fertility treatment. SSCs can be cultured indefinitely, transplanted into recipient mice and colonize the seminiferous tubule, and maintain stem cell function despite freezing and thawing (Avarbock et al., 1996; Brinster and Avarbock, 1994; Kanatsu-Shinohara et al., 2005). These techniques have great implications for treatment of male infertility, including preserving the germline of prepubertal boys undergoing radiation or chemotherapy causing infertility (Brinster, 2007).

Our findings indicate that methylation at paternally-methylated DMRs was stable throughout extreme aging both *in vivo* and *in vitro*. Additionally, cryopreservation for

~14 years and thawing of SSCs did not disrupt genomic methylation or methylation at imprinted loci. Furthermore, aged or cryopreserved SSCs could be transplanted into a donor mouse and produce sperm to be used for ICSI. Importantly, all mice born from ICSI had normal methylation at all imprinted loci assessed, regardless of stresses undergone by the SSCs.

These results confirm the potential of using these techniques for fertility treatment in humans. As treatments for pediatric cancers improve, many survivors are left infertile as a side-effect. Cryopreservation of testicular tissue, prior to cancer therapies provides an approach to preserve the patient's germline. Our results here indicate that in mice, fertility can be acquired by transplantation of SSCs that had undergone a variety of environmental stresses, and emphasizes the need to study and improve these techniques for human SSCs.

6.14 Decreased stem cell function in aged SSCs

Little is known about how aging influences SSC function, although there is evidence that fertility in male mice begins to decline at about 12 to 24 months of age (Ryu et al., 2006). Whereas *in vivo* and *in vitro* aged SSCs stably maintain DNA methylation at the paternally-methylated *H19* ICR and IG-DMR (figure 5.4), stem cell deficiencies were observed in the aged SSCs. Gene expression analysis indicates that the decision to differentiate or self-renew shifts from self-renewal in younger SSCs to differentiation in aged SSCs. While methylation at imprinted loci has been identified as being particularly sensitive to environmental stresses, this study highlights the

importance of also assessing more global gene expression changes to fully understand cellular deficiencies. Future research should focus on elucidating the underlying mechanisms directing gene expression changes, particularly at the identified candidate genes. One possibility is that there is a change in chromatin compaction specifically at these loci. Analysis of DNA methylation and histone modifications at these loci will give greater insight into the mechanism of age related SSC deficiencies.

6.15 ICSI and disruption of imprinting

The studies presented here were proof-of-principal experiments in which we showed that normal offspring could be born from either aged or cryopreserved SSCs. However, further examination is required to fully define the effects of these environmental influences on imprinting. Whereas we find normal imprinting in mice born from ICSI (figures 5.4, 5.6-5.8), numerous reports indicate disruption of imprinting associated with various procedures involved in ICSI (de Waal et al., 2012b; Doherty et al., 2000; Fauque et al., 2007; Fauque et al., 2010b; Fortier et al., 2008; Mann et al., 2004; Rivera et al., 2008; Sato et al., 2007). By analyzing mice that had been born, we might have biased our analysis towards assessing only mice that had normal imprinting. Previous studies indicate that many more blastocysts than post-implantation embryos derived from ART displayed imprinting defects (Fauque et al., 2010a). This could suggest that embryos with major epigenetic abnormalities could not implant. Additionally, the placenta has been reported to be particularly susceptible to disruption of imprinting due to manipulations associated with ART (Fauque et al., 2010b; Fortier et al.,

2008; Mann et al., 2004; Rivera et al., 2008). Therefore, to fully assess the effects of long-term cryopreservation or aging of SSCs and subsequent ICSI to obtain offspring, it will be necessary to repeat analysis at ~E9.5, which is the time when previous studies have detected loss of imprinting in both embryonic and placental tissues.

Nonetheless, loss of methylation at imprinted DMRs and behavioral abnormalities have been reported for adult mice born of ART procedures (de Waal et al., 2012a; Ecker et al., 2004; Fernandez-Gonzalez et al., 2004). One study reported loss of imprinting at several genes in adult mice born of ICSI. Loss of methylation was tissue-specific and detected either in muscle or brain (de Waal et al., 2012a). Here, our analysis was limited to liver, and thus we could have missed aberrant methylation marks by not analyzing a wider range of tissues. Therefore, future research should include methylation analysis in a variety of tissues in order to capture any tissue-specific loss of imprinting. Additional studies should also investigate more subtle defects, such as behavioral abnormalities, which have also been detected in adult mice born of ART (Ecker et al., 2004; Fernandez-Gonzalez et al., 2004).

Our analysis of the paternal *H19*^{ICR-8nrCG} allele clearly demonstrated that biallelic expression can be detected even though the ICR remains hypermethylated. Likewise, examples of normal or only slightly affected methylation and abnormal expression have been indicated in ART studies (Fauque et al., 2007; Market-Velker et al., 2010a; Market-Velker et al., 2010b). It is therefore of interest to examine if expression changes occur despite normal methylation patterns in our ICSI-derived mice.

6.16 Conclusion

Overall, the data presented in this dissertation provides novel insights into the mechanisms by which DNA methylation confers imprints. This work has identified *cis*-elements and *trans*-factors either necessary or dispensable for maintenance of allele-specific repression in somatic cells and resetting of imprints in the germline. Our analysis of a mutant paternal *H19* ICR with lowered CpG density provides a novel regulatory role for non-promoter CpG content in regulating expression in *cis*. Furthermore, we have shown that individually MBD1 and MBD2, proteins involved in DNA methylation dependent repression, are not necessary for allele-specific silencing at imprinted loci. Therefore, the MBD proteins either work redundantly in coordinating silencing, or are not involved in imprinted repression. We have also described locus-specific TET-mediated erasure of imprints in the germline. Although further research is necessary to define the mechanism of demethylation, these data provide evidence that active DNA demethylation has a role in imprint demethylation in PGCs. Lastly, our investigation into possible deregulation of imprints upon environmental stress has proven that imprints can be stably maintained in SSCs throughout extreme aging and cryopreservation. Importantly, upon transplantation, these SSCs produce viable sperm that can be used in ICSI to derive normal offspring. These data confirms the potential use of these techniques for germline preservation. The findings presented in this dissertation highlight the multifaceted nature of DNA methylation dynamics and repression. Continued investigation to better define mechanisms involved in normal imprint regulation and identification of environmental perturbations that result in

disruption of these processes will provide important insights into the causes and consequences of improper gene expression.

CHAPTER SEVEN

MATERIALS AND METHODS

7.1 Targeting and mouse generation of the *H19*^{ICR-8nrCG} allele

129/SvJ genomic DNA fragment spanning the *H19* ICR [described in (Engel et al., 2004)] was mutated at each of the four regions indicated below using the Quikchange site-directed mutagenesis kit (Stratagene) : GTACCTCGTGGACT[CG->CA]GACTC, TGGTGATTTG[CG->GC]CTTT[CG->GC]TAT, ACACAGCC[CG->CT]AGAT[CG->CT]TCAGT, CCTTCA[CG->CT]AT[CG->CT]AT[CG->CT]GTTCA (mutations italicized). The targeting vector was generated as described previously (Engel et al., 2004) using this mutated ICR in place of the DMD-9CG mutation. Mutations of CpGs were confirmed by sequencing.

Targeting vectors were linearized and electroporated into E14.1 ES cells (Kuhn 1991). G418-resistant positive clones were isolated and targeting to the *H19/Igf2* locus was confirmed by restriction digestion followed by southern hybridization (figure 2.3). Correctly targeted ES cell clones were injected into C57BL/6J (B6) blastocysts and mice were generated by the Transgenic & Chimeric Mouse Facility at the University of Pennsylvania. Chimeras were obtained and mated to B6 mice. Germline transmission of the targeted mutant alleles was confirmed in the agouti progeny by DNA isolated from tails and analyzed by Southern blot (figure 2.3).

The *neo^r* cassette (flanked by loxP sites) was excised in the mouse by mating heterozygous mutant mice to mice expressing Cre recombinase under the control of the human cytomegalovirus promoter on a B6 genetic background (obtained from Dr. Edward Morissey, University of Pennsylvania). *neo^r* excision was confirmed in the progeny by Southern blot (figure 2.3).

7.2 Mice

All mouse studies adhered to procedures approved by the Institutional Animal Care and Use Committee at the University of Pennsylvania.

8nrCG heterozygous mutant mice were maintained by mating to C57BL/6 (B6) (The Jackson Laboratory). For imprinting analysis 8nrCG heterozygous mutant mice were crossed with C57BL/6(CAST7) (C7). C7 mice contain a *Mus musculus castaneus* (CAST; The Jackson Laboratory) chromosome 7s on a B6 background. Matings were carried out in both directions to obtain F1 hybrids for analysis.

Mice carrying a null *Mbd1* mutation (*Mbd1*^{+/-}; from the mutant mouse regional resource centers) were mated either to B6 or C7 for maintenance. To generate *Mbd1* null mice, *Mbd1*^{+/-} are mated with *Mbd1*^{+/-} of the same background (B6 or C7). For imprinting analysis *Mbd1*^{+/-} (B6) were mated with *Mbd1*^{+/-} (C7). Matings were carried out in both directions to obtain F1 hybrids for analysis.

Mice carrying a null *Mbd2* mutation (*Mbd2*^{+/-}; from Dr. Steven Reiner, University of Pennsylvania) were mated either to B6 or C7 for maintenance. To generate *Mbd2* null mice, *Mbd2*^{+/-} are mated with *Mbd2*^{+/-} of the same background (B6 or C7). For

imprinting analysis *Mbd1*^{+/-} (B6) were mated with *Mbd1*^{+/-} (C7). Matings were carried out in both directions to obtain F1 hybrids for analysis.

To obtain *Mbd1*^{-/-}*Mbd2*^{-/-} double mutant mice, we cross *Mbd1*^{+/-}*Mbd2*^{+/-} mice with *Mbd1*^{-/-} mice of the same background (either B6 or C7).

7.3 Genotyping

Genotyping is performed on DNA isolated from an ear clip. DNA is prepped by incubating an ear clip in 100µL of solution A (25mM NaOH, .2mM EDTA) at 95°C for one hour followed by addition of 100µL solution B (40mM Tris). 2µL of DNA is used for each genotyping PCR.

For each PCR reaction DNA was added to 1X GoTaq (Promega) and .25-.5µM primer master mix. All PCR cycling conditions were as follows: 2 min at 95°C; 36 cycles of 15 sec at 95°C, 15 sec at annealing temperature (listed in table 7.1), 20 sec at 72°C.

Breeding to obtain null *Mbd1* or *Mbd2* mutant alleles on a C7 background, the following MIT markers were used; 7.305, 7.57, 7.112, 7.52 7.27, 7.211, 7.163, 7.148, 7.5 7.222, 7.285, 7.207, 7.140, 7.362.

Mutant/region	Primer sequence (5'-3')	Expected size (bp)	Annealing Temperature (°C)	notes
CAST 7	MIT markers	NA	55	
8nrCG	NR3F:GGGTCACCCAAATAGGGATT NR3R:TGACCCATGAGTTTGCCATA	221	58	AvaI will cut mutant; BglII will cut WT
8nrCG	H19-2.3F: CAATGTTTCATAAGGGTCATGGGGTG H19-2.0R: CGTAAGGTGTCACAAATGCCTGATCCC	Mut:250 WT:200	58	
Mbd1	XYZ59: TCTTCTCAGACTGAGAAGGGTGA XYZ60: CACTGAACATTGCCAGAGCACA XYZ:61 AAACGGCGGATTGACCGTAATGG	Mut:500 Wt: 300	55	1µL of 10 µM primer used for each
Mbd2	P61: ACG CTG GCC TAG TGC CGT GC P62: TTG TGG TTG TGC TCA GTT C ENP1: TCC GCA AAC TTC TAT TTC TG	Mut:200 WT:600	55	1 µL of 10 µM primer used for each

7.4 DNA isolation

Tissues were incubated overnight at 55°C in 500µL of lysis buffer (50mM Tris-HCl (pH8), 100mM EDTA, .5% SDS, .5mg/ml proteinase K). DNA was then isolated by performing two phenol/chloroform extractions. DNA was dissolved in 50µL of dH₂O.

Sperm were taken from the cauda epididymis and incubated overnight at 55°C in 500µl sperm lysis buffer (10mM Tris-HCl (pH 7.5-8), 10mM EDTA, 2%SDS) with 5µL β-mercaptoethanol and 12µL proteinase K. DNA was then isolated by performing two phenol/chloroform extractions. DNA was dissolved in 50µL of dH₂O.

7.5 Methylation sensitive southern at *H19*

10µg genomic DNA was digested with *PvuII* and *StuI* in combination with *HapII* or *MspI* to analyze the methylation at the *H19* promoter and structural gene. A 2.5-kb *EcoRI-StuI* fragment was used as a probe (figure 2.9).

7.6 Bisulfite mutagenesis

For SSC aging studies, bisulfite mutagenesis of DNA was carried out in agarose beads (Olek et al., 1996).

For 8nrCG mutant studies, bisulfite mutagenesis was performed using MOD50 Imprint DNA Modification Kit (Sigma-Aldrich) according to manufacturer's protocol.

For all other studies, bisulfite mutagenesis was performed using EpiTect Bisulfite Kit (Qiagen) following manufacturer's protocols.

7.7 PCR amplification of bisulfite DNA for sequencing or COBRA

Nested PCR was performed on bisulfite treated DNA. 50ng of DNA was used for the first round of PCR and 1µL of amplified DNA was used for second round PCR. For PCR reaction PuReTaq Ready-to-go PCR beads (GE Healthcare) were used with .3µM primers in a final volume of 25µL. All primers and PCR conditions are listed in bisulfite assays section. For COBRA, 5-10µL of second round PCR product was cut with the appropriate enzyme as listed in section 7.8.

For sequencing, second round PCR products were separated by gel electrophoresis on a 1% agarose gel. The band was excised and purified using the QiaQuick Gel Extraction kit (Qiagen) according to manufacturer's protocol and eluted in 30µL dH₂O. Purified PCR product was cloned using the TOPO-TA kit (Invitrogen) follow manufacturer's protocol. A minimum of 10 clones from each sample were sequenced by the University of Pennsylvania Sequencing Facility. Sequencing results were analyzed using MacVector.

7.8 Bisulfite assays

Region: *H19* ICR Repeat1-2

Accession: U19619

Reference: (Tremblay et al., 1997)

First round:

Primer 1: BMsp2t1

Sequence (5'-3'): GAG TAT TTA GGA GGT ATA AGA ATT

Primer 2: BHha1t3

Sequence (5'-3'): ATC AAA AAC TAA CAT AAA CCC CT

Second round:

Primer 1: Bmsp2t2c

Sequence (5'-3'): GTA AGG AGA TTA TGT TTA TTT TTG G

Primer 2: BHha1t4ct

Sequence (5'-3'): CTA ACC TCA TAA AAC CCA TAA CTA T

Product size: 423 bp

For COBRA: *HinfI* will cut a methylated sequence to produce 200 and 210bp fragments.

PCR Conditions: denature 94 °C 2min; 35 cycles of denature 94°C for 10 sec, anneal 55°C 30 sec, extend 72°C 1 min

NOTE- decrease ramping speed to annealing temp to .5°C/sec

Region: *H19* ICR Repeat 3

Accession: U19619

Reference: (Davis et al., 2000)

First Round:

Primer 1: BHha5t2

Sequence (5'-3'): TTG TGA GTG GAA AGA TTA ATT GTT TGG

Primer 2: BHha5t3

Sequence (5'-3'): ATA CAC ACA TCT TAG CAC CCC TAT AAA TCC
C

Second Round:

Primer 1: BHha5t

Sequence (5'-3'): TAG AGA TAG TTA AAG TTA AGG TTT GTT TAT
G

Primer 2: BHha5t3

Sequence (5'-3'): ATA CAC ACA TCT TAG CAC CCC TAT AAA TCC
C

Product size: 333 bp

PCR Conditions: denature 94 °C 2min; 35 cycles of denature 94°C for 10 sec,
anneal 55°C 30 sec, extend 72°C 1 min

NOTE- decrease ramping speed to annealing temp to .5°C/sec

Region: *H19* ICR Repeat 4

Accession: U19619

Reference: (Thorvaldsen et al., 2002)

First Round:

Primer 1: BTV3-1

Sequence (5'-3'): GGT AAA TTT ATG GGT TAT TTA AGG

Primer 2: BTV3-4

Sequence (5'-3'): CCC AAC CTC TAC TTT TAT AAC

Second Round:

Primer 1: BTV3-2

Sequence (5'-3'): AAT GTT TAT AAG GGT TAT GGG GTG G

Primer 2: BTV3-3

Sequence (5'-3'): CCT AAA TTC AAT AAA ACA TTA CAA

Product size: 425 bp

PCR Conditions: denature 94 °C 2min; 35 cycles of denature 94°C for 10 sec,
anneal 55°C 30 sec, extend 72°C 1 min

NOTE- decrease ramping speed to annealing temp to .5°C/sec

Region: *H19* Promoter Proximal

Accession: U19619

Reference: (Thorvaldsen et al., 2006)

First Round:

Primer 1: B12 (BH19-0.9f)

Sequence (5'-3'): GTT GAG GAT TTG TTA AGG TGT TAT TGT

Primer 2: B14 (BH19-0.5r)

Sequence: AAT AAT AAC TAA TTT AAA CAC TCC TCA CC

Second Round:

Primer 1: B13 (BH19-0.8f)

Sequence (5'-3'): GAG TGG TTA TGA TTG GTT AGT TTT TGA G

Primer 2: B14 (BH19-0.5r)

Sequence: AAT AAT AAC TAA TTT AAA CAC TCC TCA CC

Product size: 380 bp

PCR Conditions: denature 94 °C 2min; 35 cycles of denature 94°C for 10 sec, anneal 55°C 30 sec, extend 72°C 1 min

NOTE- decrease ramping speed to annealing temp to .5°C/sec

Region: *Snrpn* DMR

Accession: AF081460

Reference: (Lucifero et al., 2002)

First round:

Primer 1: *SnrpnA*

Sequence: TAT GTA ATA TGA TAT AGT TTA GAA ATT AG

Primer 2: *SnrpnD*

Sequence (5'-3'): AAT AAA CCC AAA TCT AAA ATA TTT TAA TC

Second round:

Primer 1: *SnrpnB*

Sequence (5'-3'): AAT TTG TGT GAT GTT TGT AAT TAT TTG G

Primer 2: *SnrpnC*

Sequence (5'-3'): ATA AAA TAC ACT TTC ACT ACT AAA ATC C

Product Size: 451

For COBRA: *HinfI* will cut only methylated sequence at positions 262 and 316.

PCR Conditions: 2 cycles; 94°C for 4 min, 55°C for 2 min, 72°C for 2 min. 35 cycles; 94°C for 1 min, 55°C for 2 min, 72°C for 2 min

Region: IG-DMR

Accession: AJ320506.1

Reference: (Takada et al., 2002)

First round:

Primer 1: IGDMRF1

Sequence (5'-3'): TTA AGG TAT TTT TTA TTG ATA AAA TAA TGT
AGT TT

Primer 2: IGDMRR1

Sequence (5'-3'): CCT ACT CTA TAA TAC CCT ATA TAA TTA TAC
CAT AA

Second round:

Primer 1: IGDMR2FG

Sequence (5'-3'): TTA GGA GTT AAG GAA AAG AAA GAA ATA
GTA TAG T

Primer 2: IGDMR2RG

Sequence (5'-3'): TAT ACA CAA AAA TAT ATC TAT ATA ACA CCA
TAC AA

Product Size: 483

For COBRA: *HinfI* will cut methylated fragment at positions 62 and 231.

PCR Conditions: 5 cycles of denature 94°C for 1 min, 50°C for 2 min, 72°C for 3 min; 30 cycles of denature 94°C for 30 sec, 50°C for 2 min, 72°C for 1.5 min

Region: *Peg3* DMR

Accession: AF105262.1

Reference: (Ma et al., 2010)

First Round:

Primer 1: Peg3A-BL

Sequence (5'-3'): TTT TGA TAA GGA GGT GTT T

Primer 2: Peg3D-BL

Sequence (5'-3'): ACT CTA ATA TCC ACT ATA ATA A

Second Round:

Primer 1: Peg3B-BL

Sequence (5'-3'): AGT GTG GGT GTA TTA GAT T

Primer 2: Peg3C-BL

Sequence (5'-3'): TAA CAA AAC TTC TAC ATC ATC

Product size: 446

For COBRA: *EcoRV* will cut methylated sequence to produce 114bp and 332bp fragments

PCR Conditions: denature 94 °C 2min; 35 cycles of denature 94°C for 10 sec, anneal 55°C 30 sec, extend 72°C 1 min

NOTE- decrease ramping speed to annealing temp to .5°C/sec

7.9 Luminometric Methylation Assay

500 ng of DNA was digested with 5 units of *MspI* and 5 units of *EcoRI* or 5 units of *HpaII* and 5 units of *EcoRI* in 20µL reactions. After a 4-hour incubation 15µL of Pyrosequencing annealing buffer (Qiagen) was added to each sample. 30µL of each sample was loaded into the Pyrosequencer and analyzed using the PyroMark MD (Qiagen) program with a nucleotide dispensation order of GTGTCACATGTGTG. The ratio of the *MspI/EcoRI* peaks (corresponding to nucleotides 9/10) was compared to the ratio the *HpaII/EcoRI* peaks (nucleotides 9/10) to determine genome-wide methylation levels.

7.10 Pyrosequencing of bisulfite treated DNA

50-100 ng of bisulfite treated DNA was used for PCR. The PyroMark PCR kit (Qiagen) was used following the manufacturers protocol in a 25µL reaction. PCR conditions were: 95°C for 15 min followed by 45 cycles of 95°C for 15 sec, 55°C for 30 sec and 72°C for 15 sec. For *Grb10* annealing temperature was 54°C. 5µL of the biotinylated PCR product was used for each sequencing assay with the appropriate sequencing primer (see chart). Pyrosequencing was performed using PyroMark Q96MD (Qiagen) system following the manufacturer’s protocol and the PyroMark Gold 96 reagents kit (Qiagen). Methylation was analyzed using Qiagen’s Pyro Q- CpG software. See table 7.2 for primer sequences and number of CpGs analyzed.

Table 7.2 Pyrosequencing assays				
DMR analyzed	Forward PCR Primer (5'-3')	Reverse Biotinylated PCR Primer (5'-3')	Sequencing Primer (5'-3')	Number of CpGs Analyzed
<i>H19</i>	GGGTAGGATATA TGTATTTTTTAGG TTG	CTCATAAAACCCATAA CTATAAAATCAT	TGTAAAGATT AGGGTTGT	6
IG-DMR	GTGGTTTGTTATG GGTAAGTTT	CCCTTCCCTCACTCAA AAATTAA	GTTATGGATTG GTGTTAAG	5
<i>Snrpn</i>	GGTAGTTGTTTT TGGTAGGATAT	ACTAAAATCCACAAAC CCAACCTAACCT	AAAAATGTGA GTATGTGTAGT TA	7
<i>Peg3</i>	GGTTTTTAAGGGT AATTGATAAGG	CCCTATCACCTAAATAA CATCCC	AATTGATAAG GTTGTAGATT	6
<i>Kcnq1ot1</i>	TTTTGTGTGATTT TATTTGGAGAGT	CCTCAAACCACCCCT ACT	GTAAGTATTTA AGGTTAGAAG TAGA	7
<i>Mest</i>	GGAGGTTTTATAT AAGTATTTGTTTT T	ACCACCCAACCTAACAC TAAA	GGTTTTATATA AGTATTTGTTT TTT	5
<i>Grb10</i>	GTTGTTTATTATT TGGTTGAGAG	CTACAATAATCCAAAT AATAACAACCTCC	GTTGTTTATTA TTTGGTTGAGA G	4

7.11 RNA extraction

RNA was isolated using Trizol Reagent (Invitrogen) following manufacturer's protocol. RNA was dissolved in 50 μ L RNase free dH₂O. RNA was isolated from E6.5 conceptuses using the Absolutely RNA Microprep Kit (Agilent Technologies) according to manufacturer's protocol and eluted in 30 μ L Elution. All RNA samples were stored at -80°C.

7.12 Reverse transcription

800ng of RNA was DNase treated using RQ1 DNase (Promega) following manufacturer's protocol. Half of the DNase treated RNA was used for reverse transcription with SSIII RT (Invitrogen) following the manufacturer's protocol. The remaining half of the DNase treated RNA was used as a negative control and underwent the same conditions except water was added instead of SSIII RT. cDNA was diluted to ~2ng/ μ L concentration.

7.13 *H19* allele-specific RNase protection assay

For *H19* RNase protection assay 5 μ g of RNA was used with the RPAIII RNase protection assay kit (Ambion) following manufacturer's protocol. The probe was prepared from a 754 bp *Bam*HI-*Stu*I genomic DNA fragment. RNase protection gels were exposed to storage phosphor screens that were scanned on a Typhoon Trio variable mode imager. Band intensities were quantified using ImageJ.

7.14 Allele-Specific expression by RT-PCR and restriction digest

~2ng of cDNA was used for an RT-PCR reaction. For each reaction a master mix was prepared with a final concentration of 1x GoTaq (promega), .3 μ M primers (listed in table 7.3) in a final volume of 15 μ L. PCR conditions were as follows 2 min at 95°C; 30-35 cycles of 15 sec at 95°C, 15 sec at annealing temperature (listen in table 7.3), 20 sec at 72°C. Linear range for individual samples was determined and was usually between 30-35 cycles. 10 μ L of amplification product was cut with appropriate restriction enzyme (listed in table 7.3). Restriction Digests were resolved on a 12% acrylamide gel and band intensities were quantified using ImageJ.

Table 7.3 Allele-specific RT-PCR assays for imprinted genes on mouse chromosome 7						
Gene	Primers (5'-3')	Annealing Temp (°C)	Product Size (BP)	Restriction Enzyme	Digested B allele band size (BP)	Digested C allele band size (BP)
<i>Ascl2</i>	Mas1: TGAGCATCCCACC CCCCTA Mas2: CCAAACATCAGCG TCAGTATAG	58	474	SfcI	474	266, 207
<i>Cdkn1c</i>	P57-L: GCCAATGCGAACGGTG CG P57-4: TACACCTTGGGACCAG CGTACTCC	60	364	TaqAI	306, 58	257, 58, 49
<i>H19</i>	HE2: TGATGGAGAGGAC AGAAGGG HE4: TTGATTCAGAACG AGACGGAC	55	235	Cac8I	173, 62	2235
<i>Igf2</i>	Igf2-18: ATCTGTGACCTCTTGAG CAGG Igf2-20: GGGTTGTTTAGAGCCA ATCAA	58	200	MluCI	180, 20	165, 20, 15
<i>Kcnq1</i>	Lqt1: CATCGGTGCCCGT CTGAACACG Lqt3: TTGCTGGGTAGGA AGAGCTCAG	60	189	BsmFI	189	113, 76
<i>Kcnq1ot1</i>	Lit1F: AATTGGGAACTTG GGGTGGAGGC Lit1R: GGCACACGGTAT GAGAAAAGATTG	60	814	StuI	814	601, 213
<i>Peg3</i>	Pg4: ATGCCCCTCCGTC AGCG Pg7: GCTCATCCTTGTGA ACTTTG	60	487	MnlI	110, 377	487
<i>Zim1</i>	Zm1: CTTCAAGCAGAGC ACAAAGC Zm3: GTGGCACACGAAA GGTTTCTC	59	490	FauI	490	236, 254

7.15 Allele-Specific Lightcycler assay

Allele-specific analysis of *Snrpn* expression was performed using the LightCycler Real-Time PCR system (Roche). ~2ng of cDNA was used for each sample. Each reaction had primers (Sn1: 5'-CTCCACCAGGAATTAGAGGC-3'; Sn3: 5'-GCAGTAAGAGGGGTCAAAGC-3') at .6μM concentration, probes at a .3μM concentration (SnMut: 5'-GAAGCATTGTAGGGGAAGAGAA-FL-3'; SnAnc: 5'-RED40-GGCTGAGATTTATCAACTGTATCTTAGGGTC-P-3'), MgCl₂ at 3.875mM concentration, PuReTaq Ready-to-go PCR bead (GE Healthcare) in a 20μL reaction. The PCR conditions were as follows: denature 95°C 2 min; amplification 45 cycles of 95°C 1 sec, 50°C 15 sec, 72°C 6 sec ; melt 95°C 1 min, 35°C 3 min, 40°C 1 min, 45°C 1 min, 85°C 0 sec (.5°C/sec ramp); Cool 40°C 30 sec. Analysis was performed using Lightcycler3 program.

7.16 Relative quantification of expression

Relative quantification of RNA levels was performed using the LightCycler Real Time PCR System (Roche). ~2ng of cDNA was added to a PuReTaq Ready-to-go PCR bead (GE Healthcare), .3μM primers (listed in table 7.4), .38μL TaqStart Antibody (Clontech), 1x EvaGreen (Biotum, Inc.) and MgCl₂ (listed in table 7.4). All expression was normalized to the geometric mean of *Rplp0* (*acidic ribosomal phosphoprotein p0*) and *Gapdh* (*glyceraldehydes-3-phosphate dehydrogenase*).

Table 7.4 Real time PCR assays			
Gene	Primer (5'-3')	Final Mg2+ Conc. (mM)	Annealing Temp (°C)
<i>H19</i>	HE2: TGATGGAGAGGACAGAAGGG HE4: TTGATTCAGAACGAGACGGAC	3	55
<i>Igf2</i>	Igf2F: CGCTTCGTTTGTCTGTTCG Igf2R: GCAGCACTCTCCACGATG	3	58
<i>Mecp2</i>	qMecp2F: CAGGCAAAGCAGAAACATCA qMecp2R: GCAAGGTGGGGTCATCATA	3	60
<i>Mbd1</i>	qMBD1F: GAGCACAGAGAATCGCCTTC qMBD1R: CACACCCACAGTCCTCTTT	3	60
<i>Mbd2</i>	Mbd269L: AACTGGAGGAGGCACTGATG Mbd269R: GGGGAAGGTCAGTCGAAAGT	3	60
<i>Gapdh</i>	GapdhF1: ATCACTGCCACCCAGAACAC GapdhR1: ATCCACGACGGACACATTGG	3	60
<i>Rplp0</i>	Arbp0#72L: TCCCCTTACTGAAAAGGTCAAG Arbp0#72R: TCCGACTCTTCCTTTGCTTC	4.5	58

7.17 Cloning CpGfree1 and CpGfree3

For cloning of CpGfree1, *AatII* (GACGTC) and *XhoI* (GAGCTC) restriction sites were inserted upstream of the CMV enhancer in pCpGvitro-neo-lacZ (Invivogen) using the QuikChange II XL Site-Directed Mutagenesis Kit (Stratagene) and the following primer sequences: for cloning of *AatII*- sense: 5'-
 GTGAGCAAACAGCAGATTAAGGAAGACGTCTAGGTACCTTCCTGCAGGAG
 TC-3'; antisense: 5'-
 GACTCCTGCAGGAAGGTACCTAGACGTCTTCCTTTATACTGCTGTTTGCTCA
 C-3'. For cloning of *XhoI*- sense: 5'-

GTGAGCAAACAGCAGATTAAGGAAGACGTCTACTCGAGTTCCTGCAGGAG
TC-3'; antisense: 5'-

GACTCCTGCAGGAACTCGAGTAGACGTCTTCCTTTTAATCTGCTGTTTGCTCA
C-3'. For cloning of CpGfree3, an *XhoI* (GAGCTC) restriction site was cloned at the 3'
end of the CMV enhancer in the CpGfree1 vector using the QuikChange II XL Site-
Directed Mutagenesis Kit (Stratagene) using the primer sequences; sense: 5'-

TAAGGTCAATAGGGGTGCTCGAGACTAGTGGAGAAGAGCA-3'; antisense: 5'-
TGCTCTTCTCCACTAGTCTCGAGCACCCCTATTGACCTTA-3'.

Targeting vectors for the 8nrCG and 9CG mutant ICRs were digested with
HindIII to obtain a 2.2kb ICR fragment. A *HindIII* digest was also used to isolate the
wild type *H19* ICR from 129/SvJ lambda library. These 2.2kb ICR fragments were
cloned in pBluescriptII KS vector. The pBluescriptII KS vectors containing ICR
fragments were digested with *AatII* and *XhoI*. The 1.8kb fragments were cloned into the
CpGfree1 and CpGfree3 vectors.

CpGfree1 and CpGfree3 were then either left unmethylated or were methylated
using the CpG Methylase *M.SssI* (Zymoresearch) following manufacturer's protocol.
Methylation was confirmed by restriction digests with the methylation sensitive enzymes
HpaII and *HhaI*.

7.18 In vitro repressor assay in Hep3b cells

Hep3b cells were cultured in 10% FBS (Gemini), DMEM+Glutamine (Gibco).
On day 0, 1×10^6 Hep3b cells were seeded on a 10cm plate and incubated at 37°C

overnight. On day 1 these cells were transfected with 1 μ g of either methylated or unmethylated CpGfree plasmids (linearized by digestion with *NheI*) using Lipofectamine 2000 (Invitrogen) following manufacturer's protocol. On day 2, each transfected 6cm plate was passaged 1:2 onto 10cm plates. Selection with 400 μ g/mL G418 was initiated on day 3 and selected for ~10-14 days. After selection, protein lysates were collected and β -gal activity was measured using the High Sensitivity β -Galactosidase Kit (Agilent Technologies) following manufacturer's protocol. Total protein concentration was measured using the Coomassie Plus Protein Assay Reagent (Thermo Scientific) following manufacturer's protocol.

7.19 In vitro repressor assay in F9 cells

F9 cells (obtained from Dr. Hua-Ying Fan, University of Pennsylvania) were cultured in 10% FBS (Gemini), DMEM+Glutamax (Gibco) on 1% gelatinized plates. On day 0, $.3 \times 10^6$ F9 cells were seeded on a 10cm plate and incubated at 37°C overnight. On day 1 these cells were transfected with 1 μ g of either methylated or unmethylated CpGfree plasmids (linearized by digestion with *NheI*) using Lipofectamine 2000 (Invitrogen) following manufacturer's protocol. On day 2, each transfected 6cm plate was passaged 1:6 onto 10cm plates. Selection with 350 μ g/mL G418 was initiated on day 3 and selected for ~10-14 days. After selection, protein lysates were collected and β -gal activity was measured using the High Sensitivity β -Galactosidase Kit (Agilent Technologies) following manufacturer's protocol. Total protein concentration was

measured using the Coomassie Plus Protein Assay Reagent (Thermo Scientific) following manufacturer's protocol.

7.20 Isolation of F1 hybrid mouse embryonic fibroblasts

F1 hybrid MEFs were isolated from individual E12.5-14.5 embryos generated from crosses between wild type B6 females and C7 males or *Mbd2*^{+/-} (B6) females and *Mbd2*^{+/-} (C7) males. The liver was removed from embryos for genotyping. The remaining embryo was placed in a 6cm plate containing PBS (Gibco). Under the tissue culture hood the embryo was placed in 2.5 ml 0.1% Trypsin-EDTA (Gibco) and minced. After incubation at 37 °C for 30-45 min with occasional agitation, the digested cells and tissues were transferred into a T75 flask with 12 ml MEF medium (10% FBS (Gemini), DMEM +Glutamax (Gibco)). When the cells became confluent, MEFs were split or frozen at Passage 2 (P2). For knockdown experiments, P4-P6 MEFs were used.

7.21 siRNA knockdown in MEFs

3 siRNA sequences targeting *Mbd1*, *Mbd2* or *Mbd3* (sequences listed in table 7.5) were generated from Invitrogen (Invitrogen Stealth siRNA) and diluted in 1mL RNase-free water according to manufacturer's protocol. All sequences were tested using the following protocol and the sequences producing the best depletion (siMbd1#39, siMbd2#42 and siMbd3#38) were used for analysis.

1.4x10⁴ MEFs/well were plated onto a 12-well plate in 5% FBS (Gemini), DMEM+Glutamax (Gibco). These cells were transfected while in suspension using

lipofectamine 2000 (Invitrogen) and 2 μ L of individual siMbds, all 3 siMbds or a negative control siRNA which does not target any known sequence (Invitrogen), following manufacturer's protocol. Medium was changed after 4 hours and cells were cultured in 10%FBS (Gemini) in DMEM+Glutamax (Gibco). 48 hours after initial transfection, a second transfection was performed with each well passaged into a well on a 6-well plate. The cells were transfected while in suspension using Lipofectamine 2000 (Invitrogen) and 5 μ l of the appropriate siRNA. 48 hours after second transfection, 85% of the cells were lysed for protein analysis with the remaining cells spun down for expression analysis.

Table 7.5 siRNA sequences	
Name	Sequence
siMbd1#39	sense:GCACCUUAUGCCAUCCCAUUCCTAA antisense:UUGGGAAUGGGAUGGCAUAAGGUGC
siMbd1#38	sense:GAUUGCGUCCAUAUCAGACCCAUCA antisense:UGAUGGGUCUGAUUUGGACGCAAUC
siMbd1#37	sense:UGGAAACGCCGAGAGUCCUUUCGAA antisense:UUCGAAAGGACUCUCGGCGUUUCCA
siMbd2#42	sense:GGAAAUGCUGUUGACCUUAGCAGUU antisense:AACUGCUAAGGUCAACAGCAUUUCC
siMbd2#41	sense:GCGAGUCCAACAAGUACGCAAGAAA antisense:UUUCUUGCGUACUUGUUGGACUCGC
siMbd2#40	sense:CCCUGCUGUUUGGCUUACACAUCU antisense:AGAUGUGUUUAGCCAAACAGCAGGG
siMbd3#59	sense:GAGUGGGCCCUGGCUGUACAGAUGA antisense:UCAUCUGUACAGCCAGGGCCACUC
siMbd3#58	sense:CCUUUGACAUUGCAGAAGAACUGGU antisense:ACCAGUUCUUCUGCAAUGUCAAGG
siMbd3#38	sense:UCCGCACCGGAAAGAUGUUGAUGAA antisense:UUCAUCAACAUCUUCCGGUGCGGA

7.22 Culturing trophoblast stem cells

TS cells (obtained from Dr. Michael Golding, Texas A&M University) were cultured as described previously (Himeno et al., 2008). Briefly, TS cells were cultured on mitomycin-C treated MEFs in TS medium (RPMI 1640 (Gibco) supplemented with 20% FBS (HyClone), 2-mM L-glutamine (Gibco), 1mM sodium pyruvate (Gibco), 100mM 2-mercaptoethanol, 50U/mL penicillin, 50µg/mL streptomycin) with 1X FGF4 and Heparin (F4H) (Sigma) added fresh. TS cells can also be cultured in 70% MEF-conditioned medium (CM) 30% TS medium 1.5X F4H. To make the CM, mitomycin-C treated MEFs were plated at a high density and cultured in TS medium without F4H for at least 72 hours. The CM was harvested and centrifuged at 1000 rpm for 20 min to remove cellular debris. The supernatant was collected and passed through a 0.2 µm filter and frozen at -20°C.

For culturing TS cells, medium was changed every 48 hours, and fresh F4H was added each time. To passage TS cells, cells were treated with 0.05% Trypsin-EDTA at 37 °C for 3 min and were split 1:5 to 1:20. To collect TS cells without MEF contaminants, cells were trypsinized and replated in 70% CM + F4H for 45 min. The supernatant was transferred to a new plate for another 45 min. This supernatant contained predominantly TS cells.

To ensure TS cells did not differentiate we analyzed expression of the pluripotency genes *Esrrb*, *mEomes*, *Fgfr2* (table 7.6) and a marker of differentiation, *Ascl2* (as described previously in table 7.3). ~2ng of cDNA was used for each RT-PCR

reaction containing 1X GoTaq (promega) and .3 μ M of the appropriate primer. The PCR conditions for pluripotency markers were: 2 min at 95°C; 35 cycles of 15 sec at 95°C for 10 sec, 15 sec at 55°C, 20 sec at 72°C

Table 7.6 RT-PCR assays for pluripotency markers	
Gene	Primer Sequence (5'-3')
<i>Esrrb</i>	Esrrb-c286f: ACTCTGCATCCCGGACCCCC Esrrb-c473r: GCGTGGGTGCTCAGGGCAAT
<i>mEomes</i>	mEomes-F: GTGACAGAGGACGGTGTGGAGG mEomes-R: AGAGGAGGCCGTTGGTCTGTGG
<i>Fgfr2</i>	Fgfr2-F: GACAAGCCCACCAACTGCACC Fgfr2-R: CGTCCCCTGAAGAACAAGAGC

7.23 siRNA knockdown in TS cells

9.1x10⁴ TS cells/well were plated into each well of a 12-well plate in 70%CM+1.5XF4H. These cells were transfected while in suspension using lipofectamine 2000 (Invitrogen) and 2 μ L of siMbd1 #39, a negative control siRNA (Invitrogen), or a fluorescent RNA (Invitrogen) following manufacturer's protocol. Medium was changed after 4 hours and cells were cultured in 70%CM+1.5XF4H. 48 hours after initial transfection, a second transfection was performed with each well passaged into a well on a 6-well plate. Cells were transfected while in suspension using Lipofectamine 2000 (Invitrogen) and 5 μ L of the appropriate RNA. 24 hours after second transfection, fluorescence was detected to determine transfection efficiencies. 48 hours after second transfection 85% of the cells were lysed for protein analysis with the remaining cells spun down for expression analysis.

7.24 Cloning shRNA into a lentiviral vector

shRNAs against *Mbd1* and *Mecp2* were cloned into the PLKO.1(Addgene) lentivirus vector. siMbd1#39 sequence was used to target *Mbd1* and the sequence used to target *Mecp2* was that used in (Zhou et al., 2006). For converting sequences into an shRNA and cloning into PLKO.1, oligos were ordered following the scheme: forward oligo: 5'CCGG-sense sequence-CTCGAG-antisense sequence-TTTTTG3' reverse oligo: 5'AATTCAAAAA- sense sequence- CTCGAG-antisense sequence. Therefore, the following oligos were ordered to target *Mbd1*: Mbd1-39F:5'-
 CCGGGCACCTTATGCCATCCCATTCCCAACGAATTGGGAATGGGATGGCATA
 AGGTGCTTTTTG-3'; Mbd1-39R: 5'-
 AATTCAAAAAGCACCTTATGCCATCCCATTCCCAACGAATTGGGAATGGGAT
 GGCATAAGGTGC-3'. To target *Mecp2* the following oligos were ordered: Mecp2F:5'-
 CCGGGTCAGAAGACCAGGATCTCCGAAGAGATCCTGGTCTTCTGACTTTTTG-
 3'; Mecp2R:5'-
 AATTCAAAAAGTCAGAAGACCAGGATCTCCGAAGAGATCCTGGTCTTCTGAC-
 3'.

Oligos were resuspended in dH₂O to a concentration of 20μM and annealed by mixing 5μL forward oligo, 5μL reverse oligo, 5μL 10x NEB buffer 2 and 35μL dH₂O. The reaction was incubated at 95°C for 4 min. The heat block (containing the reaction) was then placed at room temperature and allowed to cool over 4 hours. The reaction was purified using Qiagen's QIAquick PCR purification kit. The annealed oligos were phosphorylated using T4 PNK (New England Biolabs) following manufacturer's protocol.

For cloning annealed oligos into the pLKO.1 vector, the vector and annealed oligos were digested with *AgeI* and *EcoRI*. The digested fragment and vector were ligated together and transformed using DH5 α chemically competent cells (Invitrogen) following manufacturer's protocol.

DNA from individual clones was digested with *EcoRI* and *NcoI* to ensure insertion of the shRNA sequence into the vector. Positive clones produce ~2kb and ~5kb fragments, whereas an empty vector will produce ~2kb and ~7kb fragments. Positive clones were sequenced with the PLKO.1 sequencing primer (5'-CAAGGCTGTTAGAGAGATAATTGG-3').

To produce viral particles, ~70% confluent 15cm plate of 293T cells (cultured in 10%FBS (Gemini), DMEM+Glutamax (Gibco)) was transfected with 15 μ g pLKO.1 shRNA plasmid, 11.25 μ g psPAX2 packaging plasmid (Addgene) and 3.75 μ g pMD2.G envelope plasmid (Addgene) using Lipofectamine 200 (Invitrogen) following manufacturer's protocol. After overnight incubation at 37°C the medium was replaced with 25mL fresh DMEM+Glutamax (Gibco) +10%FBS (Gemini) +1/100 penicillin/streptomycin (University of Pennsylvania Cell Center) +1/100 non-essential amino acids+ 1/100 sodium pyruvate (Gibco). Supernatant was harvested 76 hours later.

For concentration of Lentivirus, supernatant was filtered through a .45 μ m filter and spun for 1.5 hours at 28000 x g at 4°C. The pellet was resuspended in 500 μ L of PBS (Gibco) and left overnight at 4°C. The virus was aliquoted the following day and stored at -80°C.

To titrate the lentiviruses, 293T cells were infected with varying dilutions of virus and treated with 1.5µg/mL puromycin. Numbers of viable cells after 4-6 days of drug selection were counted and the virus titer were calculated.

7.25 shRNA knockdown in MEFs

3.5×10^5 *Mbd2*^{-/-} MEFs were plated into each well of a 6 well plate and incubated at 37°C overnight. Cells were infected with 30 MOI of viruses containing shMecp2, shMbd1, both or shControl in 8µg/mL polybrene (American Bioanalytical). 24 hours after infection cells were passaged onto a 6 cm plate and puromycin treatment (at a concentration of 1.2µg/mL) was initiated. 24 hours into selection, cells were re-infected with 30 MOI shMecp2 (only shMecp2 required 2 rounds of infection). 48 hours into selection cells were passaged onto a 10cm plate. ~7 days after selection cells were collected with ~75% of cells lysed for protein analysis and 25% of cells pelleted for RNA analysis.

7.26 shRNA knockdown in TS cells

5.5×10^5 TS cells were plated into each well of a 6 well plate (cultured in 70% CM+1.5F4H) and incubated at 37°C overnight. Cells were infected with 30 MOI of viruses containing shMbd1 or shControl in 8µg/mL polybrene (American Bioanalytical). 24 hours after infection cells were passaged onto a 6 cm plate and puromycin treatment (at a concentration of 1.75µg/mL) was initiated. 48 hours into selection cells were

passed onto a 10cm plate. ~7 days after selection cells were collected with 75% of cells lysed for protein analysis and 25% of cells pelleted for RNA analysis.

7.27 Western blot analysis

Cell pellets were lysed with TNE (100 mM Tris, pH 7.4; 1% NP-40; 10 mM EDTA) buffer with 1:100 Proteinase inhibitor cocktail (Sigma) and 1 mM DTT. Embryos and placentas were lysed in 5X RIPA buffer and vortexed for 5 min. Total protein concentration was measured using the Coomassie Plus Protein Assay Reagent (Thermo Scientific) following manufacturer's protocol. Lysates were mixed with 5X loading buffer, denatured by heating at 95°C for 10 min. 20µg of total protein was fractionated on an 8% SDS-PAGE gel. The protein was transferred to a nitrocellulose membrane (BioRad), blocked in 5% milk in TBST (0.05% Tween-20 in 1X TBS) and probed with primary antibodies (as listed in table 7.7) overnight and secondary antibodies for one hour (HRP-conjugated anti-rabbit (1:2500 dilution), GE Healthcare). The blot was visualized using chemiluminescence (ECL Plus; GE). Quantification was performed using ImageJ.

Antibody raised against	Company	Lot#	Dilution	Secondary
MBD1	Santa Cruz	C161	1:200	Rabbit
MECP2	Dr. Zhaolan Zhou , University of Pennsylvania		1:2000	Rabbit
RAD21	Bethyl	A300-080A-3	1:500	Rabbit
GAPDH	Cell Signaling	8	1:1000	Rabbit
Flag-tag	Sigma	M2	1:1000	Mouse

7.28 Cloning of MBD overexpression vector

Primers were designed to include amino acid 76 through amino acid 160 of MECP2, which deletion studies defined as the MBD (Nan et al., 1993). Primers also included sequences in order modify the MBD to contain a C-terminal flag-tag and an N-terminal SV40 nuclear localization signal. Oligos also included a *Bam*HI restriction site (GGATCC) to be included 5' of the flag sequence and a *Sal*I restriction site (GTCGAC) to be included 3' of the NLS sequence. Primer sequences were as follows:

MBDBAMAA76F:5'-

AAAAGGATCCATGGATTACAAGGATGACGACGATAAGCCTCGGCTTCCCCCA

AACAGCGG-3'; MBDA163R: 5'-

AAAAGTCGACTCAAACCTTCCGTTTCTTTTTTCGGGGGCTCCCTCTCCCAGTTA

CCGTGA-3'. 2ng of cDNA derived from a wild type adult mouse was added to a reaction mix with 1X GoTaQ (promega), .3μM of the primers listed above in a 20μl final reaction. PCR conditions were as follows 2 min at 95°C; 35 cycles of 15 sec at 95°C, 15 sec at 55°C, 20 sec at 72°C.

Amplified fragments were run out on a 1% agarose gel and the band was excised and purified using the QiaQuick Gel Extraction kit (Qiagen) according to manufacturer's protocol and eluted in 30μL dH₂O. Purified PCR product was cloned using the TOPO-TA kit (Invitrogen) follow manufacturer's protocol.

The Topo vector containing the MBD fragment and the retroviral pBabe-puro expression vector (Morgenstern and Land, 1990) (obtained from Dr. Xiaolu Yang,

University of Pennsylvania) were digested with *BamHI* and *Sall*. The pbabe-puro vector and MBD insert fragments were ligated and transformed in chemically competent Top 10F cells (Invitrogen) following manufacturer's protocol. Positive clones were identified by presence of the ~350bp fragment after digestion with *BamHI* and *Sall*. One positive clone was sequenced by the University of Pennsylvania Sequencing Facility using primers overlapping the MBD: (qMBDF: 5'-CCGGGGACCTATGTATGATG-3'; qMBDR: 5'-AGGAGGTGTCTCCACCTTT-3').

7.29 MBD overexpression in F1 hybrid MEFS

To produce viral particles, 5µg of DNA (either pBabe-MBD or pBabe) was transfected using CaCl₂ into Pheonix-E cells (obtained from Dr. Xiaolu Yang, University of Pennsylvania) and cultured in 10%FBS (Gemini), DMEM+Glutamax (Gibco). The transfected cells were incubated overnight at 37°C and medium was replaced with 2 mLs of fresh medium. The following day, the viral containing medium was harvested and spun down at 1,000 RPM for 5 minutes to collect any cellular debris. 2mLs of fresh medium was added to the transfected Pheonix-E cells. 5.5x10⁵ MEFS were resuspended in the 2mLs of viral supernatant with 8µg/mL of polybrene (American Bioanalytical) and 500µL of fresh medium in a 6 well plate. The next day, the MEFS were passaged onto a 6cm plate and resuspended in new viral medium from the Pheonix-E cells. 24 hours after the second round of infection, cells were treated with puromycin at a concentration of 1.2µg/mL. Puromycin concentration was increased daily until it reached 2µg/mL. Cells

were collected for analysis after ~7 days in selection with ~25% of cells used for RNA analysis and ~75% used for protein analysis.

Overexpression of the *Mecp2 MBD* was quantified using the the LightCycler Real-Time PCR system (Roche). ~2ng of cDNA was added to a PuReTaq Ready-to-go PCR bead (GE Healthcare), .3 μ M primers qMBDF, qMBDR (listed section 7.28), .38 μ L TaqStart Antibody (Clontech), 1x EvaGreen (Biotum, Inc.) and 3 μ M MgCl₂. PCR conditions followed those outlined in section 7.16 with and annealing temperature of 58°C. All expression was normalized to the geometric mean of *Rplp0* (*acidic ribosomal phosphoprotein p0*)

7.30 Statistical analysis

To calculate P-value for gene expression changes and β -gal activity changes, a two-tailed paired T-test was used. For analysis of DNA methylation a P-value was calculated using a chi-squared test comparing the proportion of mutant and wild type samples showing abnormal methylation (sperm: methylation levels > 15% for maternally methylated DMRs and < 85% for paternally methylated DMRs; somatic tissues: methylation levels < 40% or > 60%). A P-value was considered significant if <.05.

REFERENCES

- Abramowitz, L. K., Bartolomei, M. S., 2012. Genomic imprinting: recognition and marking of imprinted loci. *Curr Opin Genet Dev.* 22, 72-8.
- Allan, A. M., Liang, X., Luo, Y., Pak, C., Li, X., Szulwach, K. E., Chen, D., Jin, P., Zhao, X., 2008. The loss of methyl-CpG binding protein 1 leads to autism-like behavioral deficits. *Human Molecular Genetics.* 17, 2047-2057.
- Amir, R. E., Van den Veyver, I. B., Wan, M., Tran, C. Q., Francke, U., Zoghbi, H. Y., 1999. Rett syndrome is caused by mutations in X-linked MECP2, encoding methyl-CpG-binding protein 2. *Nat Genet.* 23, 185-8.
- Arney, K. L., 2003. H19 and Igf2--enhancing the confusion? *Trends Genet.* 19, 17-23.
- Avarbock, M. R., Brinster, C. J., Brinster, R. L., 1996. Reconstitution of spermatogenesis from frozen spermatogonial stem cells. *Nat Med.* 2, 693-6.
- Azad, N., Zahnow, C. A., Rudin, C. M., Baylin, S. B., 2013. The future of epigenetic therapy in solid tumours--lessons from the past. *Nat Rev Clin Oncol.*
- Ballestar, E., Ropero, S., Alaminos, M., Armstrong, J., Setien, F., Agrelo, R., Fraga, M. F., Herranz, M., Avila, S., Pineda, M., Monros, E., Esteller, M., 2005. The impact of MECP2 mutations in the expression patterns of Rett syndrome patients. *Hum Genet.* 116, 91-104.
- Bao, S., Obata, Y., Carroll, J., Domeki, I., Kono, T., 2000. Epigenetic modifications necessary for normal development are established during oocyte growth in mice. *Biol Reprod.* 62, 616-21.
- Barr, H., Hermann, A., Berger, J., Tsai, H. H., Adie, K., Prokhortchouk, A., Hendrich, B., Bird, A., 2007. Mbd2 contributes to DNA methylation-directed repression of the Xist gene. *Mol Cell Biol.* 27, 3750-7.
- Bartholdi, D., Krajewska-Walasek, M., Ounap, K., Gaspar, H., Chrzanowska, K. H., Ilyana, H., Kayserili, H., Lurie, I. W., Schinzel, A., Baumer, A., 2009. Epigenetic mutations of the imprinted IGF2-H19 domain in Silver-Russell syndrome (SRS): results from a large cohort of patients with SRS and SRS-like phenotypes. *J Med Genet.* 46, 192-7.
- Bartolomei, M. S., 2009. Genomic imprinting: employing and avoiding epigenetic processes. *Genes & Development.* 23, 2124-2133.
- Bartolomei, M. S., Zemel, S., Tilghman, S. M., 1991. Parental imprinting of the mouse H19 gene. *Nature.* 351, 153-5.
- Baubec, T., Ivánek, R., Lienert, F., Schübeler, D., 2013. Methylation-Dependent and -Independent Genomic Targeting Principles of the MBD Protein Family. *Cell.* 153, 480-492.
- Baylin, S. B., Jones, P. A., 2011. A decade of exploring the cancer epigenome - biological and translational implications. *Nat Rev Cancer.* 11, 726-34.
- Begemann, M., Spengler, S., Kanber, D., Haake, A., Baudis, M., Leisten, I., Binder, G., Markus, S., Rupprecht, T., Segerer, H., Fricke-Otto, S., Muhlenberg, R., Siebert, R., Buiting, K., Eggermann, T., 2010. Silver-Russell patients showing a broad range of ICR1 and ICR2 hypomethylation in different tissues. *Clin Genet.*

- Bell, A. C., Felsenfeld, G., 2000. Methylation of a CTCF-dependent boundary controls imprinted expression of the *Igf2* gene. *Nature*. 405, 482-5.
- Bell, A. C., West, A. G., Felsenfeld, G., 1999. The protein CTCF is required for the enhancer blocking activity of vertebrate insulators. *Cell*. 98, 387-96.
- Bhogal, B., Arnaudo, A., Dymkowski, A., Best, A., Davis, T. L., 2004. Methylation at mouse *Cdkn1c* is acquired during postimplantation development and functions to maintain imprinted expression. *Genomics*. 84, 961-70.
- Bird, A. P., Wolffe, A. P., 1999. Methylation-induced repression--belts, braces, and chromatin. *Cell*. 99, 451-4.
- Boeke, J., Ammerpohl, O., Kegel, S., Moehren, U., Renkawitz, R., 2000. The minimal repression domain of MBD2b overlaps with the methyl-CpG-binding domain and binds directly to Sin3A. *J Biol Chem*. 275, 34963-7.
- Bogdanović, O., Veenstra, G. J. C., 2009. DNA methylation and methyl-CpG binding proteins: developmental requirements and function. *Chromosoma*. 118, 549-565.
- Booth, M. J., Branco, M. R., Ficz, G., Oxley, D., Krueger, F., Reik, W., Balasubramanian, S., 2012. Quantitative sequencing of 5-methylcytosine and 5-hydroxymethylcytosine at single-base resolution. *Science*. 336, 934-7.
- Bourc'his, D., Bestor, T. H., 2004. Meiotic catastrophe and retrotransposon reactivation in male germ cells lacking Dnmt3L. *Nature*. 431, 96-9.
- Bourc'his, D., Xu, G. L., Lin, C. S., Bollman, B., Bestor, T. H., 2001. Dnmt3L and the establishment of maternal genomic imprints. *Science*. 294, 2536-9.
- Brinster, R. L., 2007. Male germline stem cells: from mice to men. *Science*. 316, 404-5.
- Brinster, R. L., Avarbock, M. R., 1994. Germline transmission of donor haplotype following spermatogonial transplantation. *Proc Natl Acad Sci U S A*. 91, 11303-7.
- Butler, M. G., 2009. Genomic imprinting disorders in humans: a mini-review. *J Assist Reprod Genet*. 26, 477-86.
- Campanero, M. R., Armstrong, M. I., Flemington, E. K., 2000. CpG methylation as a mechanism for the regulation of E2F activity. *Proc Natl Acad Sci U S A*. 97, 6481-6.
- Chen, R. Z., Akbarian, S., Tudor, M., Jaenisch, R., 2001. Deficiency of methyl-CpG binding protein-2 in CNS neurons results in a Rett-like phenotype in mice. *Nat Genet*. 27, 327-31.
- Chen, Y., Dhupelia, A., Schoenherr, C. J., 2008. The *Igf2/H19* imprinting control region exhibits sequence-specific and cell-type-dependent DNA methylation-mediated repression. *Nucleic Acids Research*. 37, 793-803.
- Chotalia, M., Smallwood, S. A., Ruf, N., Dawson, C., Lucifero, D., Frontera, M., James, K., Dean, W., Kelsey, G., 2009. Transcription is required for establishment of germline methylation marks at imprinted genes. *Genes & Development*. 23, 105-117.
- Choufani, S., Shuman, C., Weksberg, R., 2010. Beckwith-Wiedemann syndrome. *Am J Med Genet C Semin Med Genet*. 154C, 343-54.
- Ciccone, D. N., Su, H., Hevi, S., Gay, F., Lei, H., Bajko, J., Xu, G., Li, E., Chen, T., 2009. KDM1B is a histone H3K4 demethylase required to establish maternal genomic imprints. *Nature*. 461, 415-418.

- Cirio, M. C., Ratnam, S., Ding, F., Reinhart, B., Navara, C., Chaillet, J. R., 2008. Preimplantation expression of the somatic form of Dnmt1 suggests a role in the inheritance of genomic imprints. *BMC Dev Biol.* 8.
- Clouaire, T., Stancheva, I., 2008. Methyl-CpG binding proteins: specialized transcriptional repressors or structural components of chromatin? *Cellular and Molecular Life Sciences.* 65, 1509-1522.
- Cortellino, S., Xu, J., Sannai, M., Moore, R., Caretti, E., Cigliano, A., Le Coz, M., Devarajan, K., Wessels, A., Soprano, D., Abramowitz, L. K., Bartolomei, M. S., Rambow, F., Bassi, M. R., Bruno, T., Fanciulli, M., Renner, C., Klein-Szanto, A. J., Matsumoto, Y., Kobi, D., Davidson, I., Alberti, C., Larue, L., Bellacosa, A., 2011. Thymine DNA glycosylase is essential for active DNA demethylation by linked deamination-base excision repair. *Cell.* 146, 67-79.
- Davis, T. L., Yang, G. J., McCarrey, J. R., Bartolomei, M. S., 2000. The H19 methylation imprint is erased and re-established differentially on the parental alleles during male germ cell development. *Hum Mol Genet.* 9, 2885-94.
- Dawlaty, M. M., Breiling, A., Le, T., Raddatz, G., Barrasa, M. I., Cheng, A. W., Gao, Q., Powell, B. E., Li, Z., Xu, M., Faull, K. F., Lyko, F., Jaenisch, R., 2013. Combined deficiency of Tet1 and Tet2 causes epigenetic abnormalities but is compatible with postnatal development. *Dev Cell.* 24, 310-23.
- Dawlaty, Meelad M., Ganz, K., Powell, Benjamin E., Hu, Y.-C., Markoulaki, S., Cheng, Albert W., Gao, Q., Kim, J., Choi, S.-W., Page, David C., Jaenisch, R., 2011. Tet1 Is Dispensable for Maintaining Pluripotency and Its Loss Is Compatible with Embryonic and Postnatal Development. *Cell Stem Cell.* 9, 166-175.
- de Waal, E., Yamazaki, Y., Ingale, P., Bartolomei, M., Yanagimachi, R., McCarrey, J. R., 2012a. Primary epimutations introduced during intracytoplasmic sperm injection (ICSI) are corrected by germline-specific epigenetic reprogramming. *Proc Natl Acad Sci U S A.* 109, 4163-8.
- de Waal, E., Yamazaki, Y., Ingale, P., Bartolomei, M. S., Yanagimachi, R., McCarrey, J. R., 2012b. Gonadotropin stimulation contributes to an increased incidence of epimutations in ICSI-derived mice. *Hum Mol Genet.* 21, 4460-72.
- DeChiara, T. M., Efstratiadis, A., Robertson, E. J., 1990. A growth-deficiency phenotype in heterozygous mice carrying an insulin-like growth factor II gene disrupted by targeting. *Nature.* 345, 78-80.
- DeChiara, T. M., Robertson, E. J., Efstratiadis, A., 1991. Parental imprinting of the mouse insulin-like growth factor II gene. *Cell.* 64, 849-59.
- Dhayalan, A., Rajavelu, A., Rathert, P., Tamas, R., Jurkowska, R. Z., Ragozin, S., Jeltsch, A., 2010. The Dnmt3a PWWP Domain Reads Histone 3 Lysine 36 Trimethylation and Guides DNA Methylation. *Journal of Biological Chemistry.* 285, 26114-26120.
- Doherty, A. S., Mann, M. R., Tremblay, K. D., Bartolomei, M. S., Schultz, R. M., 2000. Differential effects of culture on imprinted H19 expression in the preimplantation mouse embryo. *Biol Reprod.* 62, 1526-35.
- Drewell, R. A., Brenton, J. D., Ainscough, J. F., Barton, S. C., Hilton, K. J., Arney, K. L., Dandolo, L., Surani, M. A., 2000. Deletion of a silencer element disrupts H19

- imprinting independently of a DNA methylation epigenetic switch. *Development*. 127, 3419-28.
- Drewell, R. A., Goddard, C. J., Thomas, J. O., Surani, M. A., 2002. Methylation-dependent silencing at the H19 imprinting control region by MeCP2. *Nucleic Acids Res.* 30, 1139-44.
- Ecker, D. J., Stein, P., Xu, Z., Williams, C. J., Kopf, G. S., Bilker, W. B., Abel, T., Schultz, R. M., 2004. Long-term effects of culture of preimplantation mouse embryos on behavior. *Proc Natl Acad Sci U S A.* 101, 1595-600.
- Engel, N., Thorvaldsen, J. L., Bartolomei, M. S., 2006. CTCF binding sites promote transcription initiation and prevent DNA methylation on the maternal allele at the imprinted H19/Igf2 locus. *Human Molecular Genetics.* 15, 2945-2954.
- Engel, N., West, A. G., Felsenfeld, G., Bartolomei, M. S., 2004. Antagonism between DNA hypermethylation and enhancer-blocking activity at the H19 DMD is uncovered by CpG mutations. *Nature Genetics.* 36, 883-888.
- Eroglu, A., Layman, L. C., 2012. Role of ART in imprinting disorders. *Semin Reprod Med.* 30, 92-104.
- Fang, R., Barbera, A. J., Xu, Y., Rutenberg, M., Leonor, T., Bi, Q., Lan, F., Mei, P., Yuan, G.-C., Lian, C., Peng, J., Cheng, D., Sui, G., Kaiser, U. B., Shi, Y., Shi, Y. G., 2010. Human LSD2/KDM1b/AOF1 Regulates Gene Transcription by Modulating Intragenic H3K4me2 Methylation. *Molecular Cell.* 39, 222-233.
- Fauque, P., Jouannet, P., Lesaffre, C., Ripoche, M. A., Dandolo, L., Vaiman, D., Jammes, H., 2007. Assisted Reproductive Technology affects developmental kinetics, H19 Imprinting Control Region methylation and H19 gene expression in individual mouse embryos. *BMC Dev Biol.* 7, 116.
- Fauque, P., Ripoche, M. A., Tost, J., Journot, L., Gabory, A., Busato, F., Le Digarcher, A., Mondon, F., Gut, I., Jouannet, P., Vaiman, D., Dandolo, L., Jammes, H., 2010a. Modulation of imprinted gene network in placenta results in normal development of in vitro manipulated mouse embryos. *Human Molecular Genetics.* 19, 1779-1790.
- Fauque, P., Ripoche, M. A., Tost, J., Journot, L., Gabory, A., Busato, F., Le Digarcher, A., Mondon, F., Gut, I., Jouannet, P., Vaiman, D., Dandolo, L., Jammes, H., 2010b. Modulation of imprinted gene network in placenta results in normal development of in vitro manipulated mouse embryos. *Hum Mol Genet.* 19, 1779-90.
- Ferguson-Smith, A. C., 2011. Genomic imprinting: the emergence of an epigenetic paradigm. *Nature Reviews Genetics.* 12, 565-575.
- Fernandez-Gonzalez, R., Moreira, P., Bilbao, A., Jimenez, A., Perez-Crespo, M., Ramirez, M. A., Rodriguez De Fonseca, F., Pintado, B., Gutierrez-Adan, A., 2004. Long-term effect of in vitro culture of mouse embryos with serum on mRNA expression of imprinting genes, development, and behavior. *Proc Natl Acad Sci U S A.* 101, 5880-5.
- Fitzpatrick, G. V., Pugacheva, E. M., Shin, J. Y., Abdullaev, Z., Yang, Y., Khatod, K., Lobanenkova, V. V., Higgins, M. J., 2007. Allele-specific binding of CTCF to the multipartite imprinting control region KvDMR1. *Mol Cell Biol.* 27, 2636-47.

- Fitzpatrick, G. V., Soloway, P. D., Higgins, M. J., 2002. Regional loss of imprinting and growth deficiency in mice with a targeted deletion of KvDMR1. *Nat Genet.* 32, 426-31.
- Fortier, A. L., Lopes, F. L., Darricarrere, N., Martel, J., Trasler, J. M., 2008. Superovulation alters the expression of imprinted genes in the midgestation mouse placenta. *Hum Mol Genet.* 17, 1653-65.
- Fournier, C., Goto, Y., Ballestar, E., Delaval, K., Hever, A. M., Esteller, M., Feil, R., 2002. Allele-specific histone lysine methylation marks regulatory regions at imprinted mouse genes. *EMBO J.* 21, 6560-70.
- Frevel, M. A., Hornberg, J. J., Reeve, A. E., 1999. A potential imprint control element: identification of a conserved 42 bp sequence upstream of H19. *Trends Genet.* 15, 216-8.
- Frost, J. M., Moore, G. E., 2010. The importance of imprinting in the human placenta. *PLoS Genet.* 6, e1001015
- Fujita, N., Watanabe, S., Ichimura, T., Tsuruzoe, S., Shinkai, Y., Tachibana, M., Chiba, T., Nakao, M., 2003. Methyl-CpG binding domain 1 (MBD1) interacts with the Suv39h1-HP1 heterochromatic complex for DNA methylation-based transcriptional repression. *J Biol Chem.* 278, 24132-8.
- Fuks, F., Burgers, W. A., Brehm, A., Hughes-Davies, L., Kouzarides, T., 2000. DNA methyltransferase Dnmt1 associates with histone deacetylase activity. *Nat Genet.* 24, 88-91.
- Garfield, A. S., Cowley, M., Smith, F. M., Moorwood, K., Stewart-Cox, J. E., Gilroy, K., Baker, S., Xia, J., Dalley, J. W., Hurst, L. D., Wilkinson, L. S., Isles, A. R., Ward, A., 2011. Distinct physiological and behavioural functions for parental alleles of imprinted Grb10. *Nature.* 469, 534-8.
- Geiman, T. M., Sankpal, U. T., Robertson, A. K., Zhao, Y., Robertson, K. D., 2004. DNMT3B interacts with hSNF2H chromatin remodeling enzyme, HDACs 1 and 2, and components of the histone methylation system. *Biochem Biophys Res Commun.* 318, 544-55.
- Gicquel, C., Rossignol, S., Cabrol, S., Houang, M., Steunou, V., Barbu, V., Danton, F., Thibaud, N., Le Merrer, M., Burglen, L., Bertrand, A. M., Netchine, I., Le Bouc, Y., 2005. Epimutation of the telomeric imprinting center region on chromosome 11p15 in Silver-Russell syndrome. *Nat Genet.* 37, 1003-1007.
- Girardot, M., Cavaille, J., Feil, R., 2012. Small regulatory RNAs controlled by genomic imprinting and their contribution to human disease. *Epigenetics.* 7, 1341-8.
- Golding, M. C., Mann, M. R., 2011. A bidirectional promoter architecture enhances lentiviral transgenesis in embryonic and extraembryonic stem cells. *Gene Ther.* 18, 817-26.
- Goll, M. G., Kirpekar, F., Maggert, K. A., Yoder, J. A., Hsieh, C. L., Zhang, X., Golic, K. G., Jacobsen, S. E., Bestor, T. H., 2006. Methylation of tRNA^{Asp} by the DNA methyltransferase homolog Dnmt2. *Science.* 311, 395-8.
- Green, K., Lewis, A., Dawson, C., Dean, W., Reinhart, B., Chaillet, J. R., Reik, W., 2007. A developmental window of opportunity for imprinted gene silencing mediated

- by DNA methylation and the Kcnq1ot1 noncoding RNA. *Mamm Genome*. 18, 32-42.
- Gregory, R. I., Randall, T. E., Johnson, C. A., Khosla, S., Hatada, I., O'Neill, L. P., Turner, B. M., Feil, R., 2001. DNA methylation is linked to deacetylation of histone H3, but not H4, on the imprinted genes *Snrpn* and *U2af1-rs1*. *Mol Cell Biol*. 21, 5426-36.
- Gu, T. P., Guo, F., Yang, H., Wu, H. P., Xu, G. F., Liu, W., Xie, Z. G., Shi, L., He, X., Jin, S. G., Iqbal, K., Shi, Y. G., Deng, Z., Szabo, P. E., Pfeifer, G. P., Li, J., Xu, G. L., 2011. The role of Tet3 DNA dioxygenase in epigenetic reprogramming by oocytes. *Nature*. 477, 606-10.
- Guibert, S., Forne, T., Weber, M., 2012. Global profiling of DNA methylation erasure in mouse primordial germ cells. *Genome Res*. 22, 633-41.
- Gunther, K., Rust, M., Leers, J., Boettger, T., Scharfe, M., Jarek, M., Bartkuhn, M., Renkawitz, R., 2013. Differential roles for MBD2 and MBD3 at methylated CpG islands, active promoters and binding to exon sequences. *Nucleic Acids Res*.
- Guy, J., Cheval, H., Selfridge, J., Bird, A., 2011. The role of MeCP2 in the brain. *Annu Rev Cell Dev Biol*. 27, 631-52.
- Guy, J., Hendrich, B., Holmes, M., Martin, J. E., Bird, A., 2001. A mouse *Mecp2*-null mutation causes neurological symptoms that mimic Rett syndrome. *Nat Genet*. 27, 322-6.
- Hackett, J. A., Sengupta, R., Zyllicz, J. J., Murakami, K., Lee, C., Down, T. A., Surani, M. A., 2013. Germline DNA demethylation dynamics and imprint erasure through 5-hydroxymethylcytosine. *Science*. 339, 448-52.
- Hajkova, P., Ancelin, K., Waldmann, T., Lacoste, N., Lange, U. C., Cesari, F., Lee, C., Almouzni, G., Schneider, R., Surani, M. A., 2008. Chromatin dynamics during epigenetic reprogramming in the mouse germ line. *Nature*. 452, 877-881.
- Hajkova, P., Erhardt, S., Lane, N., Haaf, T., El-Maarri, O., Reik, W., Walter, J., Surani, M. A., 2002. Epigenetic reprogramming in mouse primordial germ cells. *Mech Dev*. 117, 15-23.
- Hajkova, P., Jeffries, S. J., Lee, C., Miller, N., Jackson, S. P., Surani, M. A., 2010. Genome-wide reprogramming in the mouse germ line entails the base excision repair pathway. *Science*. 329, 78-82.
- Hao, Y., Crenshaw, T., Moulton, T., Newcomb, E., Tycko, B., 1993. Tumour-suppressor activity of H19 RNA. *Nature*. 365, 764-7.
- Hark, A. T., Schoenherr, C. J., Katz, D. J., Ingram, R. S., Levorse, J. M., Tilghman, S. M., 2000. CTCF mediates methylation-sensitive enhancer-blocking activity at the *H19/Igf2* locus. *Nature*. 405, 486-9.
- Hashimoto, H., Liu, Y., Upadhyay, A. K., Chang, Y., Howerton, S. B., Vertino, P. M., Zhang, X., Cheng, X., 2012. Recognition and potential mechanisms for replication and erasure of cytosine hydroxymethylation. *Nucleic Acids Res*. 40, 4841-9.
- Henckel, A., Chebli, K., Kota, S. K., Arnaud, P., Feil, R., 2011. Transcription and histone methylation changes correlate with imprint acquisition in male germ cells. *EMBO J*.

- Hendrich, B., 2001. Closely related proteins MBD2 and MBD3 play distinctive but interacting roles in mouse development. *Genes & Development*. 15, 710-723.
- Hendrich, B., Bird, A., 1998. Identification and characterization of a family of mammalian methyl-CpG binding proteins. *Mol Cell Biol*. 18, 6538-47.
- Hendrich, B., Hardeland, U., Ng, H. H., Jiricny, J., Bird, A., 1999. The thymine glycosylase MBD4 can bind to the product of deamination at methylated CpG sites. *Nature*. 401, 301-4.
- Hikichi, T., Kohda, T., Kaneko-Ishino, T., Ishino, F., 2003. Imprinting regulation of the murine *Meg1/Grb10* and human *GRB10* genes; roles of brain-specific promoters and mouse-specific CTCF-binding sites. *Nucleic Acids Res*. 31, 1398-406.
- Himeno, E., Tanaka, S., Kunath, T., 2008. Isolation and manipulation of mouse trophoblast stem cells. *Curr Protoc Stem Cell Biol*. Chapter 1, Unit 1E 4.
- Hirasawa, R., Chiba, H., Kaneda, M., Tajima, S., Li, E., Jaenisch, R., Sasaki, H., 2008. Maternal and zygotic *Dnmt1* are necessary and sufficient for the maintenance of DNA methylation imprints during preimplantation development. *Genes Dev*. 22, 1607-16.
- Holmgren, C., Kanduri, C., Dell, G., Ward, A., Mukhopadhyaya, R., Kanduri, M., Lobanenkova, V., Ohlsson, R., 2001. CpG methylation regulates the *Igf2/H19* insulator. *Curr Biol*. 11, 1128-30.
- Horike, S., Cai, S., Miyano, M., Cheng, J. F., Kohwi-Shigematsu, T., 2005. Loss of silent-chromatin looping and impaired imprinting of *DLX5* in Rett syndrome. *Nat Genet*. 37, 31-40.
- Howell, C. Y., Bestor, T. H., Ding, F., Latham, K. E., Mertineit, C., Trasler, J. M., Chaillet, J. R., 2001. Genomic imprinting disrupted by a maternal effect mutation in the *Dnmt1* gene. *Cell*. 104, 829-38.
- Hutchins, A. S., Mullen, A. C., Lee, H. W., Sykes, K. J., High, F. A., Hendrich, B. D., Bird, A. P., Reiner, S. L., 2002. Gene silencing quantitatively controls the function of a developmental trans-activator. *Mol Cell*. 10, 81-91.
- Ideraabdullah, F. Y., Abramowitz, L. K., Thorvaldsen, J. L., Krapp, C., Wen, S. C., Engel, N., Bartolomei, M. S., 2011. Novel cis-regulatory function in ICR-mediated imprinted repression of *H19*. *Dev Biol*. 355, 349-57.
- Iguchi-Arigo, S. M., Schaffner, W., 1989. CpG methylation of the cAMP-responsive enhancer/promoter sequence TGACGTCA abolishes specific factor binding as well as transcriptional activation. *Genes Dev*. 3, 612-9.
- Inoue, A., Shen, L., Dai, Q., He, C., Zhang, Y., 2011. Generation and replication-dependent dilution of 5fC and 5caC during mouse preimplantation development. *Cell Res*. 21, 1670-6.
- Inoue, A., Zhang, Y., 2011. Replication-dependent loss of 5-hydroxymethylcytosine in mouse preimplantation embryos. *Science*. 334, 194.
- Iqbal, K., Jin, S. G., Pfeifer, G. P., Szabo, P. E., 2011. Reprogramming of the paternal genome upon fertilization involves genome-wide oxidation of 5-methylcytosine. *Proc Natl Acad Sci U S A*. 108, 3642-7.
- Ito, S., D'Alessio, A. C., Taranova, O. V., Hong, K., Sowers, L. C., Zhang, Y., 2010. Role of Tet proteins in 5mC to 5hmC conversion, ES-cell self-renewal and inner cell mass specification. *Nature*. 466, 1129-33.

- Jia, D., Jurkowska, R. Z., Zhang, X., Jeltsch, A., Cheng, X., 2007. Structure of Dnmt3a bound to Dnmt3L suggests a model for de novo DNA methylation. *Nature*. 449, 248-251.
- Jones, P. L., Veenstra, G. J., Wade, P. A., Vermaak, D., Kass, S. U., Landsberger, N., Strouboulis, J., Wolffe, A. P., 1998. Methylated DNA and MeCP2 recruit histone deacetylase to repress transcription. *Nat Genet*. 19, 187-91.
- Kaffer, C. R., Grinberg, A., Pfeifer, K., 2001. Regulatory Mechanisms at the Mouse *Igf2/H19* Locus. *Molecular and Cellular Biology*. 21, 8189-8196.
- Kaffer, C. R., Srivastava, M., Park, K. Y., Ives, E., Hsieh, S., Battle, J., Grinberg, A., Huang, S. P., Pfeifer, K., 2000. A transcriptional insulator at the imprinted *H19/Igf2* locus. *Genes Dev*. 14, 1908-19.
- Kagiwada, S., Kurimoto, K., Hirota, T., Yamaji, M., Saitou, M., 2013. Replication-coupled passive DNA demethylation for the erasure of genome imprints in mice. *EMBO J*. 32, 340-53.
- Kaji, K., Caballero, I. M., MacLeod, R., Nichols, J., Wilson, V. A., Hendrich, B., 2006. The NuRD component Mbd3 is required for pluripotency of embryonic stem cells. *Nat Cell Biol*. 8, 285-92.
- Kaji, K., Nichols, J., Hendrich, B., 2007. Mbd3, a component of the NuRD co-repressor complex, is required for development of pluripotent cells. *Development*. 134, 1123-32.
- Kanatsu-Shinohara, M., Ogonuki, N., Iwano, T., Lee, J., Kazuki, Y., Inoue, K., Miki, H., Takehashi, M., Toyokuni, S., Shinkai, Y., Oshimura, M., Ishino, F., Ogura, A., Shinohara, T., 2005. Genetic and epigenetic properties of mouse male germline stem cells during long-term culture. *Development*. 132, 4155-63.
- Kanduri, C., Pant, V., Loukinov, D., Pugacheva, E., Qi, C. F., Wolffe, A., Ohlsson, R., Lobanenko, V. V., 2000. Functional association of CTCF with the insulator upstream of the *H19* gene is parent of origin-specific and methylation-sensitive. *Curr Biol*. 10, 853-6.
- Kaneda, M., Okano, M., Hata, K., Sado, T., Tsujimoto, N., Li, E., Sasaki, H., 2004. Essential role for de novo DNA methyltransferase Dnmt3a in paternal and maternal imprinting. *Nature*. 429, 900-3.
- Karimi, M., Johansson, S., Stach, D., Corcoran, M., Grandér, D., Schalling, M., Bakalkin, G., Lyko, F., Larsson, C., Ekström, T. J., 2006. LUMA (LUMinometric Methylation Assay)—A high throughput method to the analysis of genomic DNA methylation. *Experimental Cell Research*. 312, 1989-1995.
- Kato, Y., Kaneda, M., Hata, K., Kumaki, K., Hisano, M., Kohara, Y., Okano, M., Li, E., Nozaki, M., Sasaki, H., 2007. Role of the Dnmt3 family in de novo methylation of imprinted and repetitive sequences during male germ cell development in the mouse. *Human Molecular Genetics*. 16, 2272-2280.
- Keniry, A., Oxley, D., Monnier, P., Kyba, M., Dandolo, L., Smits, G., Reik, W., 2012. The *H19* lincRNA is a developmental reservoir of miR-675 that suppresses growth and *Igf1r*. *Nat Cell Biol*. 14, 659-65.
- Kernohan, K. D., Jiang, Y., Tremblay, D. C., Bonvissuto, A. C., Eubanks, J. H., Mann, M. R. W., Bérubé, N. G., 2010. ATRX Partners with Cohesin and MeCP2 and

- Contributes to Developmental Silencing of Imprinted Genes in the Brain. *Developmental Cell*. 18, 191-202.
- Klose, R. J., Bird, A. P., 2006. Genomic DNA methylation: the mark and its mediators. *Trends in Biochemical Sciences*. 31, 89-97.
- Ko, M., Bandukwala, H. S., An, J., Lamperti, E. D., Thompson, E. C., Hastie, R., Tsangaratou, A., Rajewsky, K., Korolov, S. B., Rao, A., 2011. Ten-Eleven-Translocation 2 (TET2) negatively regulates homeostasis and differentiation of hematopoietic stem cells in mice. *Proc Natl Acad Sci U S A*. 108, 14566-71.
- Kobayashi, H., Sakurai, T., Imai, M., Takahashi, N., Fukuda, A., Yayoi, O., Sato, S., Nakabayashi, K., Hata, K., Sotomaru, Y., Suzuki, Y., Kono, T., 2012. Contribution of intragenic DNA methylation in mouse gametic DNA methylomes to establish oocyte-specific heritable marks. *PLoS Genet*. 8, e1002440.
- Koerner, M. V., Pauler, F. M., Huang, R., Barlow, D. P., 2009. The function of non-coding RNAs in genomic imprinting. *Development*. 136, 1771-1783.
- Kokura, K., Kaul, S. C., Wadhwa, R., Nomura, T., Khan, M. M., Shinagawa, T., Yasukawa, T., Colmenares, C., Ishii, S., 2001. The Ski protein family is required for MeCP2-mediated transcriptional repression. *J Biol Chem*. 276, 34115-21.
- Kriaucionis, S., Heintz, N., 2009. The nuclear DNA base 5-hydroxymethylcytosine is present in Purkinje neurons and the brain. *Science*. 324, 929-30.
- Lane, N., Dean, W., Erhardt, S., Hajkova, P., Surani, A., Walter, J., Reik, W., 2003. Resistance of IAPs to methylation reprogramming may provide a mechanism for epigenetic inheritance in the mouse. *genesis*. 35, 88-93.
- Latos, P. A., Pauler, F. M., Koerner, M. V., Senergin, H. B., Hudson, Q. J., Stocsits, R. R., Allhoff, W., Stricker, S. H., Klement, R. M., Warczok, K. E., Aumayr, K., Pasierbek, P., Barlow, D. P., 2012. Airn transcriptional overlap, but not its lncRNA products, induces imprinted *Igf2r* silencing. *Science*. 338, 1469-72.
- Le Guezennec, X., Vermeulen, M., Brinkman, A. B., Hoeijmakers, W. A., Cohen, A., Lasonder, E., Stunnenberg, H. G., 2006. MBD2/NuRD and MBD3/NuRD, two distinct complexes with different biochemical and functional properties. *Mol Cell Biol*. 26, 843-51.
- Lee, D. H., Singh, P., Tsai, S. Y., Oates, N., Spalla, A., Spalla, C., Brown, L., Rivas, G., Larson, G., Rauch, T. A., Pfeifer, G. P., Szabo, P. E., 2010. CTCF-dependent chromatin bias constitutes transient epigenetic memory of the mother at the H19-*Igf2* imprinting control region in prospermatogonia. *PLoS Genet*. 6, e1001224.
- Lefebvre, L., Viville, S., Barton, S. C., Ishino, F., Keverne, E. B., Surani, M. A., 1998. Abnormal maternal behaviour and growth retardation associated with loss of the imprinted gene *Mest*. *Nat Genet*. 20, 163-9.
- Leighton, P. A., Saam, J. R., Ingram, R. S., Stewart, C. L., Tilghman, S. M., 1995. An enhancer deletion affects both H19 and *Igf2* expression. *Genes Dev*. 9, 2079-89.
- Li, E., Beard, C., Jaenisch, R., 1993. Role for DNA methylation in genomic imprinting. *Nature*. 366, 362-5.
- Li, E., Bestor, T. H., Jaenisch, R., 1992. Targeted mutation of the DNA methyltransferase gene results in embryonic lethality. *Cell*. 69, 915-26.

- Li, H., Yamagata, T., Mori, M., Yasuhara, A., Momoi, M. Y., 2005. Mutation analysis of methyl-CpG binding protein family genes in autistic patients. *Brain Dev.* 27, 321-5.
- Li, L., Keverne, E. B., Aparicio, S. A., Ishino, F., Barton, S. C., Surani, M. A., 1999. Regulation of maternal behavior and offspring growth by paternally expressed Peg3. *Science.* 284, 330-3.
- Li, X., Ito, M., Zhou, F., Youngson, N., Zuo, X., Leder, P., Ferguson-Smith, A. C., 2008. A Maternal-Zygotic Effect Gene, *Zfp57*, Maintains Both Maternal and Paternal Imprints. *Developmental Cell.* 15, 547-557.
- Li, Z., Cai, X., Cai, C. L., Wang, J., Zhang, W., Petersen, B. E., Yang, F. C., Xu, M., 2011. Deletion of *Tet2* in mice leads to dysregulated hematopoietic stem cells and subsequent development of myeloid malignancies. *Blood.* 118, 4509-18.
- Lin, S. 2011. Roles of Protein Factors in Regulation of Imprinted Expression. Doctoral dissertation. Retrieved from Proquest Dissertations and Theses. AAI3463067.
- Lin, S., Ferguson-Smith, A. C., Schultz, R. M., Bartolomei, M. S., 2011. Nonallelic Transcriptional Roles of CTCF and Cohesins at Imprinted Loci. *Molecular and Cellular Biology.* 31, 3094-3104.
- Lin, S. P., Youngson, N., Takada, S., Seitz, H., Reik, W., Paulsen, M., Cavaille, J., Ferguson-Smith, A. C., 2003. Asymmetric regulation of imprinting on the maternal and paternal chromosomes at the *Dlk1-Gtl2* imprinted cluster on mouse chromosome 12. *Nat Genet.* 35, 97-102.
- Lister, R., Pelizzola, M., Kida, Y. S., Hawkins, R. D., Nery, J. R., Hon, G., Antosiewicz-Bourget, J., O'Malley, R., Castanon, R., Klugman, S., Downes, M., Yu, R., Stewart, R., Ren, B., Thomson, J. A., Evans, R. M., Ecker, J. R., 2011. Hotspots of aberrant epigenomic reprogramming in human induced pluripotent stem cells. *Nature.* 471, 68-73.
- Liu, C., Teng, Z. Q., McQuate, A. L., Jobe, E. M., Christ, C. C., von Hoyningen-Huene, S. J., Reyes, M. D., Polich, E. D., Xing, Y., Li, Y., Guo, W., Zhao, X., 2013. An epigenetic feedback regulatory loop involving microRNA-195 and MBD1 governs neural stem cell differentiation. *PLoS One.* 8, e51436.
- Liu, C., Teng, Z. Q., Santistevan, N. J., Szulwach, K. E., Guo, W., Jin, P., Zhao, X., 2010. Epigenetic regulation of miR-184 by MBD1 governs neural stem cell proliferation and differentiation. *Cell Stem Cell.* 6, 433-44.
- Lu, Y. C., Song, J., Cho, H. Y., Fan, G., Yokoyama, K. K., Chiu, R., 2006. Cyclophilin a protects Peg3 from hypermethylation and inactive histone modification. *J Biol Chem.* 281, 39081-7.
- Lucifero, D., 2004. Gene-specific timing and epigenetic memory in oocyte imprinting. *Human Molecular Genetics.* 13, 839-849.
- Lucifero, D., Mertineit, C., Clarke, H. J., Bestor, T. H., Trasler, J. M., 2002. Methylation dynamics of imprinted genes in mouse germ cells. *Genomics.* 79, 530-8.
- Lyko, F., Brenton, J. D., Surani, M. A., Paro, R., 1997. An imprinting element from the mouse H19 locus functions as a silencer in *Drosophila*. *Nat Genet.* 16, 171-3.
- Ma, P., Lin, S., Bartolomei, M. S., Schultz, R. M., 2010. Metastasis Tumor Antigen 2 (MTA2) Is Involved in Proper Imprinted Expression of H19 and Peg3 During Mouse Preimplantation Development. *Biology of Reproduction.* 83, 1027-1035.

- Makedonski, K., Abuhatzira, L., Kaufman, Y., Razin, A., Shemer, R., 2005. MeCP2 deficiency in Rett syndrome causes epigenetic aberrations at the PWS/AS imprinting center that affects UBE3A expression. *Hum Mol Genet.* 14, 1049-58.
- Mancini-Dinardo, D., Steele, S. J., Levorse, J. M., Ingram, R. S., Tilghman, S. M., 2006. Elongation of the *Kcnq1ot1* transcript is required for genomic imprinting of neighboring genes. *Genes Dev.* 20, 1268-82.
- Mann, M. R., Lee, S. S., Doherty, A. S., Verona, R. I., Nolen, L. D., Schultz, R. M., Bartolomei, M. S., 2004. Selective loss of imprinting in the placenta following preimplantation development in culture. *Development.* 131, 3727-35.
- Mann, M. R. W., 2003. Disruption of Imprinted Gene Methylation and Expression in Cloned Preimplantation Stage Mouse Embryos. *Biology of Reproduction.* 69, 902-914.
- Mapendano, C. K., Kishino, T., Miyazaki, K., Kondo, S., Yoshiura, K., Hishikawa, Y., Koji, T., Niikawa, N., Ohta, T., 2006. Expression of the *Snurf-Snrpn* IC transcript in the oocyte and its putative role in the imprinting establishment of the mouse 7C imprinting domain. *J Hum Genet.* 51, 236-43.
- Market-Velker, B. A., Fernandes, A. D., Mann, M. R., 2010a. Side-by-side comparison of five commercial media systems in a mouse model: suboptimal in vitro culture interferes with imprint maintenance. *Biol Reprod.* 83, 938-50.
- Market-Velker, B. A., Zhang, L., Magri, L. S., Bonvissuto, A. C., Mann, M. R., 2010b. Dual effects of superovulation: loss of maternal and paternal imprinted methylation in a dose-dependent manner. *Hum Mol Genet.* 19, 36-51.
- Mayer, W., Niveleau, A., Walter, J., Fundele, R., Haaf, T., 2000. Demethylation of the zygotic paternal genome. *Nature.* 403, 501-2.
- McCarrey, J. R., 2012. The epigenome as a target for heritable environmental disruptions of cellular function. *Molecular and Cellular Endocrinology.* 354, 9-15.
- McGrath, J., Solter, D., 1983. Nuclear transplantation in mouse embryos. *J Exp Zool.* 228, 355-62.
- McGrath, J., Solter, D., 1984. Completion of mouse embryogenesis requires both the maternal and paternal genomes. *Cell.* 37, 179-83.
- Meissner, A., Mikkelsen, T. S., Gu, H., Wernig, M., Hanna, J., Sivachenko, A., Zhang, X., Bernstein, B. E., Nusbaum, C., Jaffe, D. B., Gnirke, A., Jaenisch, R., Lander, E. S., 2008. Genome-scale DNA methylation maps of pluripotent and differentiated cells. *Nature.* 454, 766-70.
- Mellen, M., Ayata, P., Dewell, S., Kriaucionis, S., Heintz, N., 2012. MeCP2 binds to 5hmC enriched within active genes and accessible chromatin in the nervous system. *Cell.* 151, 1417-30.
- Millar, C. B., Guy, J., Sansom, O. J., Selfridge, J., MacDougall, E., Hendrich, B., Keightley, P. D., Bishop, S. M., Clarke, A. R., Bird, A., 2002. Enhanced CpG mutability and tumorigenesis in *MBD4*-deficient mice. *Science.* 297, 403-5.
- Mineno, J., Okamoto, S., Ando, T., Sato, M., Chono, H., Izu, H., Takayama, M., Asada, K., Mirochnitchenko, O., Inouye, M., Kato, I., 2006. The expression profile of microRNAs in mouse embryos. *Nucleic Acids Res.* 34, 1765-71.
- Moran-Crusio, K., Reavie, L., Shih, A., Abdel-Wahab, O., Ndiaye-Lobry, D., Lobry, C., Figueroa, M. E., Vasanthakumar, A., Patel, J., Zhao, X., Perna, F., Pandey, S.,

- Madzo, J., Song, C., Dai, Q., He, C., Ibrahim, S., Beran, M., Zavadil, J., Nimer, S. D., Melnick, A., Godley, L. A., Aifantis, I., Levine, R. L., 2011. Tet2 loss leads to increased hematopoietic stem cell self-renewal and myeloid transformation. *Cancer Cell*. 20, 11-24.
- Morgenstern, J. P., Land, H., 1990. Advanced mammalian gene transfer: high titre retroviral vectors with multiple drug selection markers and a complementary helper-free packaging cell line. *Nucleic Acids Res.* 18, 3587-96.
- Nagano, T., Mitchell, J. A., Sanz, L. A., Pauler, F. M., Ferguson-Smith, A. C., Feil, R., Fraser, P., 2008. The Air noncoding RNA epigenetically silences transcription by targeting G9a to chromatin. *Science*. 322, 1717-20.
- Nakamura, T., Arai, Y., Umehara, H., Masuhara, M., Kimura, T., Taniguchi, H., Sekimoto, T., Ikawa, M., Yoneda, Y., Okabe, M., Tanaka, S., Shiota, K., Nakano, T., 2007. PGC7/Stella protects against DNA demethylation in early embryogenesis. *Nat Cell Biol.* 9, 64-71.
- Nakamura, T., Liu, Y. J., Nakashima, H., Umehara, H., Inoue, K., Matoba, S., Tachibana, M., Ogura, A., Shinkai, Y., Nakano, T., 2012. PGC7 binds histone H3K9me2 to protect against conversion of 5mC to 5hmC in early embryos. *Nature*. 486, 415-9.
- Nan, X., Campoy, F. J., Bird, A., 1997. MeCP2 is a transcriptional repressor with abundant binding sites in genomic chromatin. *Cell*. 88, 471-81.
- Nan, X., Meehan, R. R., Bird, A., 1993. Dissection of the methyl-CpG binding domain from the chromosomal protein MeCP2. *Nucleic Acids Res.* 21, 4886-92.
- Nan, X., Ng, H. H., Johnson, C. A., Laherty, C. D., Turner, B. M., Eisenman, R. N., Bird, A., 1998. Transcriptional repression by the methyl-CpG-binding protein MeCP2 involves a histone deacetylase complex. *Nature*. 393, 386-9.
- Ng, H. H., Zhang, Y., Hendrich, B., Johnson, C. A., Turner, B. M., Erdjument-Bromage, H., Tempst, P., Reinberg, D., Bird, A., 1999. MBD2 is a transcriptional repressor belonging to the MeCP1 histone deacetylase complex. *Nat Genet.* 23, 58-61.
- Nuber, U. A., Kriaucionis, S., Roloff, T. C., Guy, J., Selfridge, J., Steinhoff, C., Schulz, R., Lipkowitz, B., Ropers, H. H., Holmes, M. C., Bird, A., 2005. Up-regulation of glucocorticoid-regulated genes in a mouse model of Rett syndrome. *Hum Mol Genet.* 14, 2247-56.
- O'Donnell, L., Soileau, B., Heard, P., Carter, E., Sebold, C., Gelfond, J., Hale, D. E., Cody, J. D., 2010. Genetic determinants of autism in individuals with deletions of 18q. *Hum Genet.* 128, 155-64.
- Ohki, I., Shimotake, N., Fujita, N., Nakao, M., Shirakawa, M., 1999. Solution structure of the methyl-CpG-binding domain of the methylation-dependent transcriptional repressor MBD1. *EMBO J.* 18, 6653-61.
- Okano, M., Bell, D. W., Haber, D. A., Li, E., 1999. DNA methyltransferases Dnmt3a and Dnmt3b are essential for de novo methylation and mammalian development. *Cell*. 99, 247-57.
- Okano, M., Xie, S., Li, E., 1998. Dnmt2 is not required for de novo and maintenance methylation of viral DNA in embryonic stem cells. *Nucleic Acids Res.* 26, 2536-40.
- Olek, A., Oswald, J., Walter, J., 1996. A modified and improved method for bisulphite based cytosine methylation analysis. *Nucleic Acids Res.* 24, 5064-6.

- Ooi, S. K. T., Qiu, C., Bernstein, E., Li, K., Jia, D., Yang, Z., Erdjument-Bromage, H., Tempst, P., Lin, S.-P., Allis, C. D., Cheng, X., Bestor, T. H., 2007. DNMT3L connects unmethylated lysine 4 of histone H3 to de novo methylation of DNA. *Nature*. 448, 714-717.
- Oswald, J., Engemann, S., Lane, N., Mayer, W., Olek, A., Fundele, R., Dean, W., Reik, W., Walter, J., 2000. Active demethylation of the paternal genome in the mouse zygote. *Curr Biol*. 10, 475-8.
- Owen, C. M., Segars, J. H., Jr., 2009. Imprinting disorders and assisted reproductive technology. *Semin Reprod Med*. 27, 417-28.
- Pachnis, V., Brannan, C. I., Tilghman, S. M., 1988. The structure and expression of a novel gene activated in early mouse embryogenesis. *EMBO J*. 7, 673-81.
- Pant, V., Kurukuti, S., Pugacheva, E., Shamsuddin, S., Mariano, P., Renkawitz, R., Klenova, E., Lobanenkova, V., Ohlsson, R., 2004. Mutation of a Single CTCF Target Site within the H19 Imprinting Control Region Leads to Loss of Igf2 Imprinting and Complex Patterns of De Novo Methylation upon Maternal Inheritance. *Molecular and Cellular Biology*. 24, 3497-3504.
- Pant, V., Mariano, P., Kanduri, C., Mattsson, A., Lobanenkova, V., Heuchel, R., Ohlsson, R., 2003. The nucleotides responsible for the direct physical contact between the chromatin insulator protein CTCF and the H19 imprinting control region manifest parent of origin-specific long-distance insulation and methylation-free domains. *Genes Dev*. 17, 586-90.
- Phesse, T. J., Parry, L., Reed, K. R., Ewan, K. B., Dale, T. C., Sansom, O. J., Clarke, A. R., 2008. Deficiency of Mbd2 attenuates Wnt signaling. *Mol Cell Biol*. 28, 6094-103.
- Poirier, F., Chan, C. T., Timmons, P. M., Robertson, E. J., Evans, M. J., Rigby, P. W., 1991. The murine H19 gene is activated during embryonic stem cell differentiation in vitro and at the time of implantation in the developing embryo. *Development*. 113, 1105-14.
- Popp, C., Dean, W., Feng, S., Cokus, S. J., Andrews, S., Pellegrini, M., Jacobsen, S. E., Reik, W., 2010. Genome-wide erasure of DNA methylation in mouse primordial germ cells is affected by AID deficiency. *Nature*. 463, 1101-5.
- Qin, C., Wang, Z., Shang, J., Bekkari, K., Liu, R., Pacchione, S., McNulty, K. A., Ng, A., Barnum, J. E., Storer, R. D., 2010. Intracisternal A particle genes: Distribution in the mouse genome, active subtypes, and potential roles as species-specific mediators of susceptibility to cancer. *Mol Carcinog*. 49, 54-67.
- Quenneville, S., Verde, G., Corsinotti, A., Kapopoulou, A., Jakobsson, J., Offner, S., Baglivo, I., Pedone, P. V., Grimaldi, G., Riccio, A., Trono, D., 2011. In embryonic stem cells, ZFP57/KAP1 recognize a methylated hexanucleotide to affect chromatin and DNA methylation of imprinting control regions. *Mol Cell*. 44, 361-72.
- Quivoron, C., Couronne, L., Della Valle, V., Lopez, C. K., Plo, I., Wagner-Ballon, O., Do Cruzeiro, M., Delhommeau, F., Arnulf, B., Stern, M. H., Godley, L., Opolon, P., Tilly, H., Solary, E., Duffourd, Y., Dessen, P., Merle-Beral, H., Nguyen-Khac, F., Fontenay, M., Vainchenker, W., Bastard, C., Mercher, T., Bernard, O. A., 2011. TET2 inactivation results in pleiotropic hematopoietic abnormalities in

- mouse and is a recurrent event during human lymphomagenesis. *Cancer Cell*. 20, 25-38.
- Reese, K. J., Lin, S., Verona, R. I., Schultz, R. M., Bartolomei, M. S., 2007. Maintenance of paternal methylation and repression of the imprinted H19 gene requires MBD3. *PLoS Genet*. 3, e137.
- Reik, W., Dean, W., Walter, J., 2001. Epigenetic reprogramming in mammalian development. *Science*. 293, 1089-93.
- Riccio, A., Aaltonen, L. A., Godwin, A. K., Loukola, A., Percesepe, A., Salovaara, R., Masciullo, V., Genuardi, M., Paravatou-Petsotas, M., Bassi, D. E., Ruggeri, B. A., Klein-Szanto, A. J., Testa, J. R., Neri, G., Bellacosa, A., 1999. The DNA repair gene MBD4 (MED1) is mutated in human carcinomas with microsatellite instability. *Nat Genet*. 23, 266-8.
- Rivera, R. M., Stein, P., Weaver, J. R., Mager, J., Schultz, R. M., Bartolomei, M. S., 2008. Manipulations of mouse embryos prior to implantation result in aberrant expression of imprinted genes on day 9.5 of development. *Hum Mol Genet*. 17, 1-14.
- Robertson, K. D., Ait-Si-Ali, S., Yokochi, T., Wade, P. A., Jones, P. L., Wolffe, A. P., 2000. DNMT1 forms a complex with Rb, E2F1 and HDAC1 and represses transcription from E2F-responsive promoters. *Nat Genet*. 25, 338-42.
- Rountree, M. R., Bachman, K. E., Baylin, S. B., 2000. DNMT1 binds HDAC2 and a new co-repressor, DMAP1, to form a complex at replication foci. *Nat Genet*. 25, 269-77.
- Ryu, B. Y., Orwig, K. E., Oatley, J. M., Avarbock, M. R., Brinster, R. L., 2006. Effects of aging and niche microenvironment on spermatogonial stem cell self-renewal. *Stem Cells*. 24, 1505-11.
- Saito, M., Ishikawa, F., 2002. The mCpG-binding domain of human MBD3 does not bind to mCpG but interacts with NuRD/Mi2 components HDAC1 and MTA2. *J Biol Chem*. 277, 35434-9.
- Saitou, M., 2009. Germ cell specification in mice. *Curr Opin Genet Dev*. 19, 386-95.
- Samaco, R. C., Hogart, A., LaSalle, J. M., 2005. Epigenetic overlap in autism-spectrum neurodevelopmental disorders: MECP2 deficiency causes reduced expression of UBE3A and GABRB3. *Hum Mol Genet*. 14, 483-92.
- Sansom, O. J., Berger, J., Bishop, S. M., Hendrich, B., Bird, A., Clarke, A. R., 2003. Deficiency of Mbd2 suppresses intestinal tumorigenesis. *Nat Genet*. 34, 145-7.
- Santoro, F., Barlow, D. P., 2011. Developmental control of imprinted expression by macro non-coding RNAs. *Seminars in Cell & Developmental Biology*. 22, 328-335.
- Sarraf, S. A., Stancheva, I., 2004. Methyl-CpG binding protein MBD1 couples histone H3 methylation at lysine 9 by SETDB1 to DNA replication and chromatin assembly. *Mol Cell*. 15, 595-605.
- Sato, A., Otsu, E., Negishi, H., Utsunomiya, T., Arima, T., 2007. Aberrant DNA methylation of imprinted loci in superovulated oocytes. *Hum Reprod*. 22, 26-35.
- Schmidt, J. A., Abramowitz, L. K., Kubota, H., Wu, X., Niu, Z., Avarbock, M. R., Tobias, J. W., Bartolomei, M. S., Brinster, R. L., 2011. In vivo and in vitro aging

- is detrimental to mouse spermatogonial stem cell function. *Biol Reprod.* 84, 698-706.
- Schoenfelder, S., Paro, R., 2004. *Drosophila* Su(Hw) regulates an evolutionarily conserved silencer from the mouse H19 imprinting control region. *Cold Spring Harb Symp Quant Biol.* 69, 47-54.
- Schoenherr, C. J., Levorse, J. M., Tilghman, S. M., 2002. CTCF maintains differential methylation at the *Igf2/H19* locus. *Nature Genetics.* 33, 66-69.
- Schoenherr, C. J., Levorse, J. M., Tilghman, S. M., 2003. CTCF maintains differential methylation at the *Igf2/H19* locus. *Nat Genet.* 33, 66-9.
- Schule, B., Armstrong, D. D., Vogel, H., Oviedo, A., Francke, U., 2008. Severe congenital encephalopathy caused by *MECP2* null mutations in males: central hypoxia and reduced neuronal dendritic structure. *Clin Genet.* 74, 116-26.
- Seisenberger, S., Andrews, S., Krueger, F., Arand, J., Walter, J., Santos, F., Popp, C., Thienpont, B., Dean, W., Reik, W., 2012. The dynamics of genome-wide DNA methylation reprogramming in mouse primordial germ cells. *Mol Cell.* 48, 849-62.
- Shahbazian, M., Young, J., Yuva-Paylor, L., Spencer, C., Antalffy, B., Noebels, J., Armstrong, D., Paylor, R., Zoghbi, H., 2002. Mice with truncated *MeCP2* recapitulate many Rett syndrome features and display hyperacetylation of histone H3. *Neuron.* 35, 243-54.
- Sharif, J., Muto, M., Takebayashi, S., Suetake, I., Iwamatsu, A., Endo, T. A., Shinga, J., Mizutani-Koseki, Y., Toyoda, T., Okamura, K., Tajima, S., Mitsuya, K., Okano, M., Koseki, H., 2007. The SRA protein Np95 mediates epigenetic inheritance by recruiting *Dnmt1* to methylated DNA. *Nature.* 450, 908-12.
- Shen, L., Wu, H., Diep, D., Yamaguchi, S., D'Alessio, A. C., Fung, H. L., Zhang, K., Zhang, Y., 2013. Genome-wide Analysis Reveals TET- and TDG-Dependent 5-Methylcytosine Oxidation Dynamics. *Cell.* 153, 692-706.
- Shin, J. Y., Fitzpatrick, G. V., Higgins, M. J., 2008. Two distinct mechanisms of silencing by the *KvDMR1* imprinting control region. *EMBO J.* 27, 168-78.
- Shmela, M. E., Gicquel, C. F., 2013. Human diseases versus mouse models: insights into the regulation of genomic imprinting at the human 11p15/mouse distal chromosome 7 region. *J Med Genet.* 50, 11-20.
- Skene, P. J., Illingworth, R. S., Webb, S., Kerr, A. R., James, K. D., Turner, D. J., Andrews, R., Bird, A. P., 2010. Neuronal *MeCP2* is expressed at near histone-octamer levels and globally alters the chromatin state. *Mol Cell.* 37, 457-68.
- Sleutels, F., Zwart, R., Barlow, D. P., 2002. The non-coding *Air* RNA is required for silencing autosomal imprinted genes. *Nature.* 415, 810-3.
- Smallwood, A., Esteve, P. O., Pradhan, S., Carey, M., 2007. Functional cooperation between *HP1* and *DNMT1* mediates gene silencing. *Genes Dev.* 21, 1169-78.
- Smallwood, S. A., Tomizawa, S.-i., Krueger, F., Ruf, N., Carli, N., Segonds-Pichon, A., Sato, S., Hata, K., Andrews, S. R., Kelsey, G., 2011. Dynamic CpG island methylation landscape in oocytes and preimplantation embryos. *Nature Genetics.* 43, 811-814.
- Smilnich, N. J., Day, C. D., Fitzpatrick, G. V., Caldwell, G. M., Lossie, A. C., Cooper, P. R., Smallwood, A. C., Joyce, J. A., Schofield, P. N., Reik, W., Nicholls, R. D.,

- Weksberg, R., Driscoll, D. J., Maher, E. R., Shows, T. B., Higgins, M. J., 1999. A maternally methylated CpG island in KvLQT1 is associated with an antisense paternal transcript and loss of imprinting in Beckwith-Wiedemann syndrome. *Proc Natl Acad Sci U S A.* 96, 8064-9.
- Smith, Z. D., Chan, M. M., Mikkelsen, T. S., Gu, H., Gnirke, A., Regev, A., Meissner, A., 2012. A unique regulatory phase of DNA methylation in the early mammalian embryo. *Nature.* 484, 339-44.
- Smits, G., Mungall, A. J., Griffiths-Jones, S., Smith, P., Beury, D., Matthews, L., Rogers, J., Pask, A. J., Shaw, G., VandeBerg, J. L., McCarrey, J. R., Renfree, M. B., Reik, W., Dunham, I., 2008. Conservation of the H19 noncoding RNA and H19-IGF2 imprinting mechanism in therians. *Nat Genet.* 40, 971-6.
- Srivastava, M., 2002. Imprint Control Element-mediated Secondary Methylation Imprints at the Igf2/H19 Locus. *Journal of Biological Chemistry.* 278, 5977-5983.
- Srivastava, M., Hsieh, S., Grinberg, A., Williams-Simons, L., Huang, S. P., Pfeifer, K., 2000. H19 and Igf2 monoallelic expression is regulated in two distinct ways by a shared cis acting regulatory region upstream of H19. *Genes Dev.* 14, 1186-95.
- Stadnick, M. P., Pieracci, F. M., Cranston, M. J., Taksel, E., Thorvaldsen, J. L., Bartolomei, M. S., 1999. Role of a 461-bp G-rich repetitive element in H19 transgene imprinting. *Dev Genes Evol.* 209, 239-48.
- Stoger, R., Kubicka, P., Liu, C. G., Kafri, T., Razin, A., Cedar, H., Barlow, D. P., 1993. Maternal-specific methylation of the imprinted mouse Igf2r locus identifies the expressed locus as carrying the imprinting signal. *Cell.* 73, 61-71.
- Suetake, I., Shinozaki, F., Miyagawa, J., Takeshima, H., Tajima, S., 2004. DNMT3L stimulates the DNA methylation activity of Dnmt3a and Dnmt3b through a direct interaction. *J Biol Chem.* 279, 27816-23.
- Surani, M. A., Barton, S. C., 1983. Development of gynogenetic eggs in the mouse: implications for parthenogenetic embryos. *Science.* 222, 1034-6.
- Surani, M. A., Barton, S. C., Norris, M. L., 1984. Development of reconstituted mouse eggs suggests imprinting of the genome during gametogenesis. *Nature.* 308, 548-50.
- Szabo, P., Tang, S. H., Rentsendorj, A., Pfeifer, G. P., Mann, J. R., 2000. Maternal-specific footprints at putative CTCF sites in the H19 imprinting control region give evidence for insulator function. *Curr Biol.* 10, 607-10.
- Szabo, P. E., Mann, J. R., 1995. Biallelic expression of imprinted genes in the mouse germ line: implications for erasure, establishment, and mechanisms of genomic imprinting. *Genes Dev.* 9, 1857-68.
- Szabo, P. E., Tang, S. H. E., Silva, F. J., Tsark, W. M. K., Mann, J. R., 2004. Role of CTCF Binding Sites in the Igf2/H19 Imprinting Control Region. *Molecular and Cellular Biology.* 24, 4791-4800.
- Tahiliani, M., Koh, K. P., Shen, Y., Pastor, W. A., Bandukwala, H., Brudno, Y., Agarwal, S., Iyer, L. M., Liu, D. R., Aravind, L., Rao, A., 2009. Conversion of 5-methylcytosine to 5-hydroxymethylcytosine in mammalian DNA by MLL partner TET1. *Science.* 324, 930-5.
- Takada, S., Paulsen, M., Tevendale, M., Tsai, C. E., Kelsey, G., Cattanach, B. M., Ferguson-Smith, A. C., 2002. Epigenetic analysis of the Dlk1-Gtl2 imprinted

- domain on mouse chromosome 12: implications for imprinting control from comparison with *Igf2-H19*. *Hum Mol Genet.* 11, 77-86.
- Tanaka, S., Kunath, T., Hadjantonakis, A. K., Nagy, A., Rossant, J., 1998. Promotion of trophoblast stem cell proliferation by FGF4. *Science.* 282, 2072-5.
- Thorvaldsen, J. L., Bartolomei, M. S., 2007. SnapShot: Imprinted Gene Clusters. *Cell.* 130, 958.e1-958.e2.
- Thorvaldsen, J. L., Duran, K. L., Bartolomei, M. S., 1998. Deletion of the H19 differentially methylated domain results in loss of imprinted expression of H19 and *Igf2*. *Genes & Development.* 12, 3693-3702.
- Thorvaldsen, J. L., Fedoriw, A. M., Nguyen, S., Bartolomei, M. S., 2006. Developmental Profile of H19 Differentially Methylated Domain (DMD) Deletion Alleles Reveals Multiple Roles of the DMD in Regulating Allelic Expression and DNA Methylation at the Imprinted H19/*Igf2* Locus. *Molecular and Cellular Biology.* 26, 1245-1258.
- Thorvaldsen, J. L., Mann, M. R. W., Nwoko, O., Duran, K. L., Bartolomei, M. S., 2002. Analysis of Sequence Upstream of the Endogenous H19 Gene Reveals Elements Both Essential and Dispensable for Imprinting. *Molecular and Cellular Biology.* 22, 2450-2462.
- Tomizawa, S. i., Kobayashi, H., Watanabe, T., Andrews, S., Hata, K., Kelsey, G., Sasaki, H., 2011. Dynamic stage-specific changes in imprinted differentially methylated regions during early mammalian development and prevalence of non-CpG methylation in oocytes. *Development.* 138, 811-820.
- Tremblay, K. D., Duran, K. L., Bartolomei, M. S., 1997. A 5' 2-kilobase-pair region of the imprinted mouse H19 gene exhibits exclusive paternal methylation throughout development. *Mol Cell Biol.* 17, 4322-9.
- Tremblay, K. D., Saam, J. R., Ingram, R. S., Tilghman, S. M., Bartolomei, M. S., 1995. A paternal-specific methylation imprint marks the alleles of the mouse H19 gene. *Nat Genet.* 9, 407-13.
- Tudor, M., Akbarian, S., Chen, R. Z., Jaenisch, R., 2002. Transcriptional profiling of a mouse model for Rett syndrome reveals subtle transcriptional changes in the brain. *Proc Natl Acad Sci U S A.* 99, 15536-41.
- Umlauf, D., Goto, Y., Cao, R., Cerqueira, F., Wagschal, A., Zhang, Y., Feil, R., 2004. Imprinting along the *Kcnq1* domain on mouse chromosome 7 involves repressive histone methylation and recruitment of Polycomb group complexes. *Nat Genet.* 36, 1296-300.
- Vire, E., Brenner, C., Deplus, R., Blanchon, L., Fraga, M., Didelot, C., Morey, L., Van Eynde, A., Bernard, D., Vanderwinden, J. M., Bollen, M., Esteller, M., Di Croce, L., de Launoit, Y., Fuks, F., 2006. The Polycomb group protein EZH2 directly controls DNA methylation. *Nature.* 439, 871-4.
- Watanabe, T., Tomizawa, S. i., Mitsuya, K., Totoki, Y., Yamamoto, Y., Kuramochi-Miyagawa, S., Iida, N., Hoki, Y., Murphy, P. J., Toyoda, A., Gotoh, K., Hiura, H., Arima, T., Fujiyama, A., Sado, T., Shibata, T., Nakano, T., Lin, H., Ichiyanagi, K., Soloway, P. D., Sasaki, H., 2011. Role for piRNAs and Noncoding RNA in de Novo DNA Methylation of the Imprinted Mouse *Rasgrf1* Locus. *Science.* 332, 848-852.

- Weaver, J. R., Sarkisian, G., Krapp, C., Mager, J., Mann, M. R. W., Bartolomei, M. S., 2010. Domain-Specific Response of Imprinted Genes to Reduced DNMT1. *Molecular and Cellular Biology*. 30, 3916-3928.
- Webber, A. L., Ingram, R. S., Levorse, J. M., Tilghman, S. M., 1998. Location of enhancers is essential for the imprinting of H19 and Igf2 genes. *Nature*. 391, 711-5.
- Weber, M., Hellmann, I., Stadler, M. B., Ramos, L., Paabo, S., Rebhan, M., Schubeler, D., 2007. Distribution, silencing potential and evolutionary impact of promoter DNA methylation in the human genome. *Nat Genet*. 39, 457-66.
- Webster, K. E., 2005. Meiotic and epigenetic defects in Dnmt3L-knockout mouse spermatogenesis. *Proceedings of the National Academy of Sciences*. 102, 4068-4073.
- Wong, E., Yang, K., Kuraguchi, M., Werling, U., Avdievich, E., Fan, K., Fazzari, M., Jin, B., Brown, A. M., Lipkin, M., Edelman, W., 2002. Mbd4 inactivation increases C>T transition mutations and promotes gastrointestinal tumor formation. *Proc Natl Acad Sci U S A*. 99, 14937-42.
- Wossidlo, M., Nakamura, T., Lepikhov, K., Marques, C. J., Zakhartchenko, V., Boiani, M., Arand, J., Nakano, T., Reik, W., Walter, J., 2011. 5-Hydroxymethylcytosine in the mammalian zygote is linked with epigenetic reprogramming. *Nat Commun*. 2.
- Wu, H., Coskun, V., Tao, J., Xie, W., Ge, W., Yoshikawa, K., Li, E., Zhang, Y., Sun, Y. E., 2010. Dnmt3a-dependent nonpromoter DNA methylation facilitates transcription of neurogenic genes. *Science*. 329, 444-8.
- Wu, X., Goodyear, S. M., Abramowitz, L. K., Bartolomei, M. S., Tobias, J. W., Avarbock, M. R., Brinster, R. L., 2012. Fertile offspring derived from mouse spermatogonial stem cells cryopreserved for more than 14 years. *Hum Reprod*. 27, 1249-59.
- Wutz, A., Smrzka, O. W., Schweifer, N., Schellander, K., Wagner, E. F., Barlow, D. P., 1997. Imprinted expression of the Igf2r gene depends on an intronic CpG island. *Nature*. 389, 745-9.
- Yamaguchi, S., Hong, K., Liu, R., Inoue, A., Shen, L., Zhang, K., Zhang, Y., 2013. Dynamics of 5-methylcytosine and 5-hydroxymethylcytosine during germ cell reprogramming. *Cell Res*. 23, 329-39.
- Yamaguchi, S., Hong, K., Liu, R., Shen, L., Inoue, A., Diep, D., Zhang, K., Zhang, Y., 2012. Tet1 controls meiosis by regulating meiotic gene expression. *Nature*. 492, 443-7.
- Yang, T., Adamson, T. E., Resnick, J. L., Leff, S., Wevrick, R., Francke, U., Jenkins, N. A., Copeland, N. G., Brannan, C. I., 1998. A mouse model for Prader-Willi syndrome imprinting-centre mutations. *Nat Genet*. 19, 25-31.
- Yao, H., Brick, K., Evrard, Y., Xiao, T., Camerini-Otero, R. D., Felsenfeld, G., 2010. Mediation of CTCF transcriptional insulation by DEAD-box RNA-binding protein p68 and steroid receptor RNA activator SRA. *Genes Dev*. 24, 2543-55.
- Yildirim, O., Li, R., Hung, J. H., Chen, P. B., Dong, X., Ee, L. S., Weng, Z., Rando, O. J., Fazio, T. G., 2011. Mbd3/NURD complex regulates expression of 5-

- hydroxymethylcytosine marked genes in embryonic stem cells. *Cell*. 147, 1498-510.
- Yoon, B., Herman, H., Hu, B., Park, Y. J., Lindroth, A., Bell, A., West, A. G., Chang, Y., Stablewski, A., Piel, J. C., Loukinov, D. I., Lobanenko, V. V., Soloway, P. D., 2005. *Rasgrf1* imprinting is regulated by a CTCF-dependent methylation-sensitive enhancer blocker. *Mol Cell Biol*. 25, 11184-90.
- Yoshimizu, T., Miroglio, A., Ripoche, M. A., Gabory, A., Vernucci, M., Riccio, A., Colnot, S., Godard, C., Terris, B., Jammes, H., Dandolo, L., 2008. The H19 locus acts in vivo as a tumor suppressor. *Proceedings of the National Academy of Sciences*. 105, 12417-12422.
- Yu, D. H., Ware, C., Waterland, R. A., Zhang, J., Chen, M. H., Gadkari, M., Kunde-Ramamoorthy, G., Nosavanh, L. M., Shen, L., 2013. Developmentally programmed 3' CpG island methylation confers tissue- and cell-type specific transcriptional activation. *Mol Cell Biol*.
- Yu, M., Hon, G. C., Szulwach, K. E., Song, C. X., Jin, P., Ren, B., He, C., 2012. Tet-assisted bisulfite sequencing of 5-hydroxymethylcytosine. *Nat Protoc*. 7, 2159-70.
- Zhang, Y., Ng, H. H., Erdjument-Bromage, H., Tempst, P., Bird, A., Reinberg, D., 1999. Analysis of the NuRD subunits reveals a histone deacetylase core complex and a connection with DNA methylation. *Genes Dev*. 13, 1924-35.
- Zhao, X., Ueba, T., Christie, B. R., Barkho, B., McConnell, M. J., Nakashima, K., Lein, E. S., Eadie, B. D., Willhoite, A. R., Muotri, A. R., Summers, R. G., Chun, J., Lee, K. F., Gage, F. H., 2003. Mice lacking methyl-CpG binding protein 1 have deficits in adult neurogenesis and hippocampal function. *Proc Natl Acad Sci U S A*. 100, 6777-82.
- Zhou, Z., Hong, E. J., Cohen, S., Zhao, W. N., Ho, H. Y., Schmidt, L., Chen, W. G., Lin, Y., Savner, E., Griffith, E. C., Hu, L., Steen, J. A., Weitz, C. J., Greenberg, M. E., 2006. Brain-specific phosphorylation of MeCP2 regulates activity-dependent *Bdnf* transcription, dendritic growth, and spine maturation. *Neuron*. 52, 255-69.